

Edge and Interfacial Vibration of a Thin Elastic Cylindrical Panel

by Victor Arulchandran

A thesis submitted for the degree of
Doctor of Philosophy

Department of Information Systems, Computing, and Mathematics

Brunel University

United Kingdom

July 2013

A youth who had begun to read geometry with Euclid, when he had learnt the first proposition, enquired, "What do I get by learning these things?" So Euclid called a slave and said "Give him threepence, since he must make a gain out of what he learns."

~ Euclid of Alexandria (325-265 BCE)

Abstract

Free vibrations of a thin elastic circular cylindrical panel localized near the rectilinear edge, propagating along the edge and decaying in its circumferential direction, are investigated in the framework of the two-dimensional equations in the Kirchoff-Love theory of shells. At first the panel is assumed to be infinite longitudinally and semi-infinite along its length of curvature (of course not realistically possible), followed by the assumption that the panel is then finite along its length of curvature and fixed and free conditions are imposed on the second resulting boundary.

Using the comprehensive asymptotic analysis detailed in Kaplunov et al. (1998) “Dynamics of Thin Walled Elastic Bodies”, leading order asymptotic solutions are derived for three types of localized vibration, they are bending, extensional, and super-low frequency. Explicit representation of the exact solutions cannot be obtained due to the degree of complexity of the solving equations and relevant boundary conditions, however, computational methods are used to find exact numerical solutions and graphs. Parameters, particularly panel thickness, wavelength, poisson’s ratio, and circumferential panel length, are varied, and their effects on vibration analyzed.

This analysis is further extended to investigate localized vibration on the interface (perfect bond) of two cylindrical panels joined at their respective rectilinear edges, propagating along the interface and decaying in the circumferential direction away from the interface. An earlier, similar, localized vibration problem presented in Kaplunov et al. (1999) “Free Localized Vibrations of a Semi-Infinite Cylindrical Shell” and Kaplunov and Wilde (2002) “Free Interfacial Vibrations in Cylindrical Shells” is replicated for comparison with all cases. The asymptotics are similar, however in this problem the numerics highlight the stronger effect of curvature on the decay of the super-low frequency vibrations, and to some extent on the leading order bending vibration.

Acknowledgement

First and foremost I would like to thank my first supervisor Dr Evgeniya Nolde for her support, encouragement and above all else, patience, with me over the last few years. I also thank my second supervisor Professor Julius Kaplunov for supporting me and giving me the enlightening opportunity to study a PhD.

I am very grateful to the EPSRC for supporting my PhD, without which I would not have been able to continue.

I would like to thank Professor Anthony D. Rawlins and Dr. Jacques Furter for their support to me as an undergraduate student.

A huge thank you to the Department of Mathematics at Brunel University, especially the administrative and support staff.

I thank my parents for supporting me in my studies.

Finally, I would like to thank Kathrine for her endless encouragement and motivation.

Contents

Abstract	ii
Acknowledgement	iii
List of Figures	x
1 Introduction	1
1.1 Dynamics of Elastic Structures	1
1.1.1 Mathematical Theories	2
1.1.2 Framework of the Thesis	9
1.2 Preliminaries	12
1.2.1 Rayleigh-Type Flexural Edge Wave	12
1.2.2 Rayleigh-Type Extensional Edge Wave	14
1.2.3 Stoneley-Type Flexural Wave	16
1.2.4 Stoneley-Type Extensional Wave	19
2 Vibration of a Thin Semi-Infinite Cylindrical Shell	21
2.1 Statement of the Problem	21
2.1.1 Problem 1A	22
2.1.2 Problem 2A	23
2.1.3 Equations of Motion	24
2.1.4 Traction-Free Boundary Conditions	24
2.2 Exact Solution	25
2.2.1 Problem 1A	25
2.2.2 Problem 2A	29
2.3 Asymptotic Analysis	32

2.3.1	Asymptotic Justification for Problem 1A	33
2.3.2	Asymptotics for Problem 2A	36
2.4	Flexural Vibrations	37
2.4.1	Numerical Results	39
2.5	Extensional Vibrations	46
2.5.1	Numerical Results	48
2.6	Super-Low Frequency Vibration	54
2.6.1	Numerical Results	57
3	Vibration of a Thin Finite Cylindrical Shell	61
3.1	Statement of the Problem	61
3.1.1	Problem 1B	61
3.1.2	Problem 2B	62
3.2	Exact Solution	63
3.2.1	Problem 1B	63
3.2.2	Problem 2B	64
3.3	Numerical Results for Flexural Vibration	65
3.3.1	Free-Free	65
3.3.2	Free-Fixed	69
3.4	Numerical Results for Extensional Vibration	72
3.4.1	Free-Free	72
3.4.2	Free-Fixed	73
3.5	Numerical Results for Super-Low Frequency	75
3.5.1	Free-Free	75
3.5.2	Free-Fixed	78
4	Interfacial Vibration of Composite Cylindrical Shell	79
4.1	Statement of the Problem	79
4.1.1	Problem 1C	79
4.1.2	Problem 2C	80
4.1.3	Equations of Motion	81
4.1.4	Perfect Contact Boundary Conditions	82
4.2	Exact Solution	83
4.2.1	Problem 1C	83

4.2.2	Problem 2C	86
4.3	Flexural Vibrations	90
4.3.1	Numerical Results	91
4.4	Extensional Vibrations	93
4.4.1	Numerical Results	94
4.5	Super-Low Frequency Vibrations	96
4.5.1	Numerical Results	97
4.6	Concluding Remarks	98

List of Figures

2.1	Panel configuration for problem 1A	22
2.2	Panel configuration for problem 2A	23
2.3	Asymptotic and numeric forms for the flexural edge waves of Problems 1A in the left column, and 2A in the right column, with given fixed parameters $\eta = 0.01$, $\gamma/n = 40$, and for (a) and (b) $\nu = 0.495$, and (c) and (d) $\nu = 0.45$	40
2.4	Asymptotic and numeric forms for the flexural edge waves of Problems 1A in the left column, and 2A in the right column, with given fixed parameters $\eta = 0.01$, $\gamma/n = 40$, and for (a) and (b) $\nu = 0.3$, and (c) and (d) $\nu = 0.2$	41
2.5	Percentage error between asymptotic and numeric forms for the flexural edge waves of Problem 1A in dark red and Problem 2A in blue, with fixed parameters $\eta = 0.01$, $\gamma/n = 40$, and ν shown below each graph.	42
2.6	Asymptotic and numeric forms for the flexural edge waves of Problems 1A in the left column, and 2A in the right column, with given fixed parameters $\eta = 0.01$, $\gamma/n = 30$, and for ν shown below each graph.	43
2.7	Percentage error between asymptotic and numeric forms for the flexural edge waves of Problem 1A in dark red and Problem 2A in blue, with fixed parameters $\eta = 0.01$, $\gamma/n = 30$, and ν shown below each graph.	44

2.8	Asymptotic and numeric forms for the extensional edge waves of Problems 1A in the left column, and 2A in the right column, with given fixed parameters $\eta = 0.001$, $\nu = 0.02$, and ν displayed under each graph.	49
2.9	Asymptotic and numeric forms for the extensional edge waves of Problems 1A in the left column, and 2A in the right column, with given fixed parameters $\eta = 0.001$, $\nu = 0.3$, and γ/n are displayed below each graph.	50
2.10	Asymptotic and numeric forms for the extensional edge waves of Problems 1A in the left column, and 2A in the right column, with given fixed parameters $\eta = 0.001$, $\nu = 0.45$, and γ/n displayed below each graph.	51
2.11	Percentage error between asymptotic and numeric forms for the extensional edge waves of Problems 1A in the left column, and 2A in the right column, with given fixed parameters $\eta = 0.001$, $\gamma/n = 5$, and ν displayed below each graph.	52
2.12	Percentage error between asymptotic and numeric forms for the extensional edge waves of Problems 1A in the left column, and 2A in the right column, with given fixed parameters $\eta = 0.001$, $\gamma/n = 15$, and ν displayed below each graph.	53
2.13	Asymptotic approximate and numeric form for the super-low frequency edge wave of Problem 1A with fixed parameters $\eta = 0.001$, $\nu = 0.3$, and $\gamma = 2$	57
2.14	Asymptotic approximate and numeric forms for the super-low frequency edge wave of Problem 1A with fixed parameters $\eta = 0.001$, $\nu = 0.3$, and $\gamma = 5$	58
2.15	Percentage error between asymptotic approximate and numeric form for the super-low frequency edge wave of Problem 1A with fixed parameters $\eta = 0.001$, $\nu = 0.3$, and $\gamma = 5$	58
2.16	Asymptotic approximate and numeric form for the super-low frequency edge wave of Problem 1A with fixed parameters $\eta = 0.001$, $\nu = 0.3$, and $\gamma = 10$	59

2.17	Percentage error between asymptotic approximate and numeric form for the super-low frequency edge wave of Problem 1A with fixed parameters $\eta = 0.001$, $\nu = 0.3$, and $\gamma = 10$.	59
3.1	Cylinder...	62
3.2	Cylinder...	62
3.3	1B	65
3.4	2B	65
3.5	1A	66
3.6	2B	67
3.7	1B	67
3.8	2B	68
3.9	1B	69
3.10	1B	70
3.11	1B	70
3.12	2B	71
3.13	1C	72
3.14	1B and 2B	73
3.15	1B and 2B	73
3.16	1B and 2B	74
3.17	Asymptotic approximate and numeric form for the super-low frequency edge wave of Problem 1B with fixed parameters $\eta = 0.001$, $\nu = 0.3$, and $\gamma = 10$	75
3.18	Asymptotic approximate and numeric form for the super-low frequency edge wave of Problem 1B with fixed parameters $\eta = 0.001$, $\nu = 0.3$, and $\gamma = 10$	76
3.19	Asymptotic approximate and numeric form for the super-low frequency edge wave of Problem 2B with fixed parameters $\eta = 0.001$, $\nu = 0.3$, and $\gamma = 10$	77
3.20	2B	77
3.21	1A	78
4.1		80
4.2		81

4.3	Asymptotic and numeric forms for the interfacial flexural edge wave of Problem 1C with fixed parameters $\eta = 0.01$, $\nu^{(1)} = 0.3$, $\nu^{(2)} = 0.4$, and $\gamma = 40$	91
4.4	Asymptotic and numeric forms for the interfacial flexural edge wave of Problem 1C with fixed parameters $\eta = 0.01$, $\nu^{(1)} = 0.3$, $\nu^{(2)} = 0.4$, and $\gamma = 35$	92
4.5	Asymptotic and numeric forms for the interfacial flexural edge wave of Problem 1C with fixed parameters $\eta = 0.01$, $\nu^{(1)} = 0.3$, $\nu^{(2)} = 0.4$, and $\gamma = 25$	92
4.6	Asymptotic and numeric forms for the interfacial flexural edge wave of Problem 2C with fixed parameters $\eta = 0.01$, $\nu^{(1)} = 0.3$, $\nu^{(2)} = 0.4$, and $n = 25$	93
4.7	Asymptotic and numeric forms for the interfacial extensional edge wave of Problem 1C with fixed parameters $\eta = 0.001$, $\nu^{(1)} = 0.3$, $\nu^{(2)} = 0.4$, and $\gamma = 15$	95
4.8	Asymptotic and numeric forms for the interfacial flexural edge wave of Problem 2C with fixed parameters $\eta = 0.001$, $\nu^{(1)} = 0.3$, $\nu^{(2)} = 0.4$, and $n = 5$	95
4.9	Asymptotic and numeric forms for the interfacial flexural edge wave of Problem 1C with fixed parameters $\eta = 0.001$, $\nu^{(1)} = 0.3$, $\nu^{(2)} = 0.4$, and $n = 10$	96
4.10	Asymptotic and numeric forms for the interfacial super-low edge wave of Problem 1C with fixed parameters $\eta = 0.001$, $\nu^{(1)} = 0.3$, $\nu^{(2)} = 0.4$, and $\gamma = 10$	97
4.11	Asymptotic and numeric forms for the interfacial flexural edge wave of Problem 2C with fixed parameters $\eta = 0.001$, $\nu^{(1)} = 0.3$, $\nu^{(2)} = 0.4$, and $\gamma = 10$	97

Chapter 1

Introduction

1.1 Dynamics of Elastic Structures

The popularity of shell dynamics over the last century has been increasing, in no small part due to the mathematical modelling of real world problems involving thin structures which vibrate and transmit waves. Since the dawn of the industrial age in the west, many problems have arisen in engineering due to the catastrophic behaviour of structures vibrating at resonant frequencies. Indeed, wave and vibration problems are widespread throughout various related subjects. Most recent developments arise from the desire to understand the behaviour of waves propagating along the edge of thin walled structures, most notably in non-destructive evaluation methods (NDE). Non-destructive evaluation techniques are being developed as a response to the growing need in industry to be able to assess the health of materials and structures, distinguish and ascertain deformities, assess safety, and potentially apply fixes without conceding excess time and resources, see Alleyne and Crawley (1992) and Alleyne and Crawley (1996) The elastic structures, waves and vibrations in these problems can be understood by mathematical modelling.

Modelling of these dynamic shell problems are carried out in the two dimensional configuration. Three dimensional configurations lead to complex systems of PDEs which are extremely difficult to solve analytically, and require complicated numerical schemes for computation. It then becomes necessary to introduce

assumptions in the case of thin bodies to simplify the three dimensional model. The assumptions are aimed at neglecting terms and quantities of such an order that they do not substantially alter the formulation and solution of the problem, but do simplify the analytical procedure. Thereby reducing the three dimensional problem into a two dimensional approximation where the explicit mathematical structure is relatively simpler and more responsive to numerical computation and qualitative analysis. It is these assumptions that are important in shell theory, and have been strengthened, refined, debated and expanded upon over many years. This idea of simplification was described by A. E. H. Love in his famous book Love (1906) “A Treatise on the Mathematical Theory of Elasticity”:

‘In a theory ideally worked out, the progress which we should be able to trace would be, in other particulars, one from less to more, but we may say that, in regard to the assumed physical principles, progress consists in passing from more to less’.

The modern approach to reduction is an asymptotic one based on a small relative thickness which originates from pioneering work by Goldenveizer (1961), Friedrichs (1955a), Green (1963), and Kolos (1965) mainly in statics.

1.1.1 Mathematical Theories

For several centuries now, philosophers alike have been analysing waves and vibration in continuous structures in order to predict the stresses and displacements which arise as a result of given forces and boundary conditions. Arguably the first philosopher (albeit self-proclaimed), Pythagoras, along with his disciples, made important contributions to various scientific subjects, but it was their investigations into the relationship between mathematics and music that led them to observe the vibrations of strings (around 500BC). They noted that the vibration of a string is influenced by several important parameters, particularly the thickness, length, and tension of the string. This experimental observation paved the way for later researchers to analyse experimental data in order to attempt to describe the physical with the mathematical.

It was not until a thousand years later that the French mathematician and theologian Marin Mersenne, known since as the father of acoustics, influenced

by his teacher René Descartes (who introduced the use of x, y, z as variables), published a book entitled “Marsenne’s Law” in which he is the first to accurately note the relationship between the frequency of the vibration to the length and cross sectional area of a string. Gallileo Gallilei, who was in contact with Marsenne, also made a meaningful contribution to shell theory by making astute observations from experimental data. It was in fact Gallilei himself who, whilst experimenting with pendulums, discovered that given a specific relationship between mass and length of string, the mass itself could swing with harmonic oscillation, or resonance. Later that century in 1678, Robert Hooke proposed his law of elasticity which stated that for relatively small deformations of a body, the deformation is directly proportional to the deforming load, which became a fundamental law in the theory of elasticity for describing stresses and strains. Hooke’s contemporary, Sir Isaac Newton, formulated ‘Newton’s laws of motion’ in 1687, whilst both he and Gottfried Leibniz independently developed infinitesimal (differential) calculus (although Newton’s version, ‘fluxions’, was disregarded after some time). What followed in the period from the late seventeenth century to the late nineteenth century were a series of instrumental discoveries and publications in the field of waves and vibration by notable academics such as Brook Taylor, Leonard Euler, Daniel Bernoulli, Le Rond d’Alembert, Ernst Chladni, Sophie Germaine, Siméon Poisson, Joseph Boussinesq, Gabriel Lamé and many more. In 1850 the German physicist Gustav Kirchhoff formulated his theory of thin elastic plates, which was the first self-contained theory of out-of-plane loaded structures (see Kurrer (2008)) where he gives differential equations for plates. His equations, although similar to those proposed by Poisson, retained Poisson’s ratio as an unknown parameter, whereas Poisson used a value of 0.5. Kirchhoff showed that Poisson’s three boundary conditions for a plate could not be satisfied, and by reducing them to two became the first to formulate consistent boundary conditions. This problem was fully resolved by Friedrichs (1950), and Goldenveizer and Kolos (1965).

Lord Rayleigh in 1885 found that a class of surface waves, which were usually apparent on the interface of two fluids with different densities, could also propagate near the free surface of an infinite homogeneous, isotropic, elastic solid. He showed that these surface waves decay very slowly with distance on the surface,

decay exponentially away from the surface, and occupy a surface layer which is of the same order of thickness as the wavelength. These ‘localised’ surface waves became known as ‘Rayleigh Waves’, and opened the field to various studies of localised phenomena such as earthquakes, crack detection, wave guides etc. For surface waves in pre-stressed elastic materials see Hayes and Rivlin (1961), and Rogerson (1997), and in anisotropic elasticity Stroh (1962), Chadwick and Smith (1977) and many more.

The behaviour of the edge wave in an isotropic plate under plane stress is rather similar to the classical Rayleigh wave in the case of plane stress, for example see appendix in Kaplunov et al. (1999) Recently such edge waves were investigated by Pichugin and Rogerson (2011) for pre-stressed, incompressible plates.

In 1888 Love proposed a theory of shells using the Kirchhoff assumptions that every straight line perpendicular to the mid-surface remain straight after deformation and perpendicular to the mid-surface, all elements of the mid-surface remain unstretched, and the thickness of the plate does not change during deformation. By this examination, Love was able to merge Rayleigh’s earlier works on shell vibration (see Lord Rayleigh (1881)) and produce a set of linear equations of motion and boundary conditions for shells experiencing both infinitesimal extensional and bending strains from three-dimensional elasticity theory. This theory was known as the Kirchhoff-Love theory of shells, a two dimensional first order approximation theory, and at the time was the foremost complete and general linear theory of thin elastic shells. Love’s shell theory and solutions to various shell problems have been improved and justified using asymptotic analysis by Kaplunov et al. (1998), Green (1963), Kolos (1965), Friedrichs (1955a), and others.

Furthermore, it should be mentioned that in 1917, Lamb discovered a guided dispersive wave in an elastic isotropic plate with traction free boundaries, and related them to bulk and Rayleigh waves. As Lamb waves can travel long distances and be guided by structures such as cylindrical pipes and tubes, they are of particular interest to research in non-destructive evaluation methods (see Alleyne and Crawley (1992), and Alleyne and Crawley (1996)).

The load applied to a Kirchhoff plate results in a transverse bending wave on the plate, also known as a *flexural wave*. The equation of motion is obtained

by balancing the bending and rotational moments, and shear forces in the plate in the absence of external loading. However, the equation of motion can also be derived from the above mentioned Kirchhoff-Love equations for a shell as the radius tends to infinity.

The existence of a flexural edge wave guided by the free edge of a semi-infinite, isotropic, elastic thin plate was first predicted in 1960 by Kononkov, but unfortunately due to certain factors his work was also not known to western researchers until much later. Also unbeknown to the west, a paper by Ishlinskii in 1954 formulated an eigenvalue problem using the theory of plate stability which was akin to flexural edge waves. Independently, Sinha (1974), and Thurston and McKenna (1974), derived expressions for the wave speed and dispersion relation. These were summarised by Norris et al. (1998) in their review of flexural edge waves as a response to Kauffmann (1998a) in which he thought he had been the first to discover the bending wave solution for the classical plate equation! (A clear example of how the hindrance of information flow can inhibit research). Many other papers on the subject of edge waves in isotropic and anisotropic plates exist (see Lawrie and Kaplunov (2011) and the references therein), however edge waves are not investigated as popularly as the Rayleigh wave due to their less explicit nature and possibly less practical value. Kononkov named this type of edge wave as a Rayleigh-type Flexural Wave because it has properties analogous to the Rayleigh surface wave on an elastic half-space in that they both decay exponentially away from the area of localisation of the wave, but it should be noted that they are not the same due to the dispersive nature of the flexural edge wave, a point stressed by Kauffmann (1998b) in his response to Norris et al. (1998).

Various refined models of the Kirchhoff-Love theory have been proposed, for example Reissner (1945) and then Mindlin (1951) took into account shear deformations and rotation inertia to calculate the bending vibrations with reference to larger plate thickness. The accuracies of these refined theories can be tested using exact analysis of three dimensional setups and then comparing the exact data to the approximate results. Asymptotic refinement was done by Goldenveizer et al. (1993), and also more recently by Zakharov (2004). S. A. Ambartsumyan (1994) used applied engineering theories for analysing edge waves.

In 1924 Stoneley questioned whether a Rayleigh type surface wave could prop-

agate along the surface of separation, or the interface, of two solids. His motivation was to further the understanding of seismic activity by investigating the behaviour of such waves within the earth's crust and mantle which propagate on the interface of two layers, and decay away from the interface. Such interfacial waves have since become known as Stoneley-waves. The derivation of this interfacial wave found by Stoneley was dependent upon the ratio of densities and elastic constants between the two concerned media to be equal, and was not stated for ranges of parameters. These were later investigated by Sezawa and Kanai (1939) who derived a range of applicability, and for a fluid-solid interface by Scholte (1942), Scholte (1947), and Gogoladse (1948). Research concerning anisotropic and pre-stressed media has been conducted by Stroh (1962), Chadwick and Jarvis (1979a), Barnett et al. (1985), Dowaiikh and Ogden (1991), Chadwick and Borejko (1994), and more. A Stoneley type flexural edge wave has been predicted to propagate at an interface by Silbergleit and Suslova (1983), with research in this area being slightly limited as mentioned earlier, see Baylis (1986) and D.P. Kouzov (1989).

Ever since Gallilei's observations, resonance has been investigated thoroughly for elastic rods, plates and shells. In 1956 Shaw experimented with vibrations on barium titanate disks and observed earlier unknown resonant edge vibrations. These localised resonances had lower cutoff frequencies and were seemingly unassociated with the thickness parameters. Mindlin and Onoe (1957) offered the first explanation of this, followed by further improvement over the years by Torvik (1967) as well as rigorous mathematical justification for zero Poisson ratio ($\nu = 0$) by I. Roitberg and Weidl (1998). The problem of edge resonance in the case of arbitrary ν was recently independently resolved by V. Zernov and Kaplunov (2006) and Pagneux (2011). See also Kaplunov et al. (2004), Zernov and Kaplunov (2008), Krushynska (2011), Lawrie and Kaplunov (2011) and Pagneux (2011). Further information on the dynamics of plates and shells can be found in Le (1999), Kaplunov et al. (1998) and Berdichevskii (1977).

In addition to the two-dimensional studies, localised edge waves have also been studied in the three-dimensional theory. Kaplunov et al. (2004) investigated three dimensional waves localised near the edge of semi-infinite isotropic (and then prestressed isotropic incompressible) plates with traction free edges

and mixed boundary conditions on its faces. For a more general case of three dimensional edge waves in plates see ?.

Edge waves and resonance can be observed not only in flat plates, but also in shells. Edge and interfacial vibrations in longitudinally semi-infinite and infinite non homogeneous elastic shells of revolution, and in particular short-waves, were investigated by Kaplunov and Wilde (2000). The authors reveal the link between localised Rayleigh-type edge waves and Stoneley-type edge waves, and show that long-wave vibrations may exist.

Andrianov (1991) and Andrianov and Awrejcewicz (2004) studied localised edge vibrations and buckling in isotropic and orthotropic cylindrical shells with free boundaries and proposed asymptotic two dimensional expressions.

G.R. Gulgazaryan and Srapionyan (2007), G.R. Gulgazaryan and Saakyan (2008), and G.R. Gulgazaryan and Srapionyan (2012) investigate the existence of localised natural vibrations of an elastic orthotropic thin-walled solid structure composed of identical cylindrical panels which are hinged at their rectilinear edges. They derive asymptotic expressions and eigenfrequencies, and show that under certain conditions are analogous to the Rayleigh type bending and extension of a strip and plate.

The most complete and through analysis of localised edge waves in thin cylindrical shells was presented by Kaplunov et al. (1999) “Free Localized Vibrations of a Semi-Infinite Cylindrical Shell(1999)”. The authors solve the problem of free localised vibrations of an isotropic, homogeneous, longitudinally semi-infinite cylindrical shell. They investigated the conditions and existence of localised and quasi-localised vibration, with complex frequency and a small oscillating part, which propagates on the circumferential edge and decays in the rectilinear direction, with the shell subject to mixed boundary conditions and governed by the Kirchhoff-Love theory of shells. Asymptotic methods from Goldenveizer (1961), Goldenveizer et al. (1979), and Kaplunov et al. (1998) were used. The authors showed that by analysis of the governing system and traction free boundary conditions for cylindrical shells, the reduction produced asymptotic equations analogous to the equations of extensional and flexural edge vibrations of a semi-infinite plate. That is, taking into consideration that shell curvature is small compared

to the wavenumber in the circumferential direction. Although the effect of the curvature is often relatively small, it causes low-level radiation damping of the extensional edge vibration, and so while the natural bending frequencies are real, the extensional ones possess small imaginary parts. Analysis also yielded a third type of vibration, super-low frequency, occurring within the so called semi-membrane shell motion as a result of the coupling between bending and extensional waves. The exact Kirchhoff-Love eigenvalues were compared with three sets of asymptotic ones. Due to the strong influence of curvature on the existence of super-low frequency vibration, there is no flat plate analogue, however it does match the asymptotic behaviour from semi-membrane theory (see Goldenveizer (1961)). It is also important to mention that related work has been carried out for thick shells, for example a numerical investigation of edge resonance in thick pipes was carried out by Ratssepp et al. (2008).

The second paper on this subject by Kaplunov and Wilde (2002) “Free Interfacial Vibrations in Cylindrical Shells (2002)”, extends the problem to free interfacial vibrations of cylindrical shells. The cylindrical shell being longitudinally non-homogeneous, infinite, and composed of two semi-infinite homogeneous shells perfectly bonded to form an interface. Analysis yielded asymptotic solutions analogous to the Stoneley type bending and extensional waves, and super-low frequency vibrations exist provided a combination of material parameters between the two shells are equal.

These assumptions and results are applicable to finite shell models where the length of the shell is much greater than the distance of decay of the vibrations, with the effect of the second boundary at the other edge of a finite shell are negligible on the behaviour of the localised vibration.

This thesis investigates the free vibrations of a thin cylindrical panel, localised near the straight rectilinear edge, propagating along the edge and decaying in the circumferential direction, an analogous problem to that mentioned above. We derive the leading order two dimensional asymptotic expressions by adopting techniques from Kaplunov et al. (1998) and Goldenveizer et al. (1979) for both a semi-infinite homogeneous panel and an infinite non-homogeneous perfectly bonded panel, and highlight that these too become analogues of the Rayleigh and

Stoneley type bending and flexural waves of a plate, and the super-low frequency - of semi-membrane theory. Two eigenvalue problems arise within each problem, one eigenvalue problem deals with solving a system to find the wavenumbers, and the second more difficult eigenvalue problem deals with solving a larger system to find the essential natural frequencies. The eigenvalue problems are solved numerically, and the vibration modes associated with each case of vibration are studied. Furthermore, in the case of localised vibration on a homogeneous panel, free and fixed boundary conditions are imposed at the other edge to make the panel finite, and are taken into account in the numerical computation. The circumferential length is varied to examine the effect of distance and the boundary conditions on the vibration fields. When solving with second boundary conditions the problem becomes more difficult as we will need to find the determinant of an eight by eight matrix system with many parameters. Here specialised computational techniques are used to isolate the modes and solutions. The results from Kaplunov et al. (1999) and Kaplunov and Wilde (2002) are replicated to draw comparisons, and specific analysis is focussed on the effect of curvature and material parameters between the two problems. The former paper is also extended in a similar manner to investigate localised vibration of a homogeneous, longitudinally finite shell. Finally we discuss some preliminary results when adding two additional boundaries to the interfacial problem, thereby creating a circumferentially finite non-homogeneous cylindrical panel.

1.1.2 Framework of the Thesis

This thesis is composed of four chapters. Chapter 1 gives a background to shell theory with an overview of the industrial motivations of studying bending and extensional waves in thin shells. Following this we consider the two dimensional edge vibration of a semi-infinite flat plate, in order to gain a better idea of the limiting problem of a thin shell.

In Chapter 2 we start by considering the two-dimensional equations of Kirchhoff-Love theory of shells, and consider the model of a cylindrical panel which is semi-infinite in the circumferential direction, and infinite in the longitudinal direction. We analyse edge vibration on the straight longitudinal edge, which propagates

on the edge and decays in the circumferential direction. This is a simplified formulation, meaning that we do not take into account the effect of the second longitudinal edge on vibration. Although this is an approximate set up, it does prove to be a good approximation as the circumferential length becomes large, as we will see in Chapter 3 where the second longitudinal edge will be taken into account, and the circumferential length will be finite. The formulation in Chapter 2 will be called ‘Problem 1A’ from here on, and when we refer to the semi-infinite panel we mean semi-infinite in the circumferential direction and infinite in the longitudinal direction. The related problem from Kaplunov et al. (1999) is replicated for comparison, with an extension to a finite shell in Chapter 3. In this paper they consider a closed semi-infinite circular cylindrical shell, which is semi-infinite in its longitudinal direction, and they analyse edge vibration on the circumferential edge, which propagates on the edge and decays in the longitudinal direction. This is a more realistic model when considering structures such as pipes and tubes, where the longitudinal length of the structure can be modelled as very large. This formulation will be called Problem 2A, and the semi-infinite setup here will be used as described.

The governing system describing edge waves is considered within the framework of the Kirchhoff-Love theory, are shown to be analogous to the bending and extensional edge vibration of a semi-infinite flat plate in the short-wave limit, and the super-low frequency vibration has no flat plate analogue. Expressions for the three types of edge eigenmodes are found. Numerical analysis of the exact system follows this with comparison to the asymptotics, the natural frequencies are tabulated and the natural modes are illustrated graphically. The main focus is on the effect of curvature and Poisson’s ratio on the decay of vibration, and how this compares with Problem 2A.

In Chapter 3 we analyse a modified formulation of Problems 1A and 2A, called Problems 1B and 2B. To formulate Problem 1B we extend 1A to take into account the effect of a second longitudinal edge at a finite circumferential distance from the first, and impose traction free and then fixed boundary conditions at that edge. Similarly with Problem 2B, we extend 2A by adding a second circumferential edge at a finite longitudinal distance from the first, and impose traction

free and then fixed boundary conditions at that edge. The exact solutions are numerically computed, along with the asymptotic forms, and results are presented for comparison. Particular attention is paid to the effect of the second edge on the decay of the vibration, the parameters mentioned previously are again varied, but this time also with a change of circumferential length in Problem 1B, and a change of longitudinal length in Problem 2B.

Chapter 4 extends Problems 1A and 2A by considering a simplified formulation of free interfacial vibration occurring at the join, or perfect bond, of two semi-infinite homogeneous cylindrical panels, without taking into account the effects of a second edge. These will be called Problems 1C and 2C. In Problem 1C the vibration propagates on the longitudinal join of the panels, and decays in the positive and negative circumferential directions of both panels. We impose boundary conditions on the longitudinal join to simulate perfect contact between the panels. In Problem 2C the semi-infinite homogeneous panels are perfectly joined at their respective circumferential edges, and vibration propagates on the join and decays in the positive and negative longitudinal directions of both panels. Asymptotic analysis of the interfacial equilibrium system for both problems are compared with the bending and extensional Stoneley type analogues. A similar numerical scheme is applied to the exact governing system as it was before, with mention of the greater variety of problem parameters that need to be considered. Numerical solutions are compared to the asymptotic solutions, and the effects of the curvature is analysed in both problems. This chapter is finalised with concluding remarks about the applicability of asymptotic models and peculiarities of the numerical schemes designed to compute the exact solutions. Further information about consistent higher order asymptotic theories in plates can be found in Goldenveizer et al. (1993) and Kaplunov et al. (1998).

1.2 Preliminaries

This section will give a brief mathematical description of the principles and equations used throughout this thesis. Those describing plate bending and extension are extensively documented in mathematics and engineering. The main equations of motion, boundary conditions, and solutions of the flexural and extensional edge waves on the edge of a semi-infinite, elastic plate, and at the interface of two semi-infinite elastic plates, are derived and shown explicitly in terms of displacements. These will be referred to in later chapters.

1.2.1 Rayleigh-Type Flexural Edge Wave

The Rayleigh-type flexural wave was first discovered by Konenkov in 1960, derivation follows below. Consider an isotropic, elastic, thin semi-infinite plate of thickness $2h$. The plate occupies the region $-\infty < y < \infty$ and $0 \leq x \leq \infty$. For time harmonic vibrations with time dependence $\exp(-i\omega t)$, the two-dimensional classical governing equation of bending of a plate in Cartesian coordinates from the Kirchhoff plate theory is

$$\frac{\partial^4 W}{\partial x^4} + 2\frac{\partial^4 W}{\partial x^2 \partial y^2} + \frac{\partial^4 W}{\partial y^4} = \frac{2\omega^2 \rho h}{D} W. \quad (1.1)$$

Here W is the transverse displacement to the plane, ρ is the density of the material, and D is the flexural rigidity of the plate and is written as

$$D = \frac{2Eh^3}{3(1-\nu^2)}, \quad (1.2)$$

where E is Young's modulus which is a measure of stress to strain, and ν is Poisson's ratio which is a measure of the proportional decrease in lateral measurement to the proportional increase in length.

At the free edge there are three boundary conditions corresponding to no bending and twisting moments, and no verticle shear forces (see Kirchhoff (1850)). Delicate asymptotic analysis by Friedrichs (1955b) showed that the three conditions can be combined to form two. So the homogeneous boundary conditions at $x = 0$ in terms of displacements are

$$\begin{aligned} \frac{\partial^2 W}{\partial x^2} + \nu \frac{\partial^2 W}{\partial y^2} &= 0, \\ \frac{\partial^3 W}{\partial x^3} + (2 - \nu) \frac{\partial^3 W}{\partial x \partial y^2} &= 0. \end{aligned} \quad (1.3)$$

We now introduce non-dimensional coordinates

$$\psi = \frac{x}{l}, \quad \text{and} \quad \xi = \frac{y}{l}, \quad (1.4)$$

and dimensionless parameters

$$\eta = \frac{h}{l}, \quad \text{and} \quad \lambda = \frac{\rho\omega^2 l^2}{E}, \quad (1.5)$$

where l is the typical wavelength, η is the relative half-thickness, and λ is the dimensionless frequency parameter.

for waves that are localised near the boundary at $\psi = 0$, and decay exponentially away from the boundary as $\psi \rightarrow \infty$. These solutions take the form of

$$W = \sum_i w_i e^{i\gamma\xi - m_i\psi}, \quad (1.6)$$

where w_i are constants and $m > 0$.

Substituting this into (1.1) gives

$$m^4 - 2m^2\gamma^2 + \gamma^4 = \frac{3\lambda(1 - \nu^2)}{\eta^2}. \quad (1.7)$$

Solving this yields four roots, two positive and two negative, and so the two possible values for m are

$$m_{1,2} = \sqrt{\gamma^2 \pm \frac{\sqrt{3\lambda(1 - \nu^2)}}{\eta}}. \quad (1.8)$$

The solution can then be rewritten as

$$W = w e^{i\gamma\xi} (e^{-m_1\psi} + C e^{-m_2\psi}), \quad (1.9)$$

where C is a constant to be determined.

Substituting (1.9) into (1.3) at $\psi = 0$ gives

$$\begin{aligned} (m_1^2 - \nu\gamma^2) + C(m_2^2 - \nu\gamma^2) &= 0, \\ m_1[m_1^2 - (2 - \nu)\gamma^2] + C m_2[m_2^2 - (2 - \nu)\gamma^2] &= 0. \end{aligned} \quad (1.10)$$

Rearranging and equating to eliminate C yields the following equation relating γ and λ

$$m_2[(2 - \nu)\gamma^2 - m_2^2](m_1^2 - \nu\gamma^2) = m_1[(2 - \nu)\gamma^2 - m_1^2](m_2^2 - \nu\gamma^2). \quad (1.11)$$

Substituting (1.8) into this gives

$$\begin{aligned} \left(\gamma^2 - \frac{\sqrt{3\lambda(1-\nu^2)}}{\eta^2}\right)^{\frac{1}{2}} \left[(1-\nu)\gamma^2 + \sqrt{\frac{3\lambda(1-\nu^2)}{\eta^2}}\right]^2 = \\ \left(\gamma^2 + \frac{\sqrt{3\lambda(1-\nu^2)}}{\eta^2}\right)^{\frac{1}{2}} \left[(1-\nu)\gamma^2 - \sqrt{\frac{3\lambda(1-\nu^2)}{\eta^2}}\right]^2. \end{aligned} \quad (1.12)$$

For this expression to have roots γ must satisfy the inequality

$$\frac{\sqrt{3\lambda(1-\nu^2)}}{\eta^2} < \gamma^2 < \frac{\sqrt{3\lambda(1+\nu)}}{\eta^2}. \quad (1.13)$$

Solving equation (1.12) gives

$$\lambda = \frac{\eta^2 \gamma^4 \left(3\nu - 1 + 2\sqrt{(1-\nu)^2 + \nu^2}\right)}{3(1+\nu)}, \quad (1.14)$$

which relates the edge wavenumber γ to the dimensionless frequency λ .

1.2.2 Rayleigh-Type Extensional Edge Wave

Consider the plate from the previous subsection, except now it is subject to generalized plane stress, where the normal and shear components of stress perpendicular to the plane are zero. In contrast to the previous subsection, here we are only interested in extensional motions of the surface. From the famous publication by Rayleigh in 1885, the system of equations governing extensional waves in the plate are

$$\frac{\partial^2 U}{\partial x^2} + \left(\frac{1-\nu}{2}\right) \frac{\partial^2 U}{\partial y^2} + \left(\frac{1+\nu}{2}\right) \frac{\partial^2 V}{\partial x \partial y} + (1-\nu^2)\lambda U = 0, \quad (1.15a)$$

$$\left(\frac{1+\nu}{2}\right) \frac{\partial^2 U}{\partial x \partial y} + \left(\frac{1-\nu}{2}\right) \frac{\partial^2 V}{\partial x^2} + \frac{\partial^2 V}{\partial y^2} + (1-\nu^2)\lambda V = 0, \quad (1.15b)$$

where U and V are the tangential displacements of the mid-surface along the x and y , and the dimensionless frequency parameter, λ , is as before.

Boundary conditions at the edge $x = 0$ are written as

$$\frac{\partial U}{\partial x} + \nu \frac{\partial V}{\partial y} = 0, \quad (1.16a)$$

$$\frac{\partial U}{\partial y} + \frac{\partial V}{\partial x} = 0. \quad (1.16b)$$

With the same notation as (1.4) and (1.5), we look for solutions of (1.15) which

satisfy (1.16), for extensional waves that are localised near the boundary at $\psi = 0$ and decay as $\psi \rightarrow \infty$. As such, solutions of the displacements will take the form

$$\begin{pmatrix} U(\psi, \xi) \\ V(\psi, \xi) \end{pmatrix} = \sum_i \begin{pmatrix} u_i \\ v_i \end{pmatrix} e^{i\gamma\xi - m_i\psi}, \quad (1.17)$$

where u_i and v_i are constants. Substituting (1.17) into the governing system (1.15) gives

$$\begin{aligned} u \left[m^2 - \gamma^2 \left(\frac{1-\nu}{2} \right) + (1-\nu^2)\lambda \right] + v \left[-i\gamma m \left(\frac{1+\nu}{2} \right) \right] &= 0, \\ u \left[-i\gamma m \frac{1+\nu}{2} \right] + v \left[m^2 \frac{1-\nu}{2} - \gamma^2(1-\nu^2)\lambda \right] &= 0, \end{aligned} \quad (1.18)$$

yielding the equation

$$\begin{aligned} m^4 \left[\frac{1}{2}(1-\nu) \right] + m^2 \gamma^2 \left[-(1-\nu) + \frac{1}{2}\lambda(3-\nu)(1+\nu) \right] + \\ \gamma^4 \frac{1}{2}(1-\nu) - \gamma^2 \lambda \frac{1}{2}(1-\nu^2)(3-\nu) + \lambda^2(1-\nu)^4 = 0, \end{aligned} \quad (1.19)$$

which solves to give four roots such that the two positive ones are

$$m_1 = \sqrt{\gamma^2 - 2\lambda(1+\nu)} \quad \text{and} \quad m_2 = \sqrt{\gamma^2 - \lambda(1-\nu^2)}. \quad (1.20)$$

We can also find the constants u_i and v_i from (1.18) and re-write the solution as

$$\begin{pmatrix} U(\psi, \xi) \\ V(\psi, \xi) \end{pmatrix} = \sum_{j=1}^2 \begin{pmatrix} u_0 \\ -iu_0 \left(\frac{m_j}{\gamma} \right)^{3-2j} \end{pmatrix} C^{j-1} e^{i\gamma\xi - m_j\psi}, \quad (1.21)$$

Substituting this into the boundary conditions (1.16) and eliminating the constant C gives an equation relating the dimensionless frequency and edge wavelength

$$(\gamma^2 - (1+\nu)\lambda)^2 = \gamma^2 \sqrt{\gamma^2 - 2\lambda(1+\nu)} \sqrt{\gamma^2 - \lambda(1-\nu^2)}. \quad (1.22)$$

For (1.22) to exist and yield a real frequency, and for the roots (1.20) to be real and different, γ and λ should satisfy the inequality

$$0 < 2(1+\nu)\lambda < \gamma^2. \quad (1.23)$$

The relation (1.22) can be re-written in the form of the secular equation for the Rayleigh wave speed

$$\left(2 - \frac{v_r^2}{v_s^2} \right)^2 = 4 \left(1 - \frac{v_r^2}{v_l^2} \right)^{\frac{1}{2}} \left(1 - \frac{v_r^2}{v_s^2} \right)^{\frac{1}{2}}, \quad (1.24)$$

where v_l is the longitudinal wave speed, v_s is the shear wave speed, and v_r is the Rayleigh wave speed. We should note that this is not the typical Rayleigh wave due to plane stress, but is an analogue of the Rayleigh wave counterpart due to plane strain.

1.2.3 Stoneley-Type Flexural Wave

The problem of a wave propagating over the surface of separation of two media was solved first by Stoneley (1924). Analysis yields two analogues in the theory of plates, flexural and extensional, thus the terms Stoneley-type bending and extensional waves arose.

We now detail the problem of a flexural wave localised at the interface of two plates perfectly bonded at their longitudinal edges, propagating on the edge and decaying away. This type of localised wave was first investigated by Silbergleit and Suslova in 1983 who found that the wave behaviour is a flexural analogue to that of the Stoneley-type surface wave at the interface of two semi-infinite media. Consider two isotropic, elastic, thin semi-infinite plates of constant thickness $2h$, perfectly joined to form an infinite non-homogeneous plate. The plates are joined at their respective edges, $x = 0$, and the non-homogeneous plate they form occupies the region $-\infty < y < \infty$ and $-\infty < x < \infty$. The plate occupying $-\infty < x \leq 0$ will be referred to as ‘plate 2’ and related quantities denoted by superscript (2). The plate occupying the region $0 \leq x < \infty$ will be referred to as ‘plate 1’ with related quantities denoted by subscript (1). The equation of motion governing the bending of the mid-surface of both plates is

$$\frac{\partial^4 W^{(k)}}{\partial x^4} + 2\frac{\partial^4 W^{(k)}}{\partial x^2 \partial y^2} + \frac{\partial^4 W^{(k)}}{\partial y^4} = \frac{2(\omega^{(k)})^2 \rho^{(k)} h}{D^{(k)}} W^{(k)}, \quad (1.25)$$

with

$$D^{(k)} = \frac{2E^{(k)}h^3}{3(1 - \nu^{(k)2})}.$$

We use the same notation as in subsection 1.2.1, only here $k = 1, 2$ correspond to the plates 1 and 2.

At the join, $x = 0$, perfect contact boundary conditions between the plates take

the form

$$\begin{aligned}
 W^{(1)} &= W^{(2)}, & \frac{\partial W^{(1)}}{\partial y} &= \frac{\partial W^{(2)}}{\partial y}, \\
 \frac{\eta^2}{3(1-\nu^{(1)^2})E^{(1)}} \left(\frac{\partial^2 W^{(1)}}{\partial x^2} + \nu^{(1)} \frac{\partial^2 W^{(1)}}{\partial y^2} \right) & & & \\
 &= \frac{\eta^2}{3(1-\nu^{(2)^2})E^{(2)}} \left(\frac{\partial^2 W^{(2)}}{\partial x^2} + \nu^{(2)} \frac{\partial^2 W^{(2)}}{\partial y^2} \right), & (1.26) \\
 \frac{\eta^2}{3(1-\nu^{(1)^2})E^{(1)}} \left(\frac{\partial^3 W}{\partial x^3} + (2-\nu^{(1)}) \frac{\partial^3 W}{\partial x \partial y^2} \right) & & & \\
 &= -\frac{\eta^2}{3(1-\nu^{(2)^2})E^{(2)}} \left(\frac{\partial^3 W}{\partial x^3} + (2-\nu^{(2)}) \frac{\partial^3 W}{\partial x \partial y^2} \right).
 \end{aligned}$$

We introduce the same non-dimensional notation as (1.4) and the notation from (1.5) is also used except λ is now

$$\lambda = \frac{\rho^{(1)} \omega^2 R^2}{E^{(1)}}, \quad (1.27)$$

A new parameter q is also introduced

$$q^{(k)} = \frac{E^{(1)} \rho^{(k)}}{E^{(k)} \rho^{(1)}}. \quad (1.28)$$

So that $\lambda q^{(k)}$ is consistent for both plates.

We seek solutions of (1.25) in the form

$$W^{(k)} = \sum_i w_i^{(k)} e^{i\gamma\xi + (-1)^k m_i^{(k)} \psi}, \quad (1.29)$$

where $w_i^{(k)}$ are constants and the $(-1)^k$ term ensures that $(-1)^k m_i^{(k)}$ is negative for $m^{(k)} > 0$ when $k = 1$, and positive when $k = 2$.

Substituting a factor of (1.29)

$$W^{(k)} = w^{(k)} e^{i\gamma\xi + (-1)^k m^{(k)} \psi}, \quad (1.30)$$

into (1.25) gives

$$(m^{(k)})^4 - 2(m^{(k)})^2 \gamma^2 + \gamma^4 = \frac{3\lambda q^{(k)} (1 - \nu^{(k)^2})}{\eta^2}. \quad (1.31)$$

We obtain the roots of this equation in the same manner as in Subsection 1.2.1 and write them as

$$m_{1,2}^{(k)} = \sqrt{\gamma^2 \pm \frac{\sqrt{3\lambda q^{(k)} (1 - \nu^{(k)^2})}}{\eta}}. \quad (1.32)$$

We can now write (1.29) with summation from $i = 1, 2$

$$W^{(k)} = \sum_{i=1}^2 w_i^{(k)} e^{i\gamma\xi + m_i^{(k)}(-1)^k}. \quad (1.33)$$

Substituting this into (1.26) gives the system of equations

$$w_1^{(1)} + w_2^{(1)} = w_1^{(2)} + w_2^{(2)}, \quad (1.34a)$$

$$w_1^{(1)} m_1^{(1)} + w_2^{(1)} m_2^{(1)} = -w_1^{(2)} m_1^{(2)} - w_2^{(2)} m_2^{(2)}, \quad (1.34b)$$

$$w_1^{(1)} \hat{\alpha}_1^{(1)} + w_2^{(1)} \hat{\alpha}_2^{(1)} = w_1^{(2)} \hat{\alpha}_1^{(2)} + w_2^{(2)} \hat{\alpha}_2^{(2)}, \quad (1.34c)$$

$$w_1^{(1)} \hat{\beta}_1^{(1)} + w_2^{(1)} \hat{\beta}_2^{(1)} = -w_1^{(2)} \hat{\beta}_1^{(2)} - w_2^{(2)} \hat{\beta}_2^{(2)} \quad (1.34d)$$

with

$$\hat{\alpha}_i^{(k)} = \frac{m_i^{(k)^2} - \nu^{(k)}\gamma^2}{(1 - \nu^{(k)^2})\hat{E}^{(k)}}, \quad \text{and} \quad \hat{\beta}_i^{(k)} = \frac{m_i^{(k)}(m_i^{(k)^2} - (2 - \nu^{(k)})\gamma^2)}{(1 - \nu^{(k)^2})\hat{E}^{(k)}}, \quad (1.35)$$

where $\hat{E}^{(k)} = \frac{E^{(1)}}{E^{(k)}}$, and we use the ‘hat’ to distinguish from notation that is used in Chapter 2.

The system of equations (1.34) can be written as

$$M_1 \cdot \bar{w} = 0, \quad (1.36)$$

where M_1 is the matrix

$$M_1 = \begin{bmatrix} 1 & 1 & -1 & -1 \\ m_1^{(1)} & m_2^{(1)} & m_1^{(2)} & m_2^{(2)} \\ \hat{\alpha}_1^{(1)} & \hat{\alpha}_2^{(1)} & -\hat{\alpha}_1^{(2)} & -\hat{\alpha}_2^{(2)} \\ \hat{\beta}_1^{(1)} & \hat{\beta}_2^{(1)} & \hat{\beta}_1^{(2)} & \hat{\beta}_2^{(2)} \end{bmatrix}, \quad (1.37)$$

and \bar{w} is the vector

$$\bar{w} = \begin{bmatrix} w_1^{(1)} \\ w_2^{(1)} \\ w_1^{(2)} \\ w_2^{(2)} \end{bmatrix} = 0. \quad (1.38)$$

The equation

$$\det M_1 = 0, \quad (1.39)$$

is an expression relating the dimensionless frequency λ to the wavenumber γ . Solving for λ and substituting into (1.37) allows us to find the constants $w_i^{(k)}$ and hence the natural form (1.33).

1.2.4 Stoneley-Type Extensional Wave

We examine here the extensional analogue of the Stoneley-type wave propagating over the surface relating to plane stress. Consider the two isotropic plates configured as in subsection 1.2.3. We are only interested in extensional motions of the mid-surface of the plate. The equations of motion governing extensional waves in the plate are

$$\frac{\partial^2 U^{(k)}}{\partial x^2} + \left(\frac{1 - \nu^{(k)}}{2} \right) \frac{\partial^2 U^{(k)}}{\partial y^2} + \left(\frac{1 + \nu^{(k)}}{2} \right) \frac{\partial^2 V^{(k)}}{\partial x \partial y} + (1 - \nu^{(k)^2}) \lambda q^{(k)} U^{(k)} = 0, \quad (1.40a)$$

$$\left(\frac{1 + \nu^{(k)}}{2} \right) \frac{\partial^2 U^{(k)}}{\partial x \partial y} + \left(\frac{1 - \nu^{(k)}}{2} \right) \frac{\partial^2 V^{(k)}}{\partial x^2} + \frac{\partial^2 V^{(k)}}{\partial y^2} + (1 - \nu^{(k)^2}) \lambda q^{(k)} V^{(k)} = 0. \quad (1.40b)$$

The continuity conditions for perfect contact at the joined edge $x = 0$ are

$$\begin{aligned} U^{(1)} &= U^{(2)}, \\ V^{(1)} &= V^{(2)}, \\ \frac{\partial U^{(1)}}{\partial x} + \nu^{(1)} \frac{\partial V^{(1)}}{\partial y} &= \frac{\partial U^{(2)}}{\partial x} + \nu^{(2)} \frac{\partial V^{(2)}}{\partial y}, \\ \frac{\partial U^{(1)}}{\partial y} + \frac{\partial V^{(1)}}{\partial x} &= \frac{\partial U^{(2)}}{\partial y} + \frac{\partial V^{(2)}}{\partial x}. \end{aligned} \quad (1.41)$$

The same notation shall be applied as in (1.4) to scale the coordinates, and we use the notation for λ and introduce the parameter $q^{(k)}$ from (1.27) and (1.28).

A possible solution to (1.40) can be written as

$$\begin{pmatrix} U^{(k)}(\psi, \xi) \\ V^{(k)}(\psi, \xi) \end{pmatrix} = \sum_i \begin{pmatrix} u_i^{(k)} \\ v_i^{(k)} \end{pmatrix} e^{i\gamma\xi + (-1)^k m_i^{(k)} \psi}. \quad (1.42)$$

Substituting a factor of this into the governing system (1.40) yields

$$\begin{aligned} u^{(k)} \left[m^{(k)^2} - \gamma^2 \left(\frac{1 - \nu^{(k)}}{2} \right) + (1 - \nu^{(k)^2}) \lambda q^{(k)} \right] + v^{(k)} \left[-i\gamma m^{(k)} \left(\frac{1 + \nu^{(k)}}{2} \right) \right] &= 0, \\ u^{(k)} \left[-i\gamma m^{(k)} \frac{1 + \nu^{(k)}}{2} \right] + v^{(k)} \left[m^{(k)^2} \frac{1 - \nu^{(k)}}{2} - \gamma^2 (1 - \nu^{(k)^2}) \lambda q^{(k)} \right] &= 0. \end{aligned} \quad (1.43)$$

we can obtain the characteristic equation

$$\begin{aligned} m^{(k)^4} \left[\frac{1}{2} (1 - \nu^{(k)}) \right] + m^{(k)^2} \gamma^2 \left[-(1 - \nu^{(k)}) + \frac{1}{2} \lambda q^{(k)} (3 - \nu^{(k)}) (1 + \nu^{(k)}) \right] + \\ \gamma^4 \frac{1}{2} (1 - \nu^{(k)}) - \gamma^2 \lambda q^{(k)} \frac{1}{2} (1 - \nu^{(k)^2}) (3 - \nu^{(k)}) + \lambda^2 q^{(k)^2} (1 - \nu)^4 = 0, \end{aligned} \quad (1.44)$$

giving the four roots

$$m_1^{(k)} = \sqrt{\gamma^2 - 2\lambda q^{(k)}(1 + \nu^{(k)})} \quad \text{and} \quad m_2^{(k)} = \sqrt{\gamma^2 - \lambda q^{(k)}(1 - \nu^{(k)})^2}. \quad (1.45)$$

Substituting these roots into (1.43) we can find the constants u_i and v_i and rewrite the solution as

$$\begin{pmatrix} U^{(k)}(\psi, \xi) \\ V^{(k)}(\psi, \xi) \end{pmatrix} = \sum_{j=1}^2 \begin{pmatrix} u_0^{(k)} \\ iu_0^{(k)} \left(\frac{(-1)^k m_j^{(k)}}{\gamma} \right)^{3-2j} \end{pmatrix} C_j^{(k)} e^{i\gamma\xi + (-1)^k m_j^{(k)}\psi}, \quad \text{with } k = 1, 2. \quad (1.46)$$

Substituting (1.46) into conditions (1.41) gives

$$\begin{aligned} C_1^{(1)} + C_2^{(1)} &= C_1^{(2)} + C_2^{(2)}, \\ -m_1^{(1)}C_1^{(1)} - \frac{\gamma^2}{m_2^{(1)}}C_2^{(1)} &= m_1^{(2)}C_1^{(2)} + \frac{\gamma^2}{m_2^{(2)}}C_2^{(2)}, \\ -m_1^{(1)}C_1^{(1)} - m_2^{(1)}C_2^{(1)} + \nu^{(1)}\gamma m_1^{(1)}C_1^{(1)} + \nu^{(1)}\frac{\gamma^2}{m_2^{(1)}}C_2^{(1)} &= \\ m_1^{(2)}C_1^{(2)} + m_2^{(2)}C_2^{(2)} - \nu^{(2)}\gamma m_1^{(2)}C_1^{(2)} - \nu^{(2)}\frac{\gamma^2}{m_2^{(2)}}C_2^{(2)}, \\ C_1^{(1)} + C_2^{(1)} + \frac{m_1^{(1)2}}{\gamma^2}C_1^{(1)} + C_2^{(1)} &= C_1^{(2)} + C_2^{(2)} + \frac{m_1^{(2)2}}{\gamma^2}C_1^{(2)} + C_2^{(2)}. \end{aligned} \quad (1.47)$$

The system above can be written as

$$M_2 \cdot \bar{C} = 0, \quad (1.48)$$

where

$$M_2 = \begin{bmatrix} 1 & 1 & -1 & -1 \\ m_1^{(1)} & \frac{\gamma^2}{m_2^{(1)}} & m_1^{(2)} & \frac{\gamma^2}{m_2^{(2)}} \\ m_1^{(1)}(\gamma\nu^{(1)} - 1) & m_2^{(1)}\left(\frac{\gamma^2\nu^{(1)}}{m_2^{(1)}} - 1\right) & m_1^{(2)}(\gamma\nu^{(2)} - 1) & m_2^{(2)}\left(\frac{\gamma^2\nu^{(2)}}{m_2^{(2)}} - 1\right) \\ 1 + \frac{m_1^{(1)2}}{\gamma^2} & 2 & -1 - \frac{m_1^{(2)2}}{\gamma^2} & -2 \end{bmatrix}, \quad (1.49)$$

and

$$\bar{C} = [C_1^{(1)}, C_2^{(1)}, C_1^{(2)}, C_2^{(2)}]'. \quad (1.50)$$

Then the equation

$$\det M_2 = 0, \quad (1.51)$$

gives the relationship between dimensionless frequency λ and wavelength γ . Substituting these values into (1.48) to find the constants $C_i^{(k)}$ allow us to find the natural form (1.46).

Chapter 2

Vibration of a Thin Semi-Infinite Cylindrical Shell

2.1 Statement of the Problem

Let an orthogonal curvilinear coordinate system be defined as (α, β) , where α and β are the two coordinates on the surface Γ . With reference to Γ , the fundamental form of the infinitesimal distance ds is

$$(ds)^2 = A^2(d\alpha)^2 + B^2(d\beta)^2, \quad (2.1)$$

where A and B are the Lamé parameters.

Now let Γ be the mid-surface of a circular cylindrical shell with radius R of the mid-surface. The curvilinear longitudinal coordinate is y , and the angular coordinate is ψ . Then $A = 1$ and $B = R$ and (2.1) becomes

$$(ds)^2 = (dy)^2 + R^2(d\psi)^2. \quad (2.2)$$

2.1.1 Problem 1A

Consider free harmonic vibrations of a homogeneous, isotropic, circular cylindrical panel assumed to be semi-infinite in the circumferential direction i.e, there is only one edge at $\psi = 0$ and no second edge, and the mid-surface Γ occupies the domain $0 \leq \psi < \infty$ and $-\infty < \xi < \infty$. The waves are localized near the longitudinal edge of the panel at $\psi = 0$, propagate on the longitudinal edge and decay in the circumferential direction.

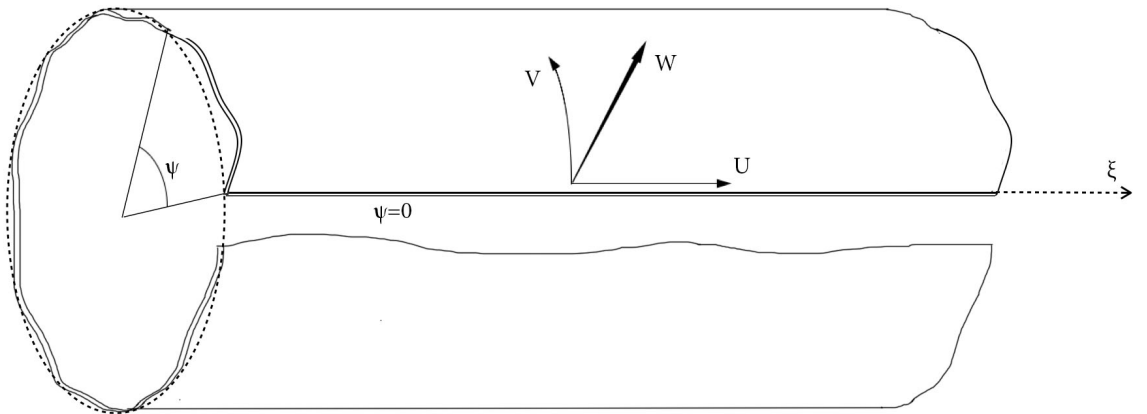


Figure 2.1: Panel configuration for problem 1A

Together with the coordinates ψ and y , the non-dimensional coordinate ξ is introduced as

$$\xi = \frac{y}{R} . \quad (2.3)$$

This is a simplified formulation in which the effect of a second longitudinal edge on vibration is not taken into account, and so although the set up is approximate in that the panel is semi-infinite circumferentially, it does become a good approximation as the circumferential length becomes large and vibrations are localised at $\psi = 0$. This assumption will be justified in chapter 3 where the panel will be considered to be finite in its circumferential length and the effect of a second longitudinal edge, at some finite distance from the first edge, will be taken into account.

The formulation outlined above for chapter 2 will be called Problem 1A from here on.

2.1.2 Problem 2A

The related problem in Kaplunov et al. (1999) is reproduced for comparison. The authors considered free harmonic vibration of a homogeneous, isotropic cylindrical shell, assumed to be semi-infinite in its longitudinal direction with only one edge at $\xi = 0$. The mid-surface Γ of the shell occupies the domains $0 \leq \psi < 2\pi$ and $0 \leq \xi < \infty$, and the waves are localised near the circumferential edge $\xi = 0$, propagating on the circumferential edge and decaying in the longitudinal direction.

Similarly to Problem 1A, this set up will be modified is also a simplified for-

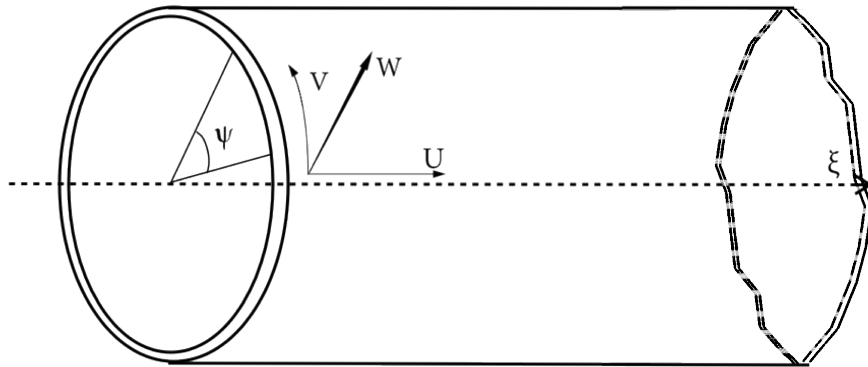


Figure 2.2: Panel configuration for problem 2A

mulation which will be verified in chapter 3 upon the introduction of a second circumferential edge at a finite distance from the first. This formulation will be called Problem 2A from here on.

2.1.3 Equations of Motion

The governing equations from the Kirchhoff-Love theory of shells (Love (1988)), expressed in terms of displacements as a system of three partial differential equations are

$$\frac{\partial^2 U}{\partial \xi^2} + \left(\frac{1-\nu}{2}\right) \frac{\partial^2 U}{\partial \psi^2} + \left(\frac{1+\nu}{2}\right) \frac{\partial^2 V}{\partial \psi \partial \xi} - \nu \frac{\partial W}{\partial \xi} + \lambda(1-\nu^2)U = 0, \quad (2.4a)$$

$$\begin{aligned} \frac{\partial^2 V}{\partial \psi^2} + \left(\frac{1-\nu}{2}\right) \frac{\partial^2 V}{\partial \xi^2} + \left(\frac{1+\nu}{2}\right) \frac{\partial^2 U}{\partial \xi \partial \psi} - \frac{\partial W}{\partial \psi} \\ + \frac{\eta^2}{3} \left[2(1-\nu) \frac{\partial^2 V}{\partial \xi^2} + \frac{\partial^2 V}{\partial \psi^2} + \frac{\partial^3 W}{\partial \psi^3} + (2-\nu) \frac{\partial^3 W}{\partial \xi^2 \partial \psi} \right] + \lambda(1-\nu^2)V = 0, \end{aligned} \quad (2.4b)$$

$$\begin{aligned} \nu \frac{\partial U}{\partial \xi} + \frac{\partial V}{\partial \psi} - W - \frac{\eta^2}{3} \left[\frac{\partial^4 W}{\partial \xi^4} + 2 \frac{\partial^4 W}{\partial \xi^2 \partial \psi^2} + \frac{\partial^4 W}{\partial \psi^4} + \frac{\partial^3 V}{\partial \psi^3} + (2-\nu) \frac{\partial^3 V}{\partial \xi^2 \partial \psi} \right] \\ + \lambda(1-\nu^2)W = 0. \end{aligned} \quad (2.4c)$$

Here λ is the non-dimensional frequency parameter written as

$$\lambda = \frac{\rho \omega^2 R^2}{E}, \quad (2.5)$$

and η is the small geometrical parameter traditional in the theory of thin shells, written as

$$\eta = \frac{h}{R}. \quad (2.6)$$

ω is the circular frequency, ρ is the mass density, E is Young's modulus, h is the half-thickness, and ν is Poisson's ratio.

The tangential displacements of the mid-surface will be denoted as U and V , while the transverse displacement which is normal to the mid-surface will be denoted as W . Equations (2.4a) and (2.4b) are the longitudinal and shear forces, which are in essence analogues of the boundary conditions for a plate. Equation (2.4c) describes the tangential shear force and bending moment.

2.1.4 Traction-Free Boundary Conditions

Problem 1A

At $\psi = 0$, traction free boundary conditions at the longitudinal edge corresponding to the longitudinal force, longitudinal shear force, bending moment,

and modified transverse shear force, take the form

$$\nu \frac{\partial U}{\partial \xi} + \frac{\partial V}{\partial \psi} - W = 0, \quad (2.7a)$$

$$\frac{\partial U}{\partial \psi} + \frac{\partial V}{\partial \xi} = 0, \quad (2.7b)$$

$$\frac{\partial V}{\partial \psi} + \frac{\partial^2 W}{\partial \psi^2} + \nu \frac{\partial^2 W}{\partial \xi^2} = 0, \quad (2.7c)$$

$$\frac{\partial^2 V}{\partial \psi^2} + 2(1 - \nu) \frac{\partial^2 V}{\partial \xi^2} + \frac{\partial^3 W}{\partial \psi^3} + (2 - \nu) \frac{\partial^3 W}{\partial \psi \partial \xi^2} = 0. \quad (2.7d)$$

Problem 2A

At $\xi = 0$ the traction free boundary conditions at the circumferential edge similarly to before are,

$$\nu \frac{\partial V}{\partial \psi} - \nu W + \frac{\partial U}{\partial \xi} = 0, \quad (2.8a)$$

$$\frac{\partial U}{\partial \psi} + \frac{\partial V}{\partial \xi} + \frac{4}{3}\eta^2 \left[\frac{\partial V}{\partial \xi} + \frac{\partial^2 W}{\partial \psi \partial \xi} \right] = 0, \quad (2.8b)$$

$$\nu \frac{\partial V}{\partial \psi} + \frac{\partial^2 W}{\partial \xi^2} + \nu \frac{\partial^2 W}{\partial \psi^2} = 0, \quad (2.8c)$$

$$\frac{\partial^3 W}{\partial \xi^3} + (2 - \nu) \frac{\partial^3 W}{\partial \psi^2 \partial \xi} + (2 - \nu) \frac{\partial^2 V}{\partial \psi \partial \xi} = 0. \quad (2.8d)$$

2.2 Exact Solution

2.2.1 Problem 1A

For Problem 1A, a solution of the governing system (2.4) can be written in the form

$$\begin{pmatrix} U(\psi, \xi) \\ V(\psi, \xi) \\ W(\psi, \xi) \end{pmatrix} = \sum_i \begin{pmatrix} u_i \\ v_i \\ w_i \end{pmatrix} e^{i\gamma\xi - m_i\psi} \quad (2.9)$$

where u_i , v_i and w_i are constants, γ is the real positive longitudinal wavenumber, and m should be chosen such that

$$\Re(m_i) > 0, \quad \text{or if } \Re(m_i) = 0 \quad \text{then } \Im(m_i) > 0, \quad (2.10)$$

where the root decays to infinity in the circumferential direction or satisfies the radiation condition (see Sommerfeld (1912)). Substituting a factor of (2.9)

$$\begin{pmatrix} U(\psi, \xi) \\ V(\psi, \xi) \\ W(\psi, \xi) \end{pmatrix} = \begin{pmatrix} u \\ v \\ w \end{pmatrix} e^{i\gamma\xi - m\psi} \quad (2.11)$$

into the governing equations (2.4) results in a linear homogeneous system of three equations with constant coefficients

$$u \left[m^2 \left(\frac{1-\nu}{2} \right) + \lambda(1-\nu^2) - \gamma^2 \right] + v \left[im\gamma \left(\frac{1+\nu}{2} \right) \right] + w[i\gamma\nu] = 0, \quad (2.12a)$$

$$u \left[im\gamma \left(\frac{1+\nu}{2} \right) \right] + v \left[m^2 \left(\frac{\eta^2}{3} + 1 \right) + \lambda(1-\nu^2) - \gamma^2 \left(\frac{1-\nu}{2} - \frac{2\eta^2}{3}(1-\nu) \right) \right] + w \left[m^3 \left(-\frac{\eta^2}{3} \right) + m \left(1 + \gamma^2 \frac{\eta^2}{3} (2-\nu) \right) \right] = 0, \quad (2.12b)$$

$$u[-i\gamma\nu] + v \left[m^3 \left(\frac{\eta^2}{3} \right) - m \left(1 + \gamma^2 \frac{\eta^2}{3} (2-\nu) \right) \right] + w \left[m^4 \left(-\frac{\eta^2}{3} \right) + m^2 \left(\gamma^2 \frac{2\eta^2}{3} \right) + \lambda(1-\nu^2) - \frac{\gamma^4 \eta^2}{3} - 1 \right] = 0. \quad (2.12c)$$

This system can be written in a matrix form as

$$M_{1A} \cdot X = 0, \quad (2.13)$$

where

$$M_{1A} = \begin{bmatrix} m^2 \tilde{a} + \tilde{b} & m\tilde{c} & -\tilde{d} \\ m\tilde{c} & m^2 \tilde{f} + \tilde{r} & -m^3 \tilde{h} + m\tilde{p} \\ \tilde{d} & -m^3 \tilde{h} + m\tilde{p} & -m^4 \tilde{h} + m^2 \tilde{q} + \tilde{s} \end{bmatrix}, \quad (2.14)$$

$$X = \begin{bmatrix} u \\ v \\ w \end{bmatrix}, \quad (2.15)$$

and

$$\begin{aligned}
 \tilde{a} &= \frac{1}{2}(1 - \nu), \quad \tilde{b} = \lambda(1 - \nu^2) - \gamma^2, \quad \tilde{c} = \frac{1}{2}\gamma(1 + \nu)i, \\
 \tilde{d} &= \gamma\nu i, \quad \tilde{f} = \frac{1}{3}\eta^2 + 1, \quad \tilde{h} = \frac{1}{3}\eta^2, \\
 \tilde{p} &= 1 + \frac{1}{3}\gamma^2\eta^2(2 - \nu), \quad \tilde{q} = \frac{2}{3}\gamma^2\eta^2, \\
 \tilde{r} &= \lambda(1 - \nu^2) - \frac{1}{2}\gamma^2(1 - \nu) - \frac{1}{3}\eta^2\gamma^2(2 - 2\nu), \\
 \tilde{s} &= \lambda(1 - \nu^2) - 1 - \frac{1}{3}\gamma^4\eta^2.
 \end{aligned}$$

The tilde terms are used to only present the problem in a simpler form and do not bring any extra physical meaning.

The system of equations (2.12) corresponds to an eigenvalue problem for m , however the final, more difficult, eigenvalue problem for λ results from solving the required boundary conditions.

Equating the determinant of matrix M_{1A} in (2.13) to zero gives an algebraic equation in m corresponding to the characteristic equation

$$\begin{aligned}
 \det|M_{1A}| &= m^8(ah^2 + afh) + m^6(h(bh - 2ap + c^2 - bf - ar) + afq) \\
 &\quad + m^4(2cdh - 2bhp + afs + arq + bfq - brh + ap^2 - c^2q) \\
 &\quad + m^2(brq + bfs + ars - 2cdp + bp^2 + d^2f - c^2s) \\
 &\quad + brs + d^2r = 0,
 \end{aligned} \tag{2.16}$$

which can be written more simply as

$$a_8m^8 + a_6m^6 + a_4m^4 + a_2m^2 + a_0 = 0, \tag{2.17}$$

where a_8 to a_0 are

$$a_8 = \eta^2, \quad a_6 = \eta^2[\lambda(1 + \nu)(3 - \nu) - 4\gamma^2 + 2],$$

$$a_4 = 2\lambda^2\eta^2(1 - \nu^2)(1 + \nu) + \lambda(1 + \nu)[-3\gamma^2\eta^2(2 - \nu) +$$

$$\eta^2(3 + \nu) - 3(1 - \nu)] - \frac{\eta^4\gamma^4}{3}(1 - \nu^2) + 6\gamma^4\eta^2 - 8\gamma^2\eta^2 + \eta^2$$

$$a_2 = -\lambda^2(1 - \nu^2)(1 + \nu)(\eta^2(4\gamma^2 + 2) + 3(3 - \nu)) - \lambda\frac{(1 + \nu)}{3}(-2\eta^4\gamma^4(1 - \nu^2) +$$

$$\eta^2(-9\gamma^4(3 - \nu) + 6\gamma^2(2 - \nu) - 6) - 18\gamma^2(1 - \nu) - 9(1 - \nu)) - \frac{4}{3}\gamma^6\eta^4 -$$

$$2\gamma^4\eta^2(3\gamma^2 - (6 - \nu^2)) - 4\gamma^2\eta^2$$

$$a_0 = -6\lambda^3(1 - \nu^2)^2(1 + \nu) + \lambda^2(1 - \nu^2)(1 + \nu)(2\gamma^4\eta^2 + 4\gamma^2\eta^2(1 - \nu) - 3\gamma^2(3 - \nu) + 6)$$

$$+ \lambda\left[\frac{1}{3}(1 + \nu)\gamma^6\eta^2(-4\eta^2(1 - \nu) - 3(3 - \nu)) - \gamma^4(1 - \nu^2)(4\eta^2 + 3) -$$

$$\gamma^2(1 - \nu^2)(4\eta^2 + 3(3 + 2\nu))\right]$$

The characteristic equation (2.17) has three parameters γ , η , and λ , assuming that ν is a constant. The natural forms of (2.4) cannot be explicitly written due to the very complicated nature of the characteristic equation above.

Solving (2.17) yields eight roots of m . The four roots chosen using (2.10) are substituted into (2.13) to find the constants u , v , and w .

A solution to (2.12) can then be written as

$$\begin{pmatrix} U(\psi, \xi) \\ V(\psi, \xi) \\ W(\psi, \xi) \end{pmatrix} = \sum_{i=1}^4 C_i \begin{pmatrix} u_i \\ v_i \\ w_i \end{pmatrix} e^{i\gamma\xi - m_i\psi}, \quad (2.18)$$

where C_i are arbitrary constants to be found by using the boundary conditions (2.7). Substituting (2.18) into (2.7) gives,

$$b_{ij}^{(1A)} C_j = 0, \quad \text{for } i, j = 1..4, \quad (2.19)$$

where

$$b_{1j}^{(1A)} = u_j(\nu\gamma i) - v_j m_j - w_j, \quad (2.20a)$$

$$b_{2j}^{(1A)} = -u_j m_j + v_j \gamma i, \quad (2.20b)$$

$$b_{3j}^{(1A)} = -v_j m_j + w_j(m_j^2 - \nu\gamma^2), \quad (2.20c)$$

$$b_{4j}^{(1A)} = v_j [m_j^2 - 2(1 - \nu)\gamma^2] + w_j [(2 - \nu)m_j\gamma^2 - m_j^3], \quad (2.20d)$$

The equation

$$\det b_{ij}^{(1A)} = 0, \quad (2.21)$$

will result in the sought for eigenvalue problem for the edge wave frequency. This is the essence of problem 1A and cannot be solved without using numerics. The characteristic equation (2.17) should first be solved numerically to find the four roots m_i satisfying (2.10). These are substituted back into the matrix (2.13) to find the vector X_i for each root. The non-dimensional frequency λ can be solved for which in turn allows the natural forms to be found using these values.

2.2.2 Problem 2A

For the problem of vibration propagating on the circumferential edge and decaying longitudinally, a solution to the equations of motion (2.4) can be written as

$$\begin{pmatrix} U(\psi, \xi) \\ V(\psi, \xi) \\ W(\psi, \xi) \end{pmatrix} = \sum_i \begin{pmatrix} u_i \\ v_i \\ w_i \end{pmatrix} \begin{pmatrix} \sin n\psi \\ \cos n\psi \\ \sin n\psi \end{pmatrix} e^{-r_i \xi}. \quad (2.22)$$

where u_i , v_i and w_i are constants, n is the real positive circumferential wavenumber, and r is chosen using

$$\Re(r_i) > 0, \quad \text{or if } \Re(r_i) = 0 \quad \text{then } \Im(r_i) > 0, \quad (2.23)$$

to satisfy the decay to infinity of the vibration in the longitudinal direction, or the radiation condition.

Substituting a factor of (2.22)

$$\begin{pmatrix} U(\psi, \xi) \\ V(\psi, \xi) \\ W(\psi, \xi) \end{pmatrix} = \begin{pmatrix} u \\ v \\ w \end{pmatrix} \begin{pmatrix} \sin n\psi \\ \cos n\psi \\ \sin n\psi \end{pmatrix} e^{-r\xi}, \quad (2.24)$$

into the equations of motion (2.4) gives

$$u \left[r^2 - \frac{1-\nu}{2} n^2 + \lambda(1-\nu^2) \right] + v \left[-\frac{1+\nu}{2} r n \right] + w [-\nu r] = 0, \quad (2.25)$$

$$u \left[\frac{1+\nu}{2} r n \right] + v \left[\frac{1-\nu}{2} r^2 - n^2 + \frac{\eta^2}{3} (2(1-\nu)r^2 - n^2) + (1-\nu^2)\lambda \right] + w \left[\frac{\eta^2}{3} n((2-\nu)r^2 - n^2) - n \right] = 0, \quad (2.26)$$

$$u [-\nu r] + v \left[n - \frac{\eta^2}{3} n((2-\nu)r^2 - n^2) \right] + w \left[1 + \frac{\eta^2}{3} (r^4 - 2n^2 r^2 + n^4) - (1-\nu^2)\lambda \right] = 0. \quad (2.27)$$

The system (2.27) can be written in matrix form as

$$M_{2A} \cdot X = 0, \quad (2.28)$$

where

$$M_{2A} = \begin{bmatrix} r^2 + \hat{b} & -r\hat{c} & -r\hat{d} \\ r\hat{c} & r^2\hat{f} + \hat{r} & r^2\hat{h} - \hat{p} \\ -r\hat{d} & -r^2\hat{h} + \hat{p} & r^4\hat{t} - r^2\hat{q} + \hat{s} \end{bmatrix}, \quad (2.29)$$

and

$$\begin{aligned} \hat{b} &= \lambda(1-\nu^2) - \frac{1-\nu}{2} n^2, & \hat{c} &= \frac{1}{2} n(1+\nu), \\ \hat{d} &= \nu r, & \hat{f} &= \frac{1-\nu}{2} + \frac{2}{3} (1-\nu)\eta^2, & \hat{h} &= \frac{1}{3} (2-\nu)\eta^2 n, \\ \hat{p} &= n \left(\frac{1}{2} \eta^2 n^2 + 1 \right), & \hat{q} &= \frac{2}{3} \gamma^2 \eta^2, \\ \hat{r} &= \lambda(1-\nu^2) - \gamma^2 \left(1 + \frac{1}{2} \eta^2 \right), \\ \hat{s} &= 1 - \lambda(1-\nu^2) + \frac{1}{3} \eta^2 n^4, & \hat{t} &= \frac{1}{3} \eta^2. \end{aligned}$$

The hat terms are only used to present the problem in a simpler form. Similarly to Problem 1A, the system of equations (2.27) corresponds to an eigenvalue problem for r , where the more complicated eigenvalue problem for λ will be formed using the boundary conditions. Equating the determinant of matrix M_{2A} in (2.28) to zero gives

$$\begin{aligned} \det M_{2A} &= r^8 (\hat{f}\hat{t}) + r^6 (\hat{c}^2\hat{t} + \hat{b}\hat{f}\hat{t} - \hat{f}\hat{q} + \hat{r}\hat{t} + \hat{h}^2) \\ &+ r^4 (\hat{b}\hat{h}^2 + \hat{b}\hat{r}\hat{t} + 2\hat{c}\hat{d}\hat{h} + \hat{f}\hat{s} - 2\hat{h}\hat{p} - \hat{b}\hat{f}\hat{q} - \hat{d}^2\hat{f} - \hat{r}\hat{q} - \hat{c}^2\hat{q}) \\ &+ r^2 (\hat{p}^2 + \hat{b}\hat{f}\hat{s} + \hat{c}^2\hat{s} + \hat{r}\hat{s} - 2\hat{b}\hat{h}\hat{p} - \hat{d}^2\hat{r} - 2\hat{c}\hat{d}\hat{p} - \hat{b}\hat{r}\hat{q}) + \hat{p}^2\hat{b} + \hat{b}\hat{r}\hat{s} = 0, \end{aligned} \quad (2.30)$$

which can be written in a simpler notation as

$$b_8 r^8 + b_6 r^6 + b_4 r^4 + b_2 r^2 + b_0 = 0, \quad (2.31)$$

where b_8 to b_0 are given in the paper Kaplunov et al. (1999).

Characteristic equation (2.31) is dependent upon three parameters, n , η , and λ , assuming ν is a constant. Similarly to problem 1A this can be numerically solved for the roots r which are used to find the constants u , v , and w , enabling a solution to (2.4) to be able to be written on the form

$$\begin{pmatrix} U(\psi, \xi) \\ V(\psi, \xi) \\ W(\psi, \xi) \end{pmatrix} = \sum_i^4 B_i \begin{pmatrix} u_i \\ v_i \\ w_i \end{pmatrix} \begin{pmatrix} \sin n\psi \\ \cos n\psi \\ \sin n\psi \end{pmatrix} e^{-r_i \xi}, \quad (2.32)$$

where B_i are arbitrary constants to be found.

Substituting (2.32) into the traction free boundary conditions for Problem 2A (2.8) yields

$$b_{ij}^{(2A)} B_j = 0, \quad \text{for } i, j = 1..4, \quad (2.33)$$

where

$$b_{1j}^{(2A)} = u_j r_j + v_j \nu n + w_j \nu, \quad (2.34a)$$

$$b_{2j}^{(2A)} = u_j n - v_j r_j - \frac{4}{3} \eta^2 r_j (v_j + w_j n), \quad (2.34b)$$

$$b_{3j}^{(2A)} = -v_j \nu n + w_j (r_j^2 - \nu n^2), \quad (2.34c)$$

$$b_{4j}^{(2A)} = v_j n r_j (2 - \nu) - w_j (r_j^3 - (2 - \nu) r_j n), \quad (2.34d)$$

with $j = 1..4$. Using matrix notation for the boundary conditions

$$\det b_{ij}^{(2A)} = 0, \quad (2.35)$$

yields an equation which can be solved to establish the relationship between the non-dimensional frequency λ and the wavenumber n , and from here the natural forms.

2.3 Asymptotic Analysis

To find the leading order behaviour to problems 1A and 2A it is possible to separate the stress-strain states (SSS) into the sum of the basic SSS, subscript (b), and the additional SSS, subscript (a). The displacements can be written as

$$\begin{pmatrix} U(\psi) \\ V(\psi) \\ W(\psi) \end{pmatrix} = \begin{pmatrix} U_b(\psi) \\ V_b(\psi) \\ W_b(\psi) \end{pmatrix} + \eta^\kappa \begin{pmatrix} U_a(\psi) \\ V_a(\psi) \\ W_a(\psi) \end{pmatrix}. \quad (2.36)$$

This is known as the separation method (Goldenveizer et al. (1979) and therein) and describes the separation of the leading order stresses and strains from the additional, less prevalent ones. The asymptotic terms associated with the basic SSS will yield homogeneous equations which represent the leading order behaviour of the forces and moments acting on the mid-surface of the panel. This thesis is only concerned with the basic SSS and will hence be referred to as the leading order behaviour.

Utilising the results of the model problems for a plate, of the Rayleigh-type flexural and extensional waves studied in subsections 1.2.1 and 1.2.2, the characteristic equation in problem 1A (2.17) is subject to asymptotic analysis by representing all terms using the small parameter η , and the leading order terms are analysed. Three types of vibration are uncovered, these are the Rayleigh-type flexural and extensional vibration, and super-low frequency vibration, and will be clarified in what follows.

The interest here is in waves which are long compared to the thickness of the panel, and short compared to the radius of the panel, thus

$$1 \ll \gamma \ll \eta^{-1}, \quad (2.37)$$

The main small geometrical parameter η is used to write the wavelength as having the order

$$\gamma \sim \eta^{-q}. \quad (2.38)$$

With $0 < q < 1$ from the consideration of (2.37). Then all parameters can be expressed through η .

2.3.1 Asymptotic Justification for Problem 1A

Flexural Vibration:

From subsection 1.2.1 the range of applicability given by the inequality (1.13) for wavelength γ and dimensionless frequency λ is

$$\frac{\sqrt{3\lambda(1-\nu^2)}}{\eta^2} < \gamma^2 < \frac{\sqrt{3\lambda(1+\nu)}}{\eta^2}. \quad (2.39)$$

Looking at the governing equation (1.7) of flexural waves on a plate

$$m^4 - 2m^2\gamma^2 + \gamma^4 = \frac{3\lambda(1-\nu^2)}{\eta^2}, \quad (2.40)$$

the edge wavelength γ and the root m have the same order such that

$$m \sim \gamma, \quad \text{and} \quad m \neq \gamma. \quad (2.41)$$

From here it is evident that λ is of order

$$\lambda \sim \eta^2\gamma^4. \quad (2.42)$$

Writing the parameters in terms of η gives

$$\gamma = \underset{*}{\gamma}\eta^{-q}, \quad m = \underset{*}{m}\eta^{-q}, \quad \lambda = \underset{*}{\lambda}\eta^{2-4q}, \quad (2.43)$$

where all starred terms are of order 1. Substituting these into the characteristic equation (2.17) of problem 1A and retaining only the leading order terms in the range $\frac{1}{2} \leq q < 1$ yields

$$\frac{1}{2}\underset{*}{\lambda}(1-\nu^2)(1-\nu)(\underset{*}{m}^2 - \underset{*}{\gamma}^2)^2 - \frac{1}{6}(1-\nu)(\underset{*}{m}^2 - \underset{*}{\gamma}^2)^4 = 0, \quad (2.44)$$

which simplifies to an equation that is equivalent to the governing equation of flexural waves on a plate (2.40).

The next order terms in characteristic equation (2.17) are of relative order η^{2-2q} and η^{4q-2}

$$\begin{aligned} & \frac{1}{2}\underset{*}{\lambda}(1-\nu^2)(1-\nu)(\underset{*}{m}^2 - \underset{*}{\gamma}^2)^2 - \frac{1}{6}(1-\nu)(\underset{*}{m}^2 - \underset{*}{\gamma}^2)^4 \\ & - \eta^{4q-2} \left\{ (1-\nu^2) \frac{(1-\nu)}{2} \gamma^4 \right\} + \eta^{2-2q} \left\{ \underset{*}{\lambda}(1-\nu^2) \frac{3-\nu}{6} (3\underset{*}{\lambda}(1-\nu^2)(\underset{*}{m}^2 - \underset{*}{\gamma}^2) - 1) \right\} = 0. \end{aligned} \quad (2.45)$$

For q in the range $\frac{2}{3} \leq q < 1$, the terms of relative order η^{2-2q} will dominate those of order η^{4q-2} . When this happens equation (2.45) reduces to (2.44) which is the leading order equation. However, when $\frac{1}{2} \leq q < \frac{2}{3}$, the terms of relative order η^{4q-2} will be dominant, giving

$$\frac{1}{2} \lambda (1 - \nu^2) (1 - \nu) (m^2 - \gamma^2)^2 - \frac{1}{6} (1 - \nu) (m^2 - \gamma^2)^4 - (1 - \nu^2) \frac{(1 - \nu)}{2} \gamma^4 = 0. \quad (2.46)$$

This special case has been investigated in Kaplunov (1990) and ?.

Extensional Vibration:

From subsection (1.2.2) the inequality (1.23) describing the relationship between the dimensionless frequency and the wavelength is

$$0 < 2\lambda(1 + \nu) < \gamma^2. \quad (2.47)$$

From this and the characteristic equation of the Rayleigh-type extensional wave in a plate

$$m^4 \left[\frac{1}{2}(1 - \nu) \right] + m^2 \gamma^2 \left[(1 - \nu) + \frac{1}{2} \lambda (3 - \nu)(1 + \nu) \right] + \gamma^4 \frac{1}{2}(1 - \nu) - \gamma^2 \lambda \frac{1}{2}(1 - \nu^2)(3 - \nu) + \lambda^2 (1 - \nu)^4 = 0, \quad (2.48)$$

the non-dimensional frequency is deduced to have order

$$\lambda \sim \gamma^2, \quad (2.49)$$

and γ and m are related as (2.41). Writing the parameters in terms of η gives

$$\gamma = \gamma \eta^{-q}, \quad m = m \eta^{-q}, \quad \lambda = \lambda \eta^{-2q}. \quad (2.50)$$

Substituting these into the characteristic equation (2.17) and retaining only the leading order terms in the range of $q \geq 0$ leaves an equation which is equivalent to equation (2.48) for extensional waves on a plate, and the range of q satisfies

$$0 < q. \quad (2.51)$$

Super-Low Frequency:

Unfortunately for this type of vibration there is no flat plate analogues. The super-low frequency vibration is typical for a curved body due to the coupling between bending and extensional motions.

It is possible to deduce from the previous analyses that for $\lambda \ll 1$ and $\gamma \gg 1$

$$\gamma^4 \sim \eta^2 m^8, \quad \text{and} \quad \lambda \sim \eta^2 m^4. \quad (2.52)$$

Writing parameters

$$\gamma = \underset{*}{\gamma} \eta^{-q}, \quad m = \underset{*}{m} \eta^{-\frac{q}{2} - \frac{1}{4}}, \quad \lambda = \underset{*}{\lambda} \eta^{1-2q}. \quad (2.53)$$

The leading order terms of the characteristic equation (2.17) are

$$- \underset{*}{m}^8 \frac{1}{3} + \underset{*}{m}^4 \underset{*}{\lambda} (1 - \nu^2) - \underset{*}{\gamma}^4 (1 - \nu^2) = 0. \quad (2.54)$$

Including the next order terms of relative order $\eta^{\frac{3}{4} - \frac{9q}{2}}$ [ηm^2] and $\eta^{1\frac{3}{4} - \frac{3q}{2}}$ [$1/m^2$] gives

$$- \frac{1}{3} [\underset{*}{m}^8 - 4 \underset{*}{m}^6 \underset{*}{\gamma}^2 + 2 \underset{*}{m}^6] + \underset{*}{\lambda} (1 - \nu^2) [\underset{*}{m}^4 - 2 \underset{*}{m}^2 \underset{*}{\gamma}^2 - \underset{*}{m}^2] - \underset{*}{\gamma}^4 (1 - \nu^2) = 0. \quad (2.55)$$

The next relative order terms $\eta^{\frac{3}{2} - 9q}$ [$\eta^2 m^4$], $\eta^{2\frac{1}{4} - 13q\frac{1}{2}}$ [$\eta^3 m^6$] and η^{4-8q} [$\eta^4 m^8$] can be taken into account to obtain

$$- \frac{1}{3} [(\underset{*}{m}^2 - \underset{*}{\gamma}^2)^4 + 2 \underset{*}{m}^6] + \underset{*}{\lambda} (1 - \nu^2) [(\underset{*}{m}^2 - \underset{*}{\gamma}^2)^2 - \underset{*}{m}^2] - \underset{*}{\gamma}^4 (1 - \nu^2) = 0. \quad (2.56)$$

This is the simplest expression of the leading order terms for super-low frequency vibration, and q satisfies the range

$$0 < q < \frac{1}{2}. \quad (2.57)$$

2.3.2 Asymptotics for Problem 2A

The asymptotics for this problem are obtained from Kaplunov et al. (1998) and Kaplunov et al. (1999).

Flexural Vibration ($\frac{1}{2} \leq q < 1$):

$$\begin{aligned} n &= n_* \eta^{-q}, & r &= r_* \eta^{-q}, & \lambda &= \lambda_* \eta^{2-4q}, \\ u &= u_* \eta^q, & v &= v_* \eta^q, & w &= w_* \eta^0. \end{aligned} \tag{2.58}$$

Extensional Vibration ($q \geq 0$):

$$\begin{aligned} n &= n_* \eta^{-q}, & r &= r_* \eta^{-q}, & \lambda &= \lambda_* \eta^{-2q}, \\ u &= u_* \eta^{-q}, & v &= v_* \eta^q, & w &= w_* \eta^0. \end{aligned} \tag{2.59}$$

Super-Low Frequency ($0 \leq q < \frac{1}{2}$):

$$\begin{aligned} n &= n_* \eta^{-q}, & r &= r_* \eta^{\frac{1}{2}-2q}, & \lambda &= \lambda_* \eta^{2-4q}, \\ u &= u_* \eta^{\frac{1}{2}}, & v &= v_* \eta^q, & w &= w_* \eta^0. \end{aligned} \tag{2.60}$$

The asymptotic analysis in Problem 2A applied to the system of equations (2.27) that are used in conjunction with a numerical scheme can be found in Kaplunov et al. (1999).

2.4 Flexural Vibrations

Substituting the leading order asymptotic behaviour from subsection (2.5.1) into the governing equations (2.12) and considering analysis of the leading order displacements, it is found that

$$u = {}_u\eta^q, \quad v = {}_v\eta^q, \quad w = {}_w\eta^0. \quad (2.61)$$

This means that the transverse displacements to the mid-surface Γ are larger, and the tangential displacements of the mid-surface are smaller.

Substituting the leading order behaviours into the governing equations (2.12) yields

$$\begin{aligned} & {}_u \left[\left(\frac{1-\nu}{2} \right) m^2 \eta^{-q} + \lambda(1-\nu^2) \eta^{2-3q} - \gamma^2 \eta^{-q} \right] + {}_v \left[\left(\frac{1+\nu}{2} \right) i\gamma m \eta^{-q} \right] \\ & + {}_w [i\nu\gamma \eta^{-q}] = 0, \end{aligned} \quad (2.62a)$$

$$\begin{aligned} & {}_u \left[im\gamma \left(\frac{1+\nu}{2} \right) \eta^{-q} \right] + {}_v \left[m^2 \left(\frac{\eta^2}{3} + 1 \right) \eta^{-q} + \lambda(1-\nu^2) \eta^{2-3q} \right. \\ & \left. - \gamma^2 \left(\frac{1-\nu}{2} - \frac{2\eta^2}{3}(1-\nu) \right) \eta^{-q} \right] \end{aligned} \quad (2.62b)$$

$$\begin{aligned} & + {}_w \left[m^3 \left(-\frac{\eta^2}{3} \right) \eta^{-3q} + m \left(\eta^{-q} + \gamma^2 \frac{\eta^{2-3q}}{3} (2-\nu) \right) \right] = 0, \\ & {}_u [-i\gamma\nu\eta^0] + {}_v \left[m^3 \left(\frac{\eta^{2-2q}}{3} \right) - m \left(\eta^0 + \gamma^2 \frac{\eta^{2-2q}}{3} (2-\nu) \right) \right] \\ & + {}_w \left[m^4 \left(-\frac{\eta^{2-4q}}{3} \right) + m^2 \left(\gamma^2 \frac{2\eta^{2-4q}}{3} \right) + \lambda(1-\nu^2) \eta^{2-4q} - \frac{\gamma^4 \eta^{2-4q}}{3} - \eta^0 \right] = 0. \end{aligned} \quad (2.62c)$$

Neglecting lower order terms and keeping only leading order terms, system (2.63) becomes,

$${}_u \left[\left(\frac{1-\nu}{2} \right) m^2 - \gamma^2 \right] \eta^{-q} + {}_v \left[\left(\frac{1+\nu}{2} \right) i\gamma m \right] \eta^{-q} + {}_w [i\nu\gamma] \eta^{-q} = 0, \quad (2.63a)$$

$${}_u \left[im\gamma \left(\frac{1+\nu}{2} \right) \right] \eta^{-q} + {}_v \left[m^2 - \gamma^2 \left(\frac{1-\nu}{2} \right) \right] \eta^{-q} + {}_w [m] \eta^{-q} = 0, \quad (2.63b)$$

$${}_w \left[m^4 \left(-\frac{1}{3} \right) + m^2 \left(\gamma^2 \frac{2}{3} \right) + \lambda(1-\nu^2) - \frac{\gamma^4}{3} \right] \eta^{2-4q} = 0. \quad (2.63c)$$

The equation (2.63c) is analogous to the governing equation of the Rayleigh-type flexural wave on a plate (1.7), and equations (2.63a) and (2.63b) can be used to find U and V .

Now substituting (2.61) and (2.43) into the boundary conditions (2.33) gives $b_{ij}^{(1A)}$ as

$$b_{1j}^{(1A)} = [u_j i \nu \gamma - v_j m_j - w_j] \eta^0,$$

$$b_{2j}^{(1A)} = [-u_j m_j + v_j i \gamma] \eta^0,$$

$$b_{3j}^{(1A)} = -v_j m_j \eta^0 + w_j (\nu \gamma^2 + m_j^2) \eta^{-2q},$$

$$b_{4j}^{(1A)} = v_j [m_j^2 - 2(1 - \nu) \gamma^2] \eta^{2-5q} + w_j [(2 - \nu) m_j \gamma^2 - m_j^3] \eta^{-3q}.$$

Eliminating the lower order terms leaves

$$b_{1j}^{(1A)} = w [\nu \gamma^2 + m^2], \quad (2.64a)$$

$$b_{2j}^{(1A)} = w [(2 - \nu) m \gamma^2 - m^3]. \quad (2.64b)$$

Where (2.64a) and (2.64b) are the same as the free boundary conditions (1.3) of flexural waves in a plate. From subsection 1.2.1 the solution to this problem is

$$W = w e^{i\gamma\xi} (e^{-m_1\psi} + C e^{-m_2\psi}), \quad (2.65)$$

and the frequency equation is

$$\lambda = \frac{\eta^2 \gamma^4 \left(3\nu - 1 + 2\sqrt{(1 - \nu)^2 + \nu^2} \right)}{3(1 + \nu)}. \quad (2.66)$$

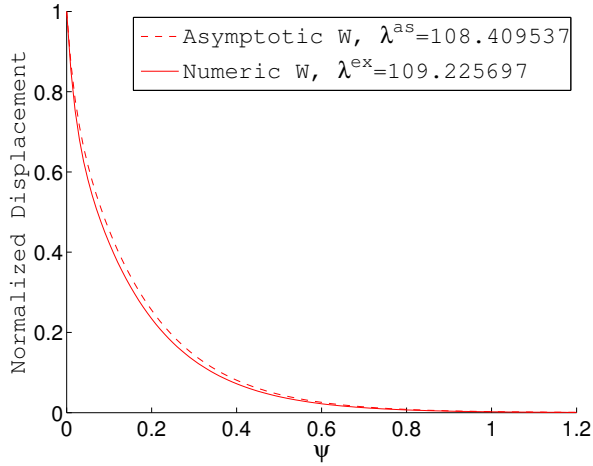
2.4.1 Numerical Results

In all results sections we refer to the numerically found frequency as λ^{ex} and the asymptotically found frequency as λ^{as} . All results in this section use a thickness of $\eta = 0.01$, and each figure displays the numerical value of the smallest root, m and r , of the asymptotic and numerical forms (m_{as} and r_{as} are the same) to illustrate their effect on decay of the wave. In addition, the graphs of displacement will only show the transverse displacement W in red, and the asymptotic displacement with a red dashed line.

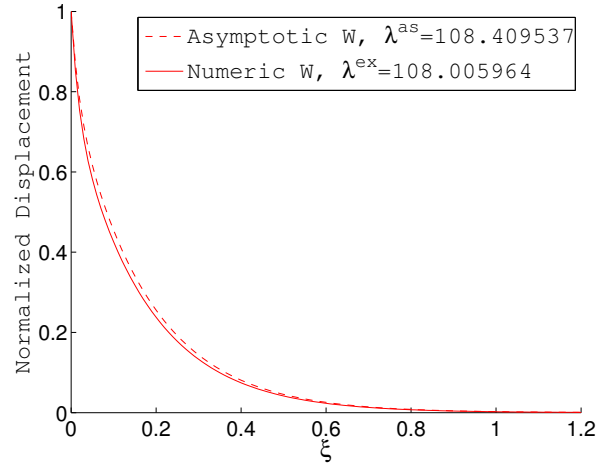
Comparing the asymptotic with the numerical results, Figures 2.3c and 2.3d show the forms of the flexural edge wave for parameters $\gamma, n = 40 \sim \eta^{-\frac{4}{5}}$ and $\nu = 0.45$. The displacements decay smoothly with no sign change, and the asymptotics are very accurate. Figures 2.3a and 2.3b for Poisson ratio of $\nu = 0.495$, close to that of incompressible material, show more rapid decay over a shorter distance, whereas in Figures 2.4c and 2.4d for $\nu = 0.2$ the decay is slower and over a longer distance. Figure 2.5 shows percentage error plots between asymptotic and numeric displacements for the cases shown in Figures 2.3 and 2.4. The dark red lines are the percentage errors in Problem 1A, and the blue lines are the percentage errors in Problem 2A. The results show that for $\gamma \sim \eta^{-\frac{4}{5}}$ the percentage error in Problem 1A drastically increases as $\nu \rightarrow 0.2$, and there is no significant difference between Figures 2.5c and 2.5d for $\nu = 0.45$ and $\nu = 0.495$.

Figure 2.6 shows three graphs for each problem with $\gamma/n = 30 \sim \eta^{-\frac{3}{4}}$ and different ν displayed under each graph. It is clear again that the asymptotics are less accurate for smaller ν . The graph for $\nu = 0.495$ has been omitted as there is no significant difference with the graph of $\nu = 0.45$.

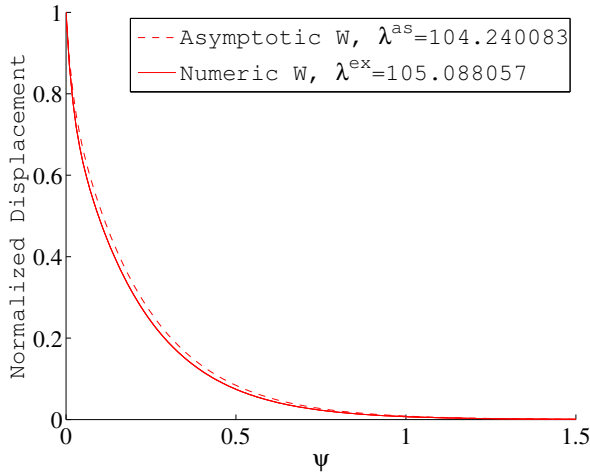
The results indicate that in Problem 1A the rate of decay of the numerical line is more rapid than the asymptotic one when compared to Problem 2A. Examining the roots m and r of the characteristic equations for both problems, we see a larger difference in Problem 1A corresponding to the larger percentage errors. The asymptotics remain accurate for Problem 2A in all cases within the applicable range of parameters. This seems to indicate that the curvature increases the rate of decay in Problem 1A more than expected, whereas in Problem 2A curvature has less effect and the asymptotics remain accurate.



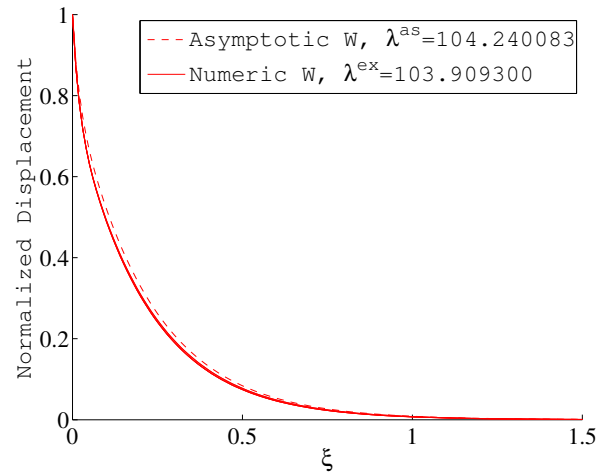
(a) $\nu = 0.495$, $m_{as} = 5.861$, $m_{ex} = 6.238$



(b) $\nu = 0.495$, $r_{as} = 5.861$, $r_{ex} = 5.810$

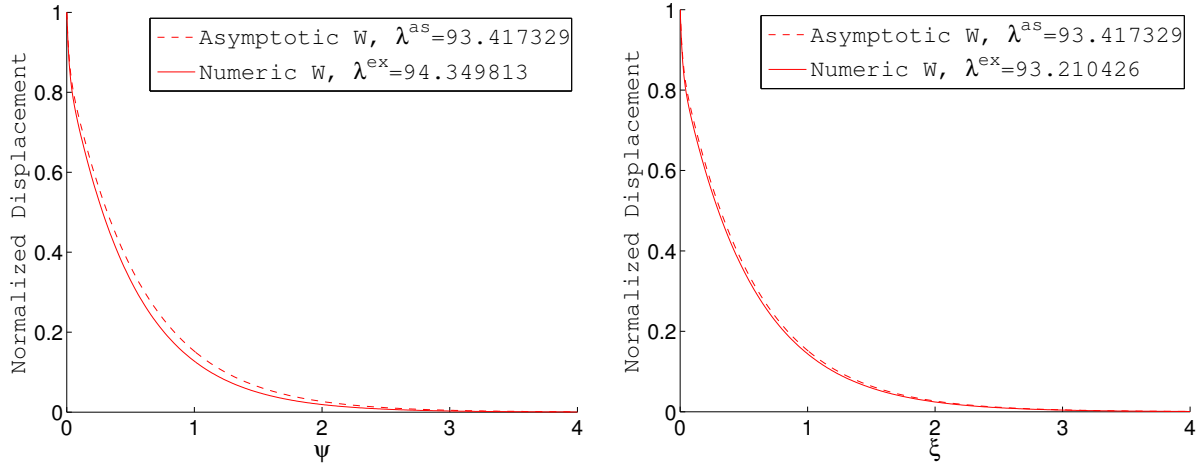


(c) $\nu = 0.45$, $m_{as} = 4.558$, $m_{ex} = 4.705$

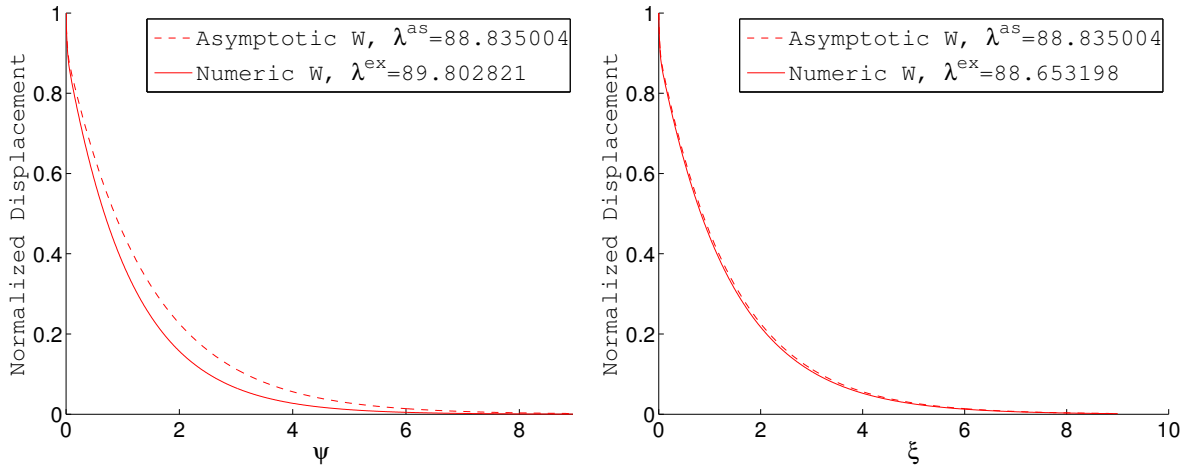


(d) $\nu = 0.45$, $r_{as} = 4.558$, $r_{ex} = 4.622$

Figure 2.3: Asymptotic and numeric forms for the flexural edge waves of Problems 1A in the left column, and 2A in the right column, with given fixed parameters $\eta = 0.01$, $\gamma/n = 40$, and for (a) and (b) $\nu = 0.495$, and (c) and (d) $\nu = 0.45$.

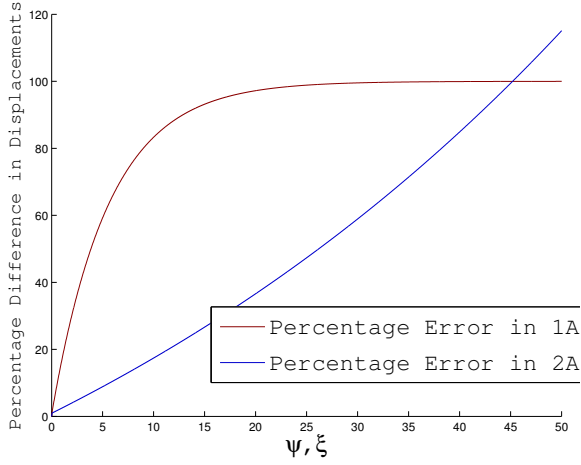


(a) $\nu = 0.3$, $m_{as} = 1.742$, $m_{ex} = 1.903$ (b) $\nu = 0.3$, $r_{as} = 1.742$, $r_{ex} = 1.778$

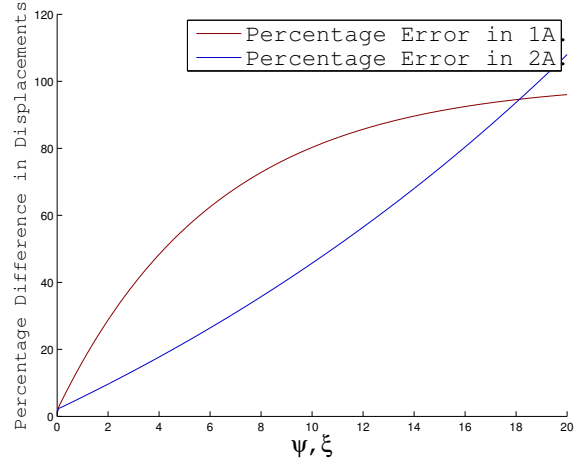


(c) $\nu = 0.2$, $m_{as} = 0.696$, $m_{ex} = 0.875$ (d) $\nu = 0.2$, $r_{as} = 0.696$ and $r_{ex} = 0.712$

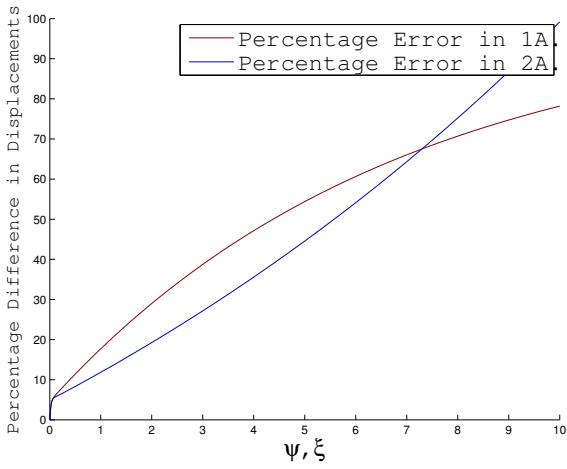
Figure 2.4: Asymptotic and numeric forms for the flexural edge waves of Problems 1A in the left column, and 2A in the right column, with given fixed parameters $\eta = 0.01$, $\gamma/n = 40$, and for (a) and (b) $\nu = 0.3$, and (c) and (d) $\nu = 0.2$.



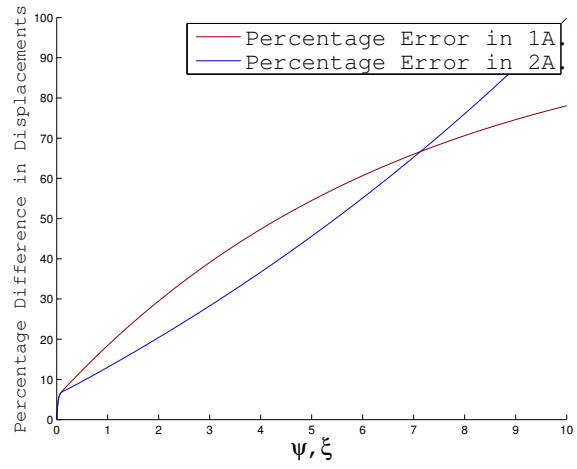
(a) $\nu = 0.2$



(b) $\nu = 0.3$

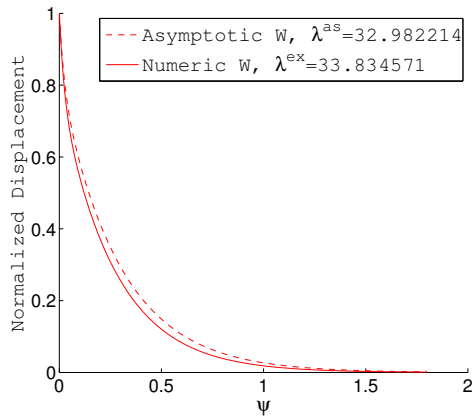


(c) $\nu = 0.45$

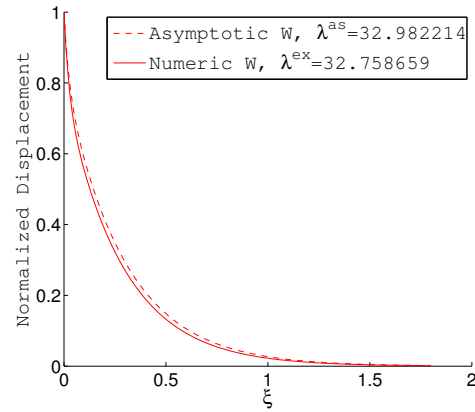


(d) $\nu = 0.495$

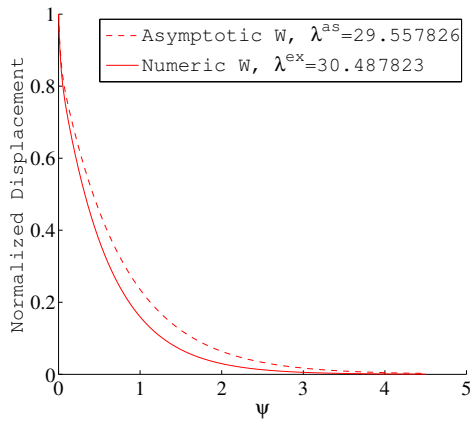
Figure 2.5: Percentage error between asymptotic and numeric forms for the flexural edge waves of Problem 1A in dark red and Problem 2A in blue, with fixed parameters $\eta = 0.01$, $\gamma/n = 40$, and ν shown below each graph.



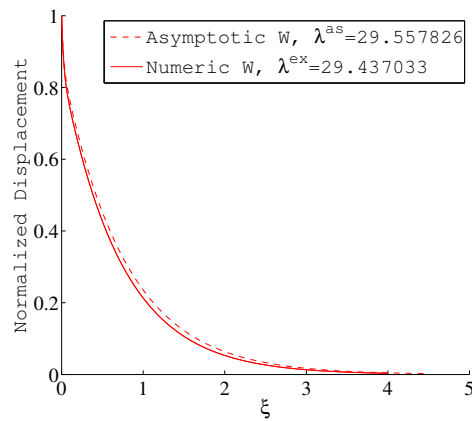
(a) $\nu = 0.45$, $m_{as} = 3.419$,
 $m_{ex} = 3.757$



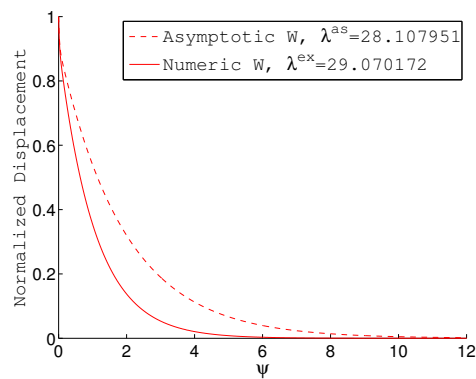
(b) $\nu = 0.45$, $r_{as} = 3.419$,
 $r_{ex} = 3.757$



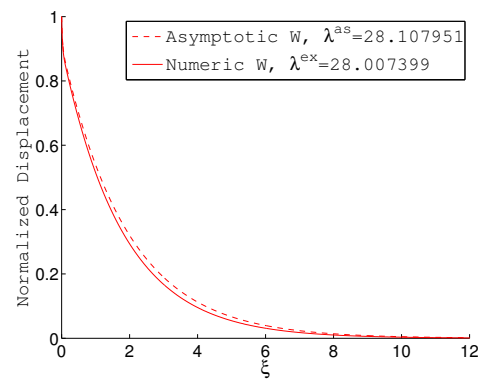
(c) $\nu = 0.3$, $m_{as} = 1.307$,
 $m_{ex} = 1.686$



(d) $\nu = 0.3$, $r_{as} = 1.307$,
 $r_{ex} = 1.373$

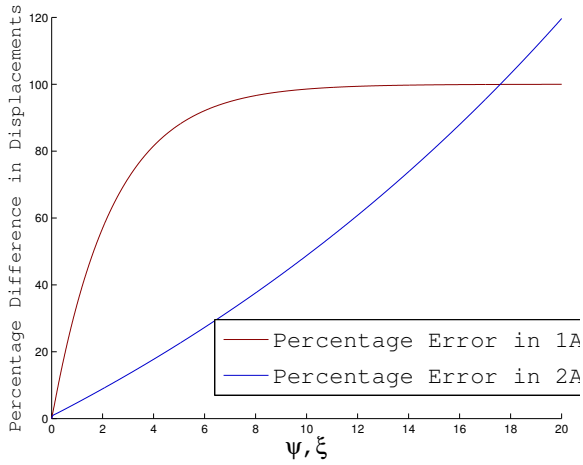


(e) $\nu = 0.2$, $m_{as} = 0.522$,
 $m_{ex} = 0.946$

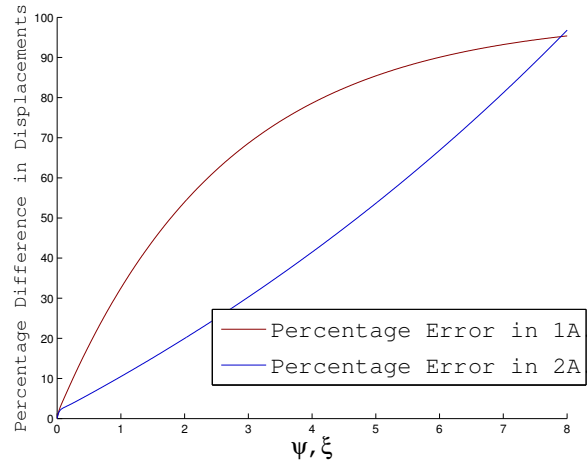


(f) $\nu = 0.2$, $r_{as} = 0.522$,
 $r_{ex} = 0.561$

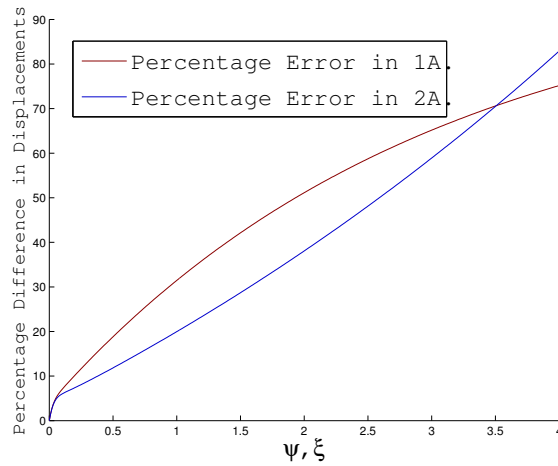
Figure 2.6: Asymptotic and numeric forms for the flexural edge waves of Problems 1A in the left column, and 2A in the right column, with given fixed parameters $\eta = 0.01$, $\gamma/n = 30$, and for ν shown below each graph.



(a) $\nu = 0.2$



(b) $\nu = 0.3$



(c) $\nu = 0.45$

Figure 2.7: Percentage error between asymptotic and numeric forms for the flexural edge waves of Problem 1A in dark red and Problem 2A in blue, with fixed parameters $\eta = 0.01$, $\gamma/n = 30$, and ν shown below each graph.

Some relevant numerical data are presented in table 2.1.

Table 2.1: Natural Frequencies with $\eta = 0.01$, and $\nu = 0.3$.

γ, n	1A λ^{ex}	2A λ^{ex}	Asymptotic λ^{as}
25	14.975647	14.179650	14.25435
30	30.319554	29.437033	29.557826
40	94.202452	93.210426	93.417329

2.5 Extensional Vibrations

Using the asymptotics from subsection 2.5.1 to analyse the governing system (2.12) yields

$$U = u\eta^{-q}, \quad V = v\eta^{-q}, \quad W = w\eta^0. \quad (2.67)$$

Which corresponds to the tangential displacements of the mid-surface being the leading order displacements.

Substituting (2.67) and (2.50) into the governing equations gives

$$\begin{aligned} u \left[m^2 \left(\frac{1-\nu}{2} \right) + \lambda(1-\nu^2) - \gamma^2 \right] \eta^{-3q} + v \left[im\gamma \left(\frac{1+\nu}{2} \right) \right] \eta^{-3q} \\ + w [i\gamma\nu] \eta^{-q} = 0, \end{aligned} \quad (2.68a)$$

$$\begin{aligned} u \left[im\gamma \left(\frac{1+\nu}{2} \right) \right] \eta^{-3q} + v \left[m^2 \left(\frac{\eta^2}{3} + 1 \right) + \lambda(1-\nu^2) \right. \\ \left. - \gamma^2 \left(\frac{1-\nu}{2} - \frac{2\eta^2}{3}(1-\nu) \right) \right] \eta^{-3q} \end{aligned} \quad (2.68b)$$

$$\begin{aligned} + w \left[m^3 \left(-\frac{1}{3} \right) \eta^{2-3q} + m \left(\eta^{-q} + \gamma^2 \frac{1}{3} (2-\nu) \eta^{2-3q} \right) \right] = 0, \\ u \left[-i\gamma\nu \right] \eta^{-2q} + v \left[m^3 \left(\frac{\eta^2}{3} \right) \eta^{2-3q} - m \left(\eta^{-2q} + \gamma^2 \frac{1}{3} (2-\nu) \eta^{2-4q} \right) \right] + \\ w \left[m^4 \left(-\frac{1}{3} \right) \eta^{2-4q} + m^2 \left(\gamma^2 \frac{2}{3} \right) \eta^{2-4q} + \lambda(1-\nu^2) \eta^{-2q} - \frac{\gamma^4}{3} \eta^{2-4q} - \eta^0 \right] = 0. \end{aligned} \quad (2.68c)$$

Keeping leading order terms gives

$$u \left[m^2 \left(\frac{1-\nu}{2} \right) + \lambda(1-\nu^2) - \gamma^2 \right] + v \left[im\gamma \left(\frac{1+\nu}{2} \right) \right] = 0, \quad (2.69a)$$

$$u \left[im\gamma \left(\frac{1+\nu}{2} \right) \right] + v \left[m^2 + \lambda(1-\nu^2) - \gamma^2 \left(\frac{1-\nu}{2} \right) \right] = 0, \quad (2.69b)$$

$$u \left[-i\gamma\nu \right] + v \left[-m \right] + w \left[\lambda(1-\nu^2) \right] = 0. \quad (2.69c)$$

Equations (2.69a) and (2.69b) are the leading order equations and are analogous to the governing equations of the Rayleigh-type extensional waves on a plate (1.15). Equation (2.69c) can be used to find W .

Then substituting (2.67) and (2.50) into the traction free boundary conditions

(2.33) where

$$b_{1j}^{(1A)} = [u_* i \nu \gamma \eta^{-2q} - v_* m_j \eta^{-2q} + w_* \eta^0], \quad (2.70a)$$

$$b_{2j}^{(1A)} = [-u_* m_j + v_* i \gamma] \eta^{-2q}, \quad (2.70b)$$

$$b_{3j}^{(1A)} = -v_* m_j \eta^{-q} - w_* (m_j^2 - \nu \gamma^2) \eta^{-2q}, \quad (2.70c)$$

$$b_{4j}^{(1A)} = [v_* [m_j^2 - 2(1 - \nu) \gamma^2] \eta^{-3q} - w_* [(2 - \nu) m_j \gamma^2 - m_j^3] \eta^{-3q}], \quad (2.70d)$$

and eliminating lower order terms leaves in particular

$$b_{1j}^{(1A)} = u_* i \nu \gamma - v_* m, \quad (2.71a)$$

$$b_{2j}^{(1A)} = -u_* m + v_* i \gamma. \quad (2.71b)$$

Equations (4.43b) and (2.71b) are the same as the free edge boundary conditions for extensional waves on a plate (1.16). As such a solution to this problem can be written as

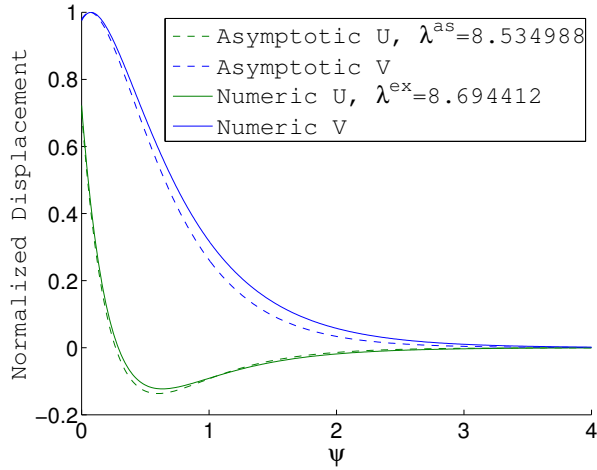
$$\begin{pmatrix} U(\psi, \xi) \\ V(\psi, \xi) \end{pmatrix} = \sum_{j=1}^2 \begin{pmatrix} u_0 \\ -i u_0 \left(\frac{m_j}{\gamma} \right)^{3-2j} \end{pmatrix} C^{j-1} e^{i\gamma\xi - m_j\psi}, \quad (2.72)$$

and the equation for the non-dimensional frequency can be written as

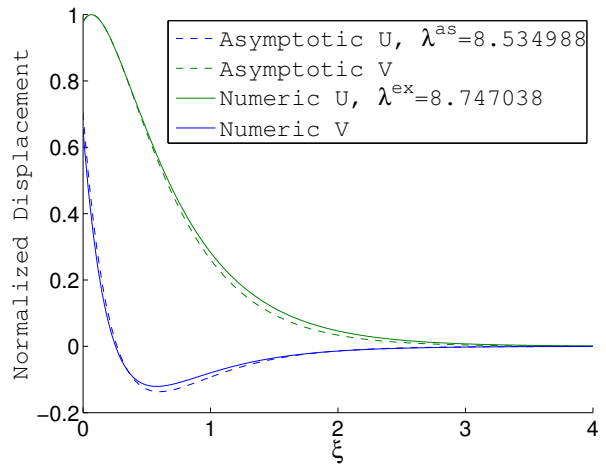
$$(\gamma^2 - (1 + \nu)\lambda)^2 = \sqrt{\gamma^2 - 2\lambda(1 + \nu)} \sqrt{\gamma^2 - \lambda(1 - \nu^2)} \gamma^2. \quad (2.73)$$

2.5.1 Numerical Results

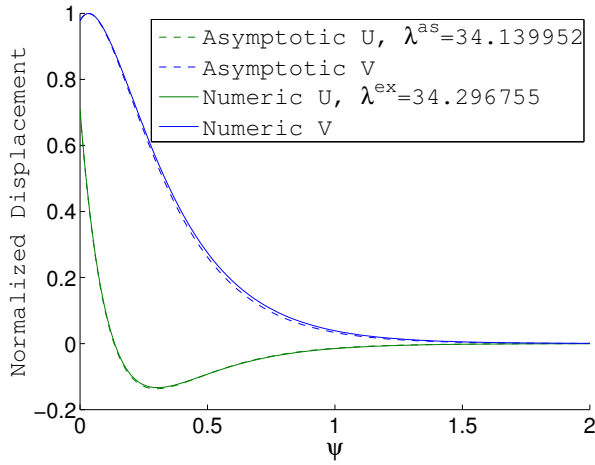
The forms of the extensional waves in this section are illustrated using green for displacement U and blue for displacement V , with their asymptotic counterparts with dashed lines. Figures 2.8, 2.9, and 2.10 show that the behaviour of U in problem 1A and V in problem 2A is very similar, with both decaying rapidly and changing sign before tending to zero. Conversely, the behaviours of V in problem 1A and U in problem 2A are similar, both decaying smoothly with no change of sign. Figure 2.11 shows the percentage difference between asymptotic and numeric forms for $\gamma/n = 5 \sim \eta^{-\frac{1}{4}}$, and in the first row $\nu = 0.2$ and the second row $\nu = 0.45$. We see that the accuracy of U in Problem 1A and V in Problem 2A spikes significantly at a shorter distance from the edge. As the distance from the edge tends to infinity the very small numbers cause numerical irregularities in the percentage errors. The erratic behaviour that can be observed in many of the percentage error figures is due to the effect of complex numerical values. Larger γ/n and change in Poisson's ratio can be seen in Figure 2.12 for $\gamma/n = 15 \sim \eta^{-\frac{2}{5}}$ with $\nu = 0.2$ and $\nu = 0.45$. These results seem to indicate that the percentage error between asymptotic and numeric forms is much greater for smaller edge wave numbers, in particular $\gamma/n < 10 \sim \eta^{-\frac{1}{3}}$.



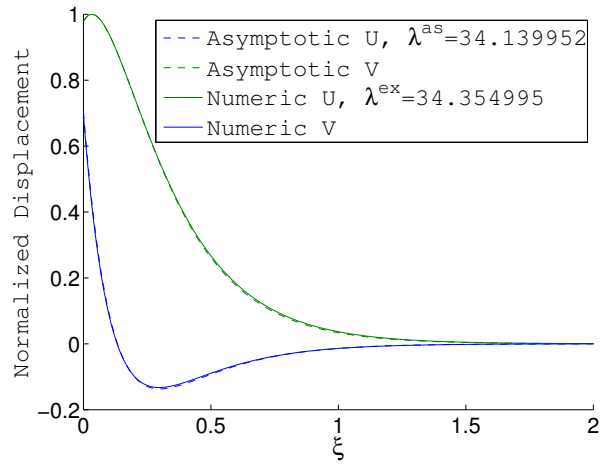
(a) $\gamma = 5$



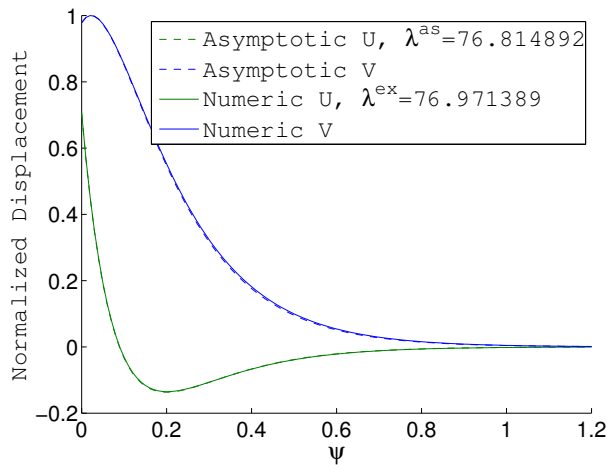
(b) $n = 5$



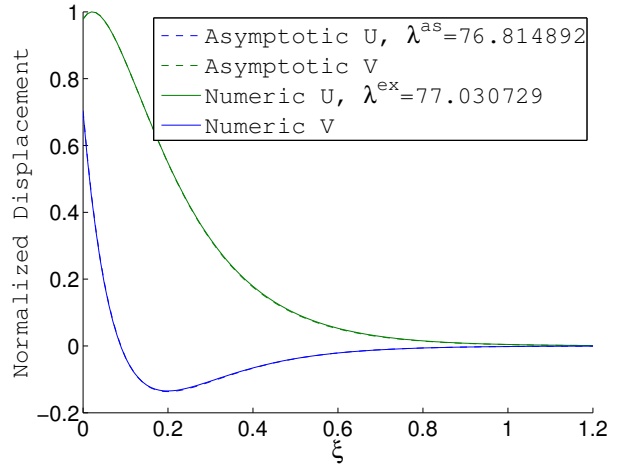
(c) $\gamma = 10$



(d) $n = 10$

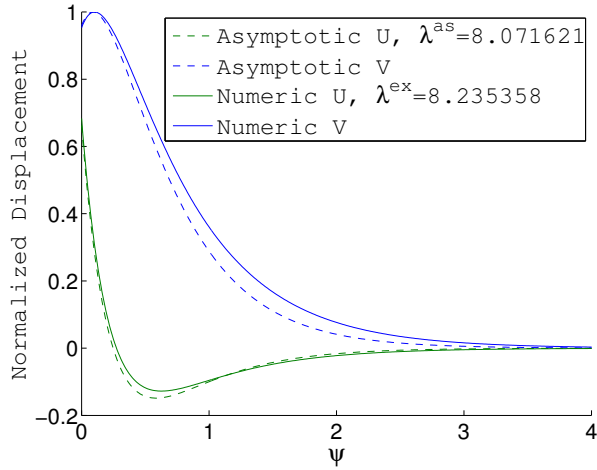


(e) $\gamma = 15$

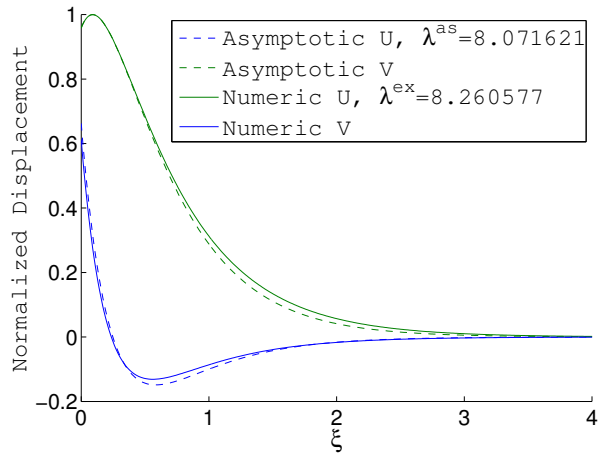


(f) $n = 15$

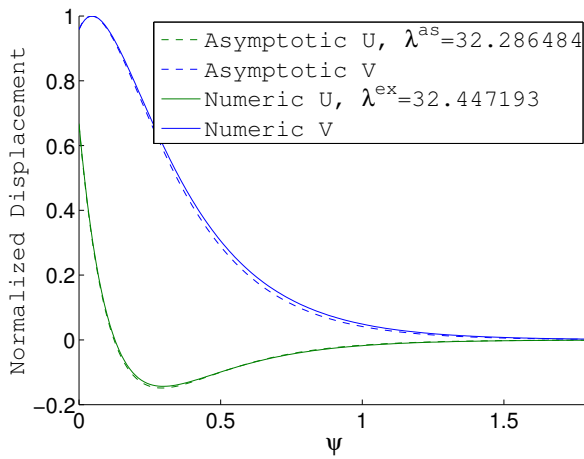
Figure 2.8: Asymptotic and numeric forms for the extensional edge waves of Problems 1A in the left column, and 2A in the right column, with given fixed parameters $\eta = 0.001$, $\nu = 0.02$, and ν displayed under each graph.



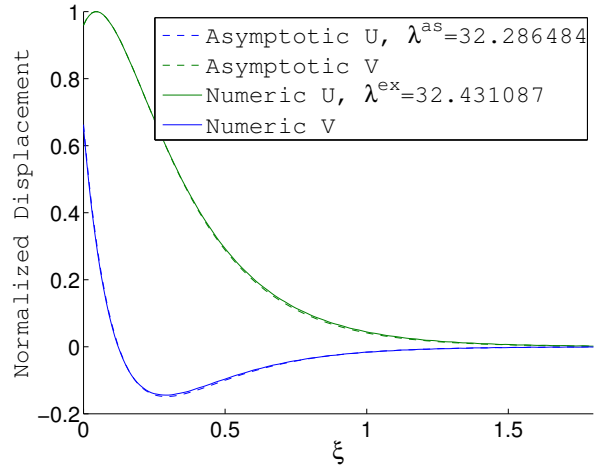
(a) $\gamma = 5$



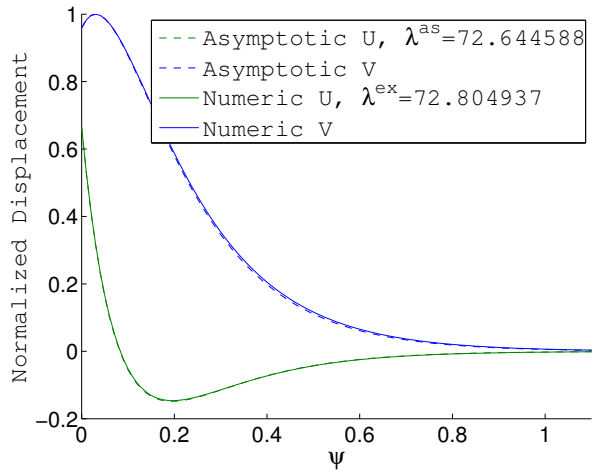
(b) $n = 5$



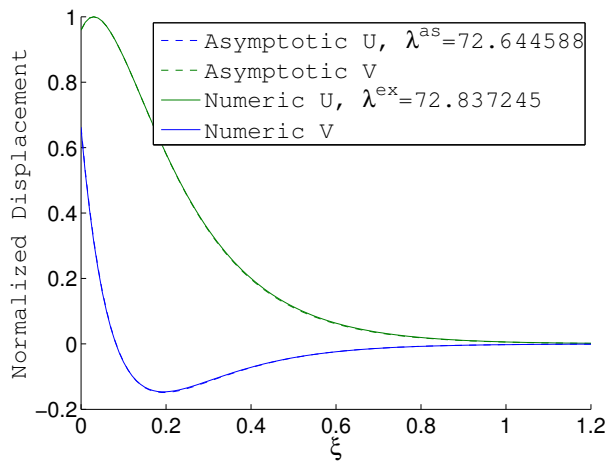
(c) $\gamma = 10$



(d) $n = 10$

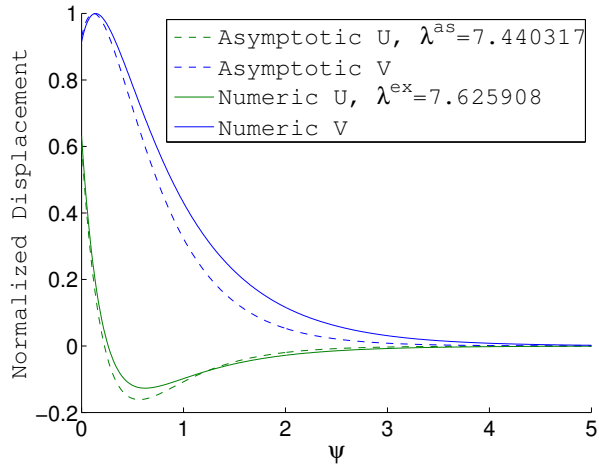


(e) $\gamma = 15$

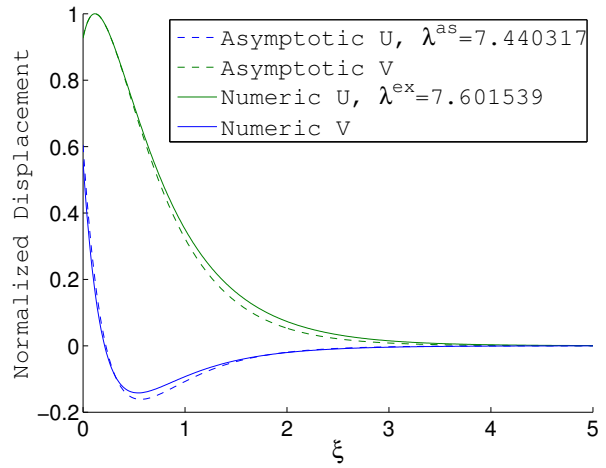


(f) $n = 15$

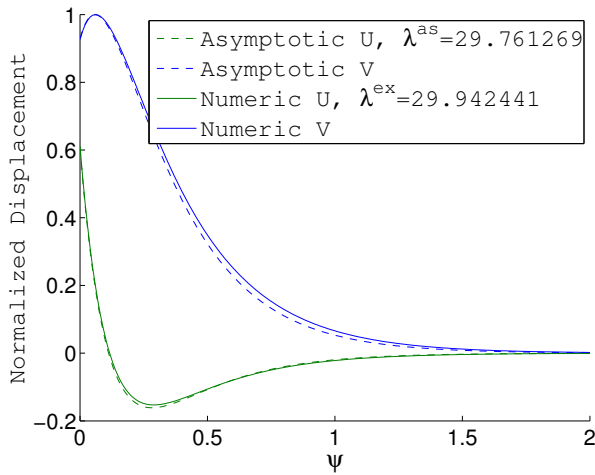
Figure 2.9: Asymptotic and numeric forms for the extensional edge waves of Problems 1A in the left column, and 2A in the right column, with given fixed parameters $\eta = 0.001$, $\nu = 0.3$, and γ/n are displayed below each graph.



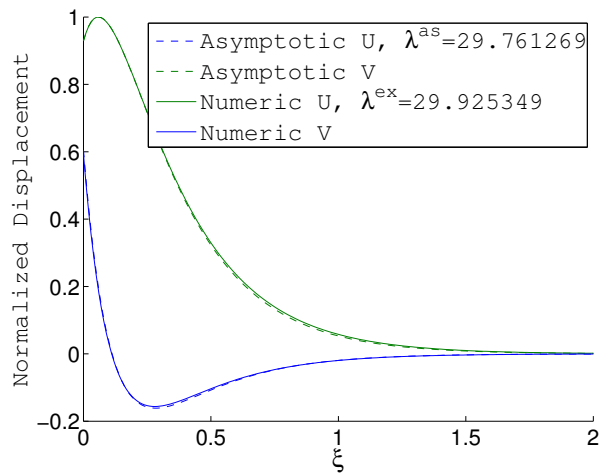
(a) $\gamma = 5$



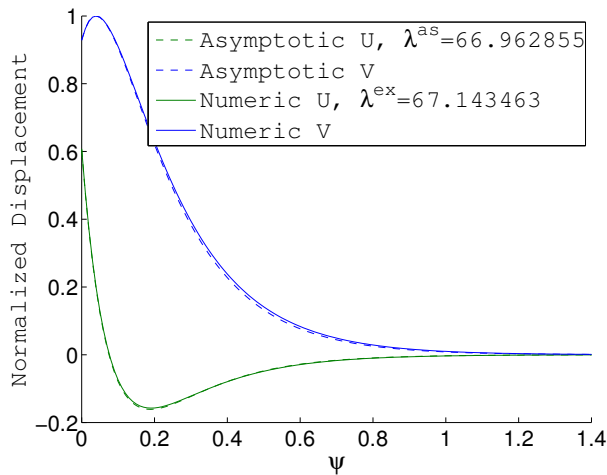
(b) $n = 5$



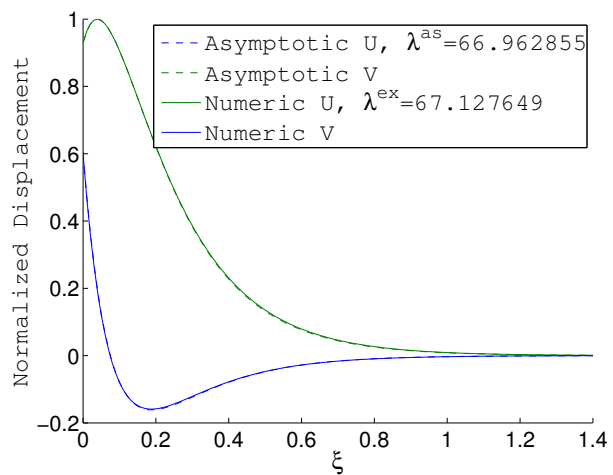
(c) $\gamma = 10$



(d) $n = 10$

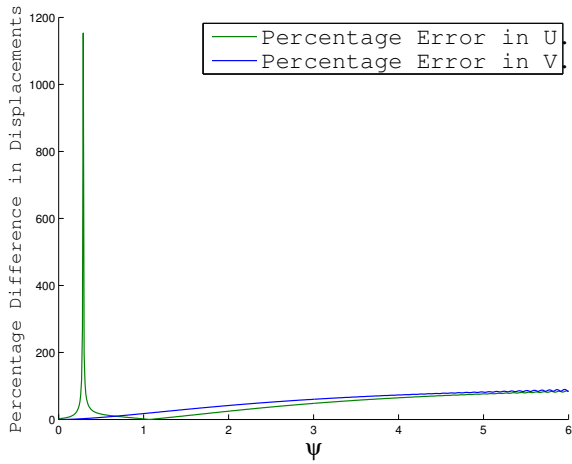


(e) $\gamma = 15$

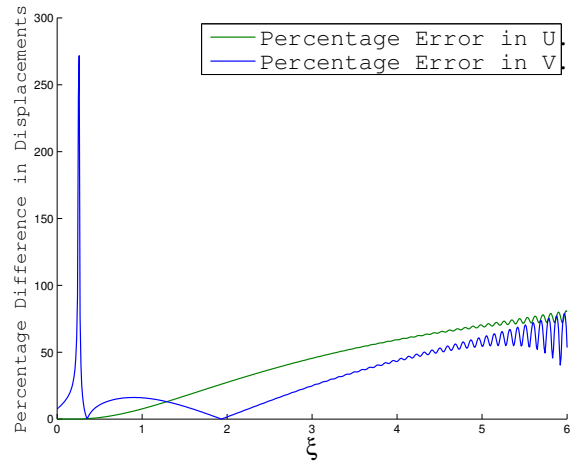


(f) $n = 15$

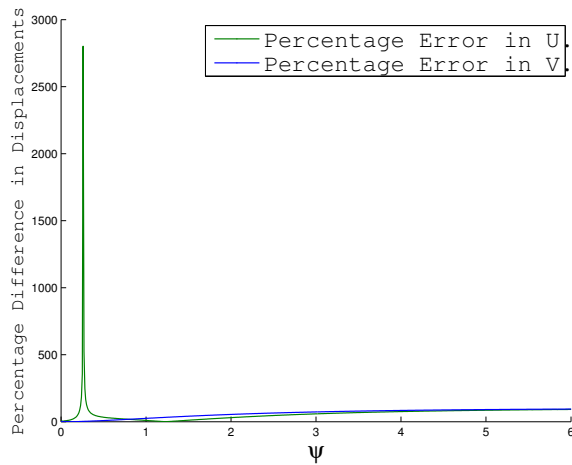
Figure 2.10: Asymptotic and numeric forms for the extensional edge waves of Problems 1A in the left column, and 2A in the right column, with given fixed parameters $\eta = 0.001$, $\nu = 0.45$, and γ/n displayed below each graph.



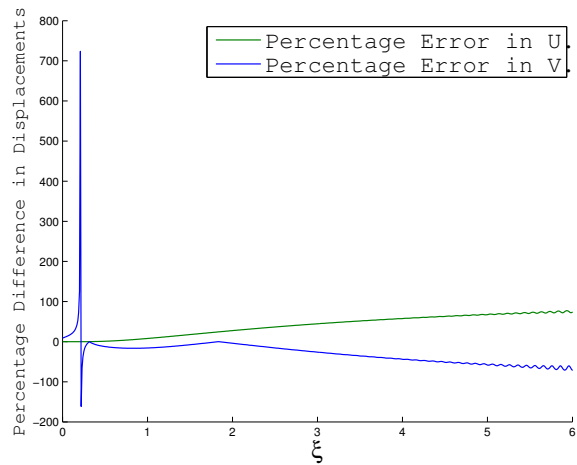
(a) $\nu = 0.2$



(b) $\nu = 0.2$



(c) $\nu = 0.45$



(d) $\nu = 0.45$

Figure 2.11: Percentage error between asymptotic and numeric forms for the extensional edge waves of Problems 1A in the left column, and 2A in the right column, with given fixed parameters $\eta = 0.001$, $\gamma/n = 5$, and ν displayed below each graph.

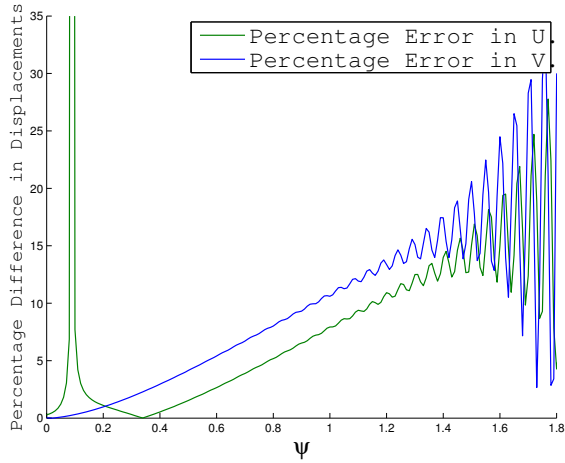
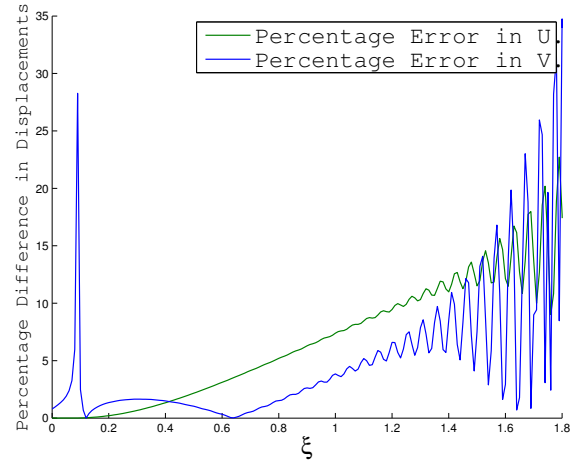
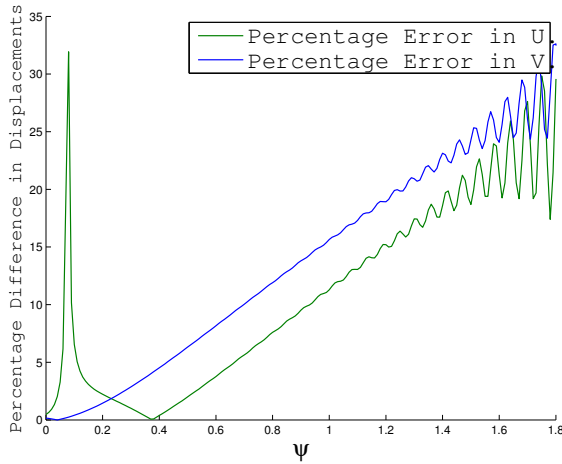
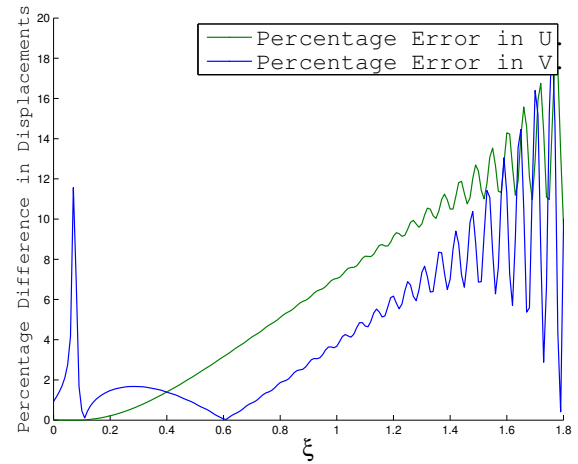

 (a) $\nu = 0.2$

 (b) $\nu = 0.2$

 (c) $\nu = 0.45$

 (d) $\nu = 0.45$

Figure 2.12: Percentage error between asymptotic and numeric forms for the extensional edge waves of Problems 1A in the left column, and 2A in the right column, with given fixed parameters $\eta = 0.001$, $\gamma/n = 15$, and ν displayed below each graph.

Table 2.2 gives some relevant numerical data about the natural frequencies for the parameters $\eta = 0.001$ and $\nu = 0.3$.

Table 2.2: Natural Frequencies with $\eta = 0.001$, and $\nu = 0.3$

γ, n	1A λ^{ex}	2A λ^{ex}	Asymptotic λ^{as}
5	8.197372	8.197371	8.071620
10	32.410630	32.994823	32.286483
15	72.768512	72.837266	72.644588

2.6 Super-Low Frequency Vibration

Taking into account the asymptotic behaviours from subsection 2.3.1 with the governing equations (2.12) and analysing the orders of the displacements gives

$$U = u_* \eta^{\frac{1}{2}}, \quad V = v_* \eta^{\frac{1}{4} + \frac{q}{2}}, \quad W = w_* \eta^0. \quad (2.74)$$

Substituting (2.74) into (2.12) gives

$$\begin{aligned} & u_* \left[m_*^2 \frac{1}{2} (1 - \nu) + \lambda_* (1 - \nu^2) \eta^{\frac{3}{2} - q} - \gamma_*^2 \eta^{\frac{1}{2} - q} \right] \\ & + v_* \left[i m_* \gamma_* \frac{1}{2} (1 + \nu) \right] + w_* [i \gamma_* \nu] = 0, \end{aligned} \quad (2.75a)$$

$$\begin{aligned} & u_* \left[i m_* \gamma_* \frac{1}{2} (1 + \nu) \eta^{\frac{1}{2} - q} \right] + v_* \left[m_*^2 \left(\frac{1}{3} \eta^2 + 1 \right) + \lambda_* (1 - \nu^2) \eta^{\frac{3}{2} - q} \right. \\ & \left. - \gamma_*^2 \left(\frac{1}{2} (1 - \nu) \eta^{\frac{1}{2} - \frac{q}{2}} - \frac{2}{3} (1 - \nu) \eta^{\frac{5}{2} - q} \right) \right] \end{aligned} \quad (2.75b)$$

$$\begin{aligned} & + w_* \left[-m_*^3 \frac{1}{3} \eta^{\frac{3}{2} - q} + m_* \left(1 + \gamma_*^2 \frac{1}{3} \eta^{2 - 2q} (2 - \nu) \right) \right] = 0, \\ & u_* \left[-i \gamma_* \nu \right] \eta^{\frac{1}{2} - q} + v_* \left[m_*^3 \frac{1}{3} \eta^{\frac{3}{2} - q} - m_* \left(1 + \gamma_*^2 \frac{1}{3} (2 - \nu) \eta^{2 - 2q} \right) \right] + \\ & w_* \left[-m_*^4 \frac{1}{3} \eta^{1 - 2q} + m_*^2 \gamma_*^2 \frac{2}{3} \eta^{\frac{3}{2} - 3q} + \lambda_* (1 - \nu^2) \eta^{1 - 2q} - \gamma_*^4 \frac{1}{3} \eta^{2 - 4q} - 1 \right] = 0. \end{aligned} \quad (2.75c)$$

Introducing the notation

$$\epsilon = \eta^{\frac{1}{2} - q}, \quad (2.76)$$

for convenience and neglecting terms $O(\eta^{\frac{3}{2} - q})$, and smaller terms of $\eta\epsilon, \eta\epsilon^2, \eta^2$ and $\eta^2\epsilon$, gives

$$u_* \left[m_*^2 \frac{1}{2} (1 - \nu) - \gamma_*^2 \epsilon \right] + v_* i m_* \gamma_* \frac{1}{2} (1 + \nu) + w_* i \gamma_* \nu = 0, \quad (2.77a)$$

$$u_* i m_* \gamma_* \frac{1}{2} (1 + \nu) \epsilon + v_* \left[m_*^2 - \gamma_*^2 \frac{1}{2} (1 - \nu) \epsilon \right] + w_* m_* = 0, \quad (2.77b)$$

$$\begin{aligned} & - u_* i \gamma_* \nu \epsilon - v_* m_* + w_* \left[-m_*^4 \frac{1}{3} \epsilon^2 + m_*^2 \gamma_*^2 \frac{2}{3} \epsilon^3 + \lambda_* (1 - \nu^2) \epsilon^2 - \gamma_*^4 \frac{1}{3} \epsilon^4 - 1 \right] = 0. \end{aligned} \quad (2.77c)$$

In the last line of the above equation the terms of order ϵ^3 and ϵ^4 are retained in order to test their influence in the asymptotics. Keeping only the leading order terms, the characteristic equation is then

$$- m_*^8 \frac{1}{3} + m_*^4 \lambda_* (1 - \nu^2) - \gamma_*^4 (1 - \nu^2) = 0. \quad (2.78)$$

This equation is the same as (2.54). A solution takes the form

$$\begin{pmatrix} U(\psi, \xi) \\ V(\psi, \xi) \\ W(\psi, \xi) \end{pmatrix} = \sum_{i=1}^4 C_i \begin{pmatrix} u_i \\ v_i \\ w_i \end{pmatrix} e^{i\gamma\xi - m_i\psi}, \quad (2.79)$$

whereby using (2.77) it is possible to write u_i and w_i as

$$u_i m_i^3 = -v_i (i\gamma) \left[m_i^2 + 2(1 + \nu)\gamma^2\epsilon + 2\frac{1}{m_i^2}\gamma^4(1 + \nu)(2 + \nu)\epsilon^2 \right], \quad (2.80)$$

and

$$w_i m_i = -v_i \left[m_i^2 + \gamma^2\nu\epsilon + \frac{1}{m_i^2}\gamma^4(1 + \nu)^2\epsilon^2 \right]. \quad (2.81)$$

The constants C_i are found from the boundary conditions (2.33). Applying the asymptotic terms to the traction free boundary conditions at $\psi = 0$ in which

$$b_{1j}^{(1A)} = u_j i\nu\gamma\epsilon - v_j m_j + w_j, \quad (2.82a)$$

$$b_{2j}^{(1A)} = \eta^{\frac{1}{4} + \frac{1}{2}q} [-u_j m_j + v_j i\gamma], \quad (2.82b)$$

$$b_{3j}^{(1A)} = \eta^{-\frac{1}{2} - q} [-\eta^{\frac{1}{2} + q} v_j m_j - w_j (m_j^2 - \nu\gamma^2\epsilon)], \quad (2.82c)$$

$$b_{4j}^{(1A)} = \eta^{-\frac{3}{4}(1+2q)} \{ \eta^{\frac{1}{2} + q} v_j [m_j^2 - 2(1 - \nu)\gamma^2\epsilon] - w_j [(2 - \nu)m_j\gamma^2\epsilon - m_j^3] \}, \quad (2.82d)$$

or taking into account (2.80) and (2.81) and neglecting terms $O(\eta\epsilon)$, (2.82) can be rewritten in terms of v as

$$b_{1j}^{(1A)} = v_j \left[-2m_j - \epsilon^2 \frac{\gamma^4}{m_j^3} (1 - \nu^2) \right], \quad (2.83a)$$

$$b_{2j}^{(1A)} = \eta^{\frac{1}{4} - \frac{1}{2}q} v_j 2i\gamma \left[1 + \epsilon \frac{\gamma^2}{m_j^2} (1 + \nu) + \epsilon^2 \frac{\gamma^4}{m_j^4} (1 + \nu)(2 + \nu) \right], \quad (2.83b)$$

$$b_{3j}^{(1A)} = \eta^{-\frac{1}{2} - q} m_j^3 v_j \left[1 + \epsilon^2 \frac{\gamma^4}{m_j^4} (1 + 2\nu) \right], \quad (2.83c)$$

$$b_{4j}^{(1A)} = \eta^{-\frac{3}{4}(1+2q)} m_j^4 v_j \left[1 - 2\epsilon \frac{\gamma^2}{m_j^2} (1 - \nu) + \epsilon^2 \frac{\gamma^4}{m_j^4} (1 + \nu^2) \right]. \quad (2.83d)$$

In comparison with the asymptotics of the super-low frequency Problem 2A investigated in Kaplunov et al. (1999), it has not yet been possible to find an explicit frequency equation for Problem 1A. Instead, the asymptotics investigated thus far will be solved using a numerical scheme and compared with the exact numerical results.

2.6.1 Numerical Results

In this results subsection an additional red dotted line will be used to illustrate the form of the asymptotic approximate result which uses the leading order terms plus some additional smaller ones. A red dashed line will be used to illustrate the approximate forms found by applying a numerical scheme to the asymptotic equations. The graphs for Problem 2A have been omitted as they do not show any significant divergence between asymptotic and numeric forms.

Figure 2.13 shows the numerical and approximate results of problem 1A for $\eta = 0.001$, $\gamma = 2 \sim \eta^{-\frac{1}{10}}$ and $\nu = 0.3$. The displacements decay and oscillate as they approach zero, with the leading order approximate line decaying more rapidly.

Figure 2.14 is for $\gamma = 5 \sim \eta^{-\frac{1}{4}}$. There is greater difference between the approximate and numeric forms with the wave decaying more rapidly. The percentage error for this case is shown in figure 2.15.

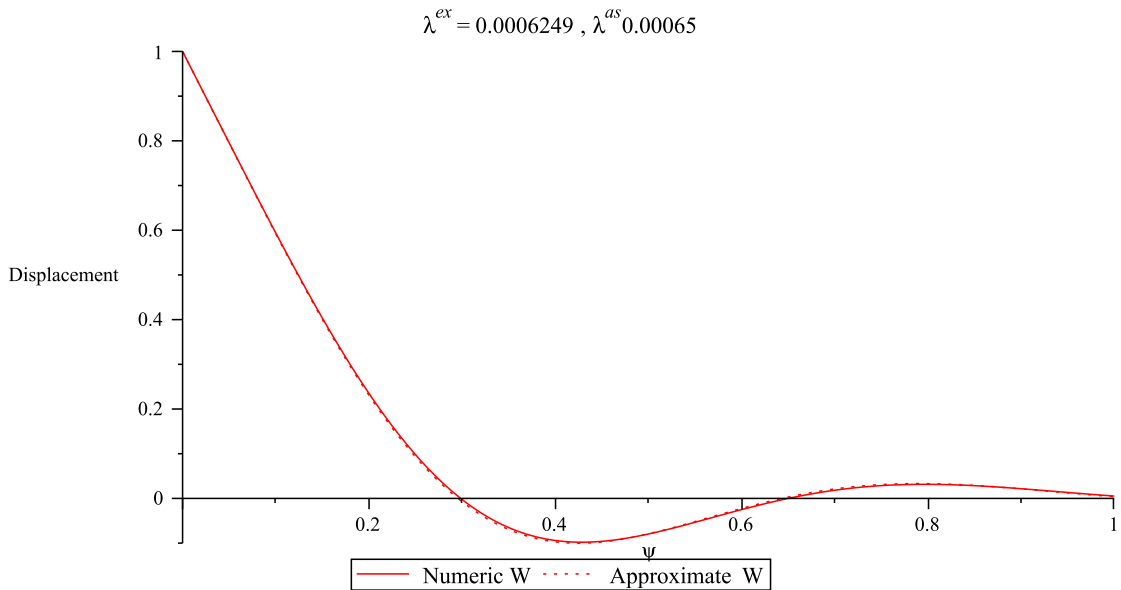


Figure 2.13: Asymptotic approximate and numeric form for the super-low frequency edge wave of Problem 1A with fixed parameters $\eta = 0.001$, $\nu = 0.3$, and $\gamma = 2$

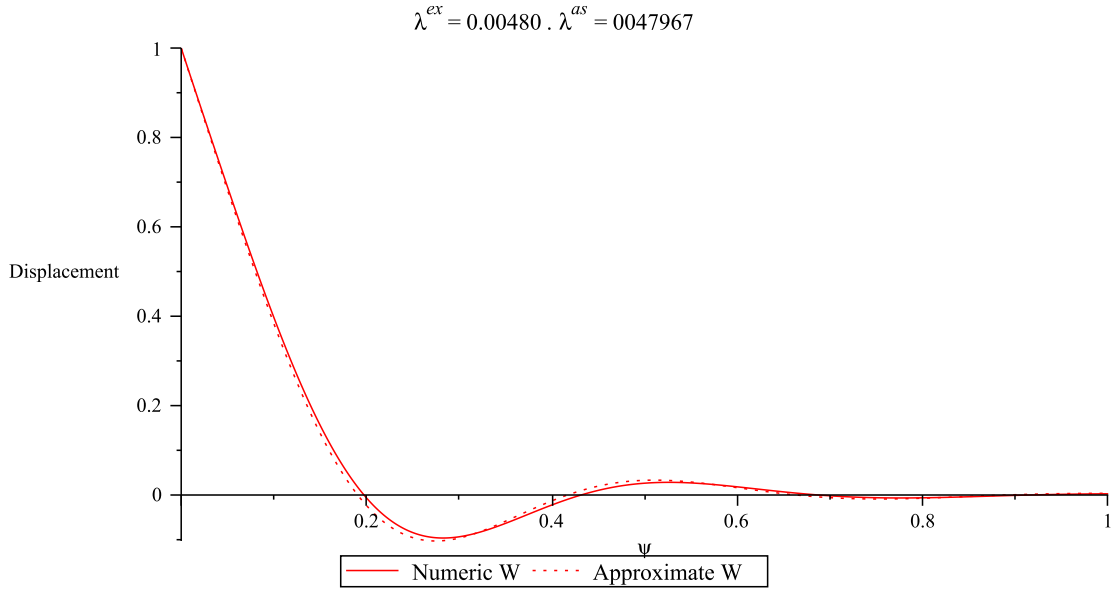


Figure 2.14: Asymptotic approximate and numeric forms for the super-low frequency edge wave of Problem 1A with fixed parameters $\eta = 0.001$, $\nu = 0.3$, and $\gamma = 5$.

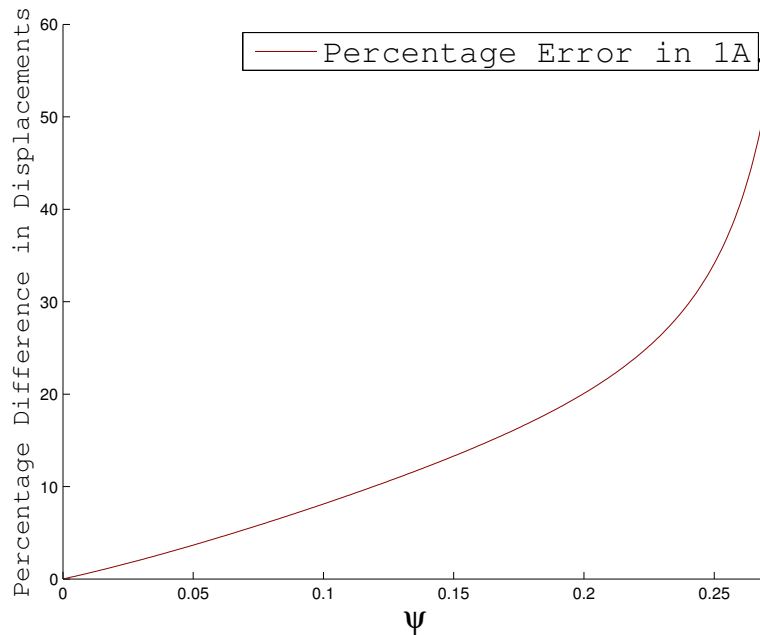


Figure 2.15: Percentage error between asymptotic approximate and numeric form for the super-low frequency edge wave of Problem 1A with fixed parameters $\eta = 0.001$, $\nu = 0.3$, and $\gamma = 5$.

Taking a larger wavenumber, this time $\gamma = 10 \sim \eta^{-\frac{1}{3}}$, the results in Figure 2.16 show that the wave decays quicker as γ increases. The percentage error for

this case is shown in Figure 2.17.

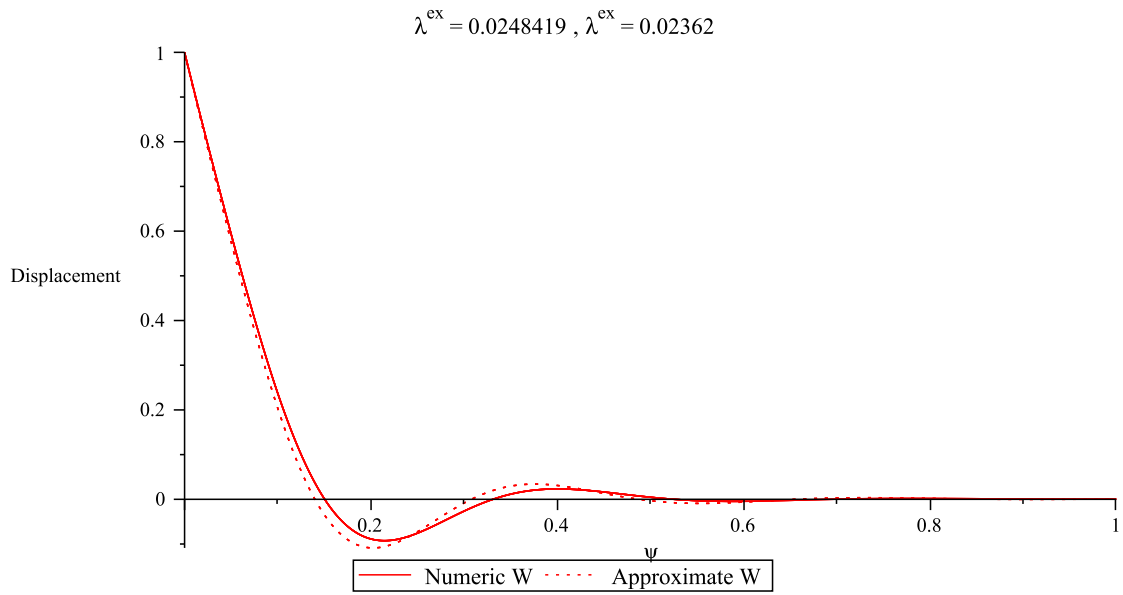


Figure 2.16: Asymptotic approximate and numeric form for the super-low frequency edge wave of Problem 1A with fixed parameters $\eta = 0.001$, $\nu = 0.3$, and $\gamma = 10$.

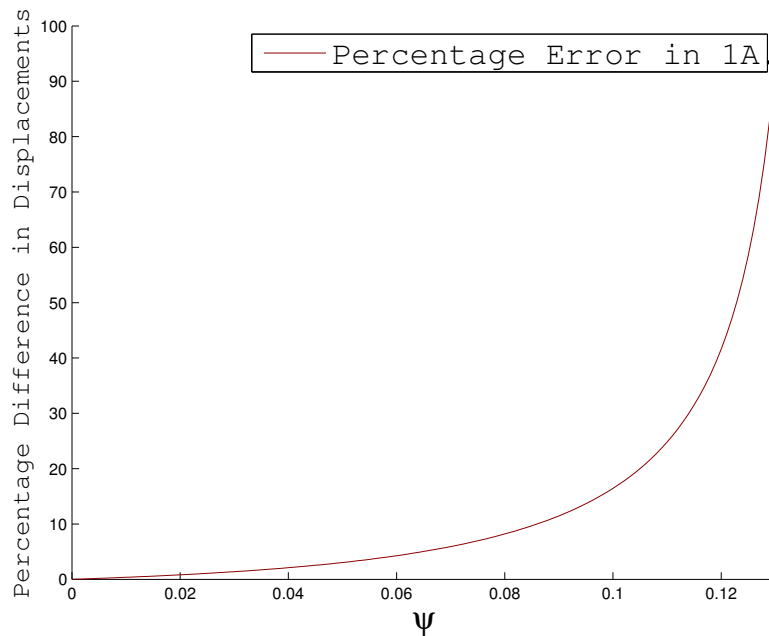


Figure 2.17: Percentage error between asymptotic approximate and numeric form for the super-low frequency edge wave of Problem 1A with fixed parameters $\eta = 0.001$, $\nu = 0.3$, and $\gamma = 10$.

Table 2.3 lists some relevant numerical data with fixed parameters $\eta = 0.001$ and $\nu = 0.3$.

Table 2.3: Natural Frequencies with $\eta = 0.001$, and $\nu = 0.3$

γ, n	1A λ^{ex}	2A λ^{ex}	1A Asymptotic λ^{as}	2A Asymptotic λ^{as}
2	0.000625	0.00000264	0.00000264	0.000653
5	0.004843	0.00020285	0.00020287	0.004797
10	0.02484	0.0035422	0.0035546	0.02362

Chapter 3

Vibration of a Thin Finite Cylindrical Shell

3.1 Statement of the Problem

In this chapter Problems 1A and 2A are modified by the addition of a second edge in the circumferential direction in 1A and the longitudinal direction in 2A, thereby the panels become finite in the direction of decay of the waves. Free and then fixed boundary conditions will be imposed on the second edge, and the numerical results will be compared with the results from chapter 2. These problems will be called problems 1B and 2B.

3.1.1 Problem 1B

Problem 1A is modified so that the effect of a second longitudinal edge at a finite circumferential distance from the first will be taken into account. The mid-surface Γ now occupies the domain $0 \leq \psi \leq \psi_1$ and $-\infty < \xi < \infty$. The edge at $\psi = 0$ remains free, and on the second edge at $\psi = \psi_1$ either traction free or fixed boundary conditions will be imposed.

The governing equations and free boundary conditions at $\psi = 0$ are the same as (2.12) and (2.20) in subsection 2.2.1, and the free or fixed boundary conditions at $\psi = \psi_1$ are

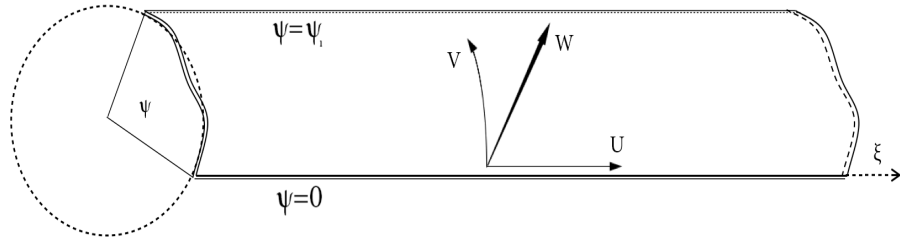


Figure 3.1: Cylinder...

$$\begin{aligned}
 \nu \frac{\partial U}{\partial \xi} + \frac{\partial V}{\partial \psi} - W &= 0, \\
 \frac{\partial U}{\partial \psi} + \frac{\partial V}{\partial \xi} &= 0, \\
 \frac{\partial V}{\partial \psi} + \frac{\partial^2 W}{\partial \psi^2} + \nu \frac{\partial^2 W}{\partial \xi^2} &= 0, \\
 \frac{\partial^2 V}{\partial \psi^2} + 2(1 - \nu) \frac{\partial^2 V}{\partial \xi^2} + \frac{\partial^3 W}{\partial \psi^3} + (2 - \nu) \frac{\partial^3 W}{\partial \psi \partial \xi^2} &= 0,
 \end{aligned} \tag{3.1}$$

or

$$U = 0, \quad V = 0, \quad W = 0, \quad \frac{dW}{d\psi} = 0. \tag{3.2}$$

The same notation is used as in chapter 2.

3.1.2 Problem 2B

Problem 2A is now similarly modified so that the effect of a second circumferential edge at a finite longitudinal distance from the first will be taken into account. The mid-surface Γ now occupies the domain $0 \leq \xi \leq \xi_1$ and $0 \leq \psi \leq 2\pi$. The circumferential edge at $\xi = 0$ remains free, and on the second edge at ξ_1 either traction free or fixed boundary conditions will be imposed.

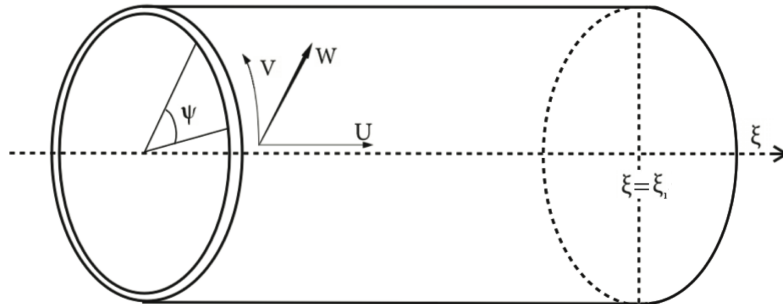


Figure 3.2: Cylinder...

As before, the governing equations and free boundary conditions at $\xi = 0$ are the same as (2.27) and (2.34) in subsection 2.2.2, and the free or fixed boundary

conditions at $\xi = \xi_1$ are

$$\begin{aligned}
 \nu \frac{\partial V}{\partial \psi} - \nu W + \frac{\partial U}{\partial \xi} &= 0, \\
 \frac{\partial U}{\partial \psi} + \frac{\partial V}{\partial \xi} + \frac{4}{3} \eta^2 \left[\frac{\partial V}{\partial \xi} + \frac{\partial^2 W}{\partial \psi \partial \xi} \right] &= 0, \\
 \nu \frac{\partial V}{\partial \psi} + \frac{\partial^2 W}{\partial \xi^2} + \nu \frac{\partial^2 W}{\partial \psi^2} &= 0, \\
 \frac{\partial^3 W}{\partial \xi^3} + (2 - \nu) \frac{\partial^3 W}{\partial \psi^2 \partial \xi} + (2 - \nu) \frac{\partial^2 V}{\partial \psi \partial \xi} &= 0,
 \end{aligned} \tag{3.3}$$

or

$$U = 0, \quad V = 0, \quad W = 0, \quad \frac{dW}{d\xi} = 0. \tag{3.4}$$

3.2 Exact Solution

3.2.1 Problem 1B

A solution to this problem can now be written as

$$\begin{pmatrix} U(\psi, \xi) \\ V(\psi, \xi) \\ W(\psi, \xi) \end{pmatrix} = \sum_{i=1}^8 \tilde{c}_i \begin{pmatrix} u_i \\ v_i \\ w_i \end{pmatrix} e^{\gamma \xi i - m_i \psi}, \tag{3.5}$$

where for computational convenience

$$\tilde{c}_i = \begin{cases} c_i & \text{for } i = 1..4 \\ c_i e^{m_i \psi_1} & \text{for } i = 5..8, \end{cases} \tag{3.6}$$

and

$$m_i = \begin{cases} \Re(m_i) > 0, \text{ or if } \Re(m_i) = 0 \text{ then } \Im(m_i) > 0 & \text{for } i = 1..4, \\ \Re(m_i) < 0, \text{ or if } \Re(m_i) = 0 \text{ then } \Im(m_i) < 0 & \text{for } i = 5..8. \end{cases} \tag{3.7}$$

A similar procedure to chapter 2 is followed in substituting (3.5) into (2.4), however this gives an eigenmatrix in m of order 8x8. Once the roots and constants are found, these must then be substituted into the boundary conditions, giving a more complicated eigenmatrix of 16x16. The solution to this problem, taking into account the second longitudinal edge, can only be numerically computed.

3.2.2 Problem 2B

A possible solution to this problem takes the form

$$\begin{pmatrix} U(\psi, \xi) \\ V(\psi, \xi) \\ W(\psi, \xi) \end{pmatrix} = \sum_{i=1}^8 \tilde{c}_i \begin{pmatrix} u_i \\ v_i \\ w_i \end{pmatrix} e^{-r_i \xi} \sin n\psi, \quad (3.8)$$

where again for computational convenience

$$\tilde{c}_i = \begin{cases} c_i & \text{for } i = 1..4 \\ c_i e^{r_i \xi_1} & \text{for } i = 5..8, \end{cases} \quad (3.9)$$

and

$$r_i = \begin{cases} \Re(r_i) > 0, \text{ or if } \Re(r_i) = 0 \text{ then } \Im(r_i) > 0 & \text{for } i = 1..4, \\ \Re(r_i) < 0, \text{ or if } \Re(r_i) = 0 \text{ then } \Im(r_i) < 0 & \text{for } i = 5..8. \end{cases} \quad (3.10)$$

This also leads to two eigenvalue problems, the first of order 8x8 in r , which leads to the essential eigen problem using the boundary conditions, to be solved numerically.

3.3 Numerical Results for Flexural Vibration

3.3.1 Free-Free

Figures 3.3 and 3.4 illustrate the comparison between both problems 1B and 2B and their asymptotics, for $\eta = 0.01$, $\nu = 0.45$, $\gamma = 30$ and length $\psi, \xi = 4$. The asymptotics work very well here and the dashed lines are hardly visible.

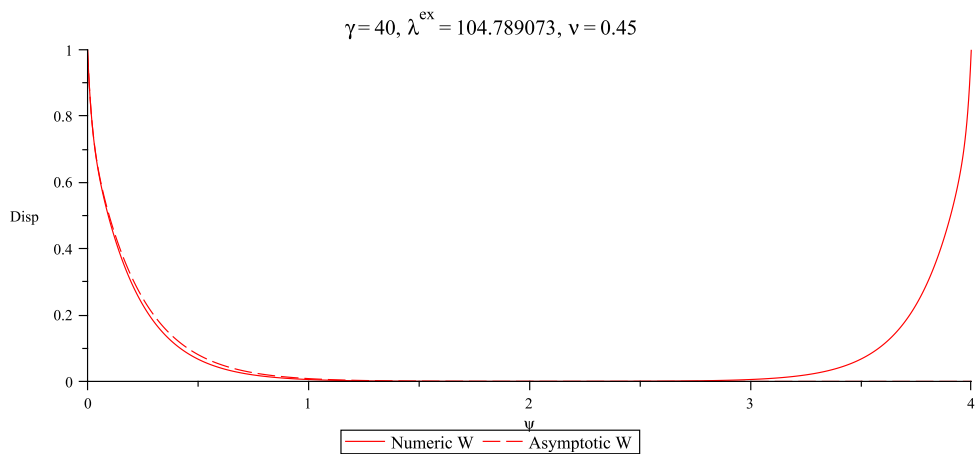


Figure 3.3: 1B

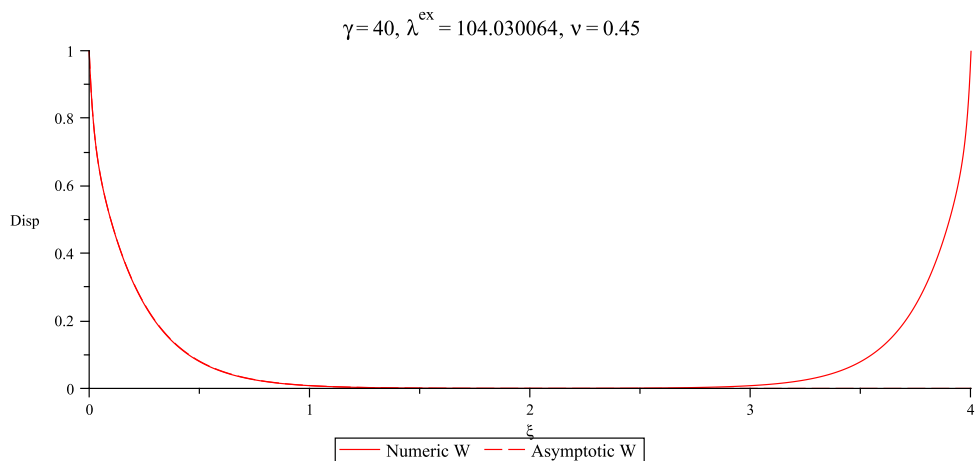


Figure 3.4: 2B

Table 3.1 shows the exact frequencies of Problems 1B and 2B for $\eta = 0.01$, $\nu = 0.3$ and $\gamma = 30$. The panel length ψ in Problem 1B, and shell length ξ in Problem 2B are varied from 1 to 4. The errors ϵ_1 and ϵ_2 are the difference between the frequencies of 1A,2A and 1B,2B.

Table 3.1: Natural Frequencies, $\eta = 0.01$, $\nu = 0.3$, and $\gamma = 30$

ψ, ξ	1B λ^{ex}	2B λ^{ex}
1	30.552841	29.354299
2	30.333525	29.428899
3	30.320804	29.447651
4	30.319437	29.447652

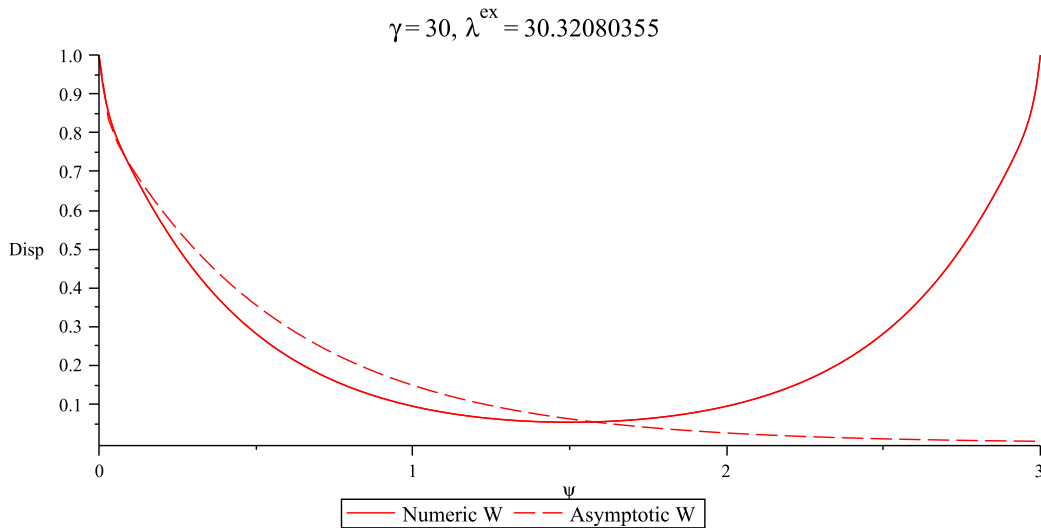


Figure 3.5: 1A

Figures 3.5 and 3.6 show the asymptotics and numerics for a length of $\psi, \xi = 3$ with $\eta = 0.01$, $\nu = 0.3$ and $\gamma = 30$ in Problems 1B and 2B.

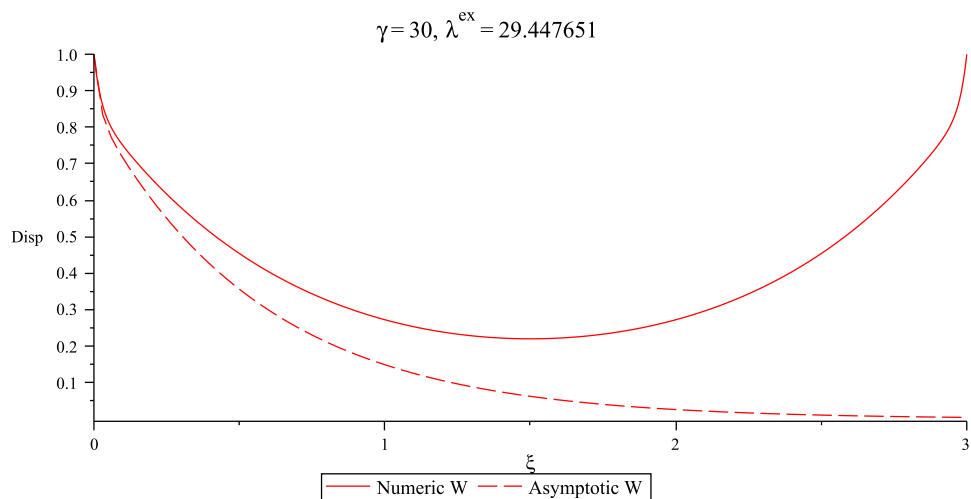


Figure 3.6: 2B

Examining a slightly longer distance of $\psi, \xi = 4$ in Figures (3.7) and (3.8) shows that the asymptotics improves for 2B but not for 1B.

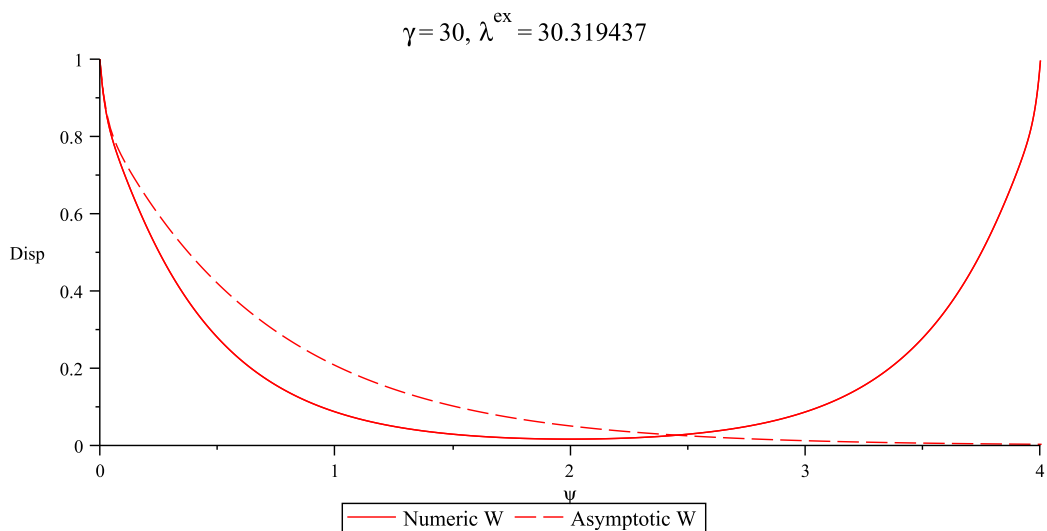


Figure 3.7: 1B

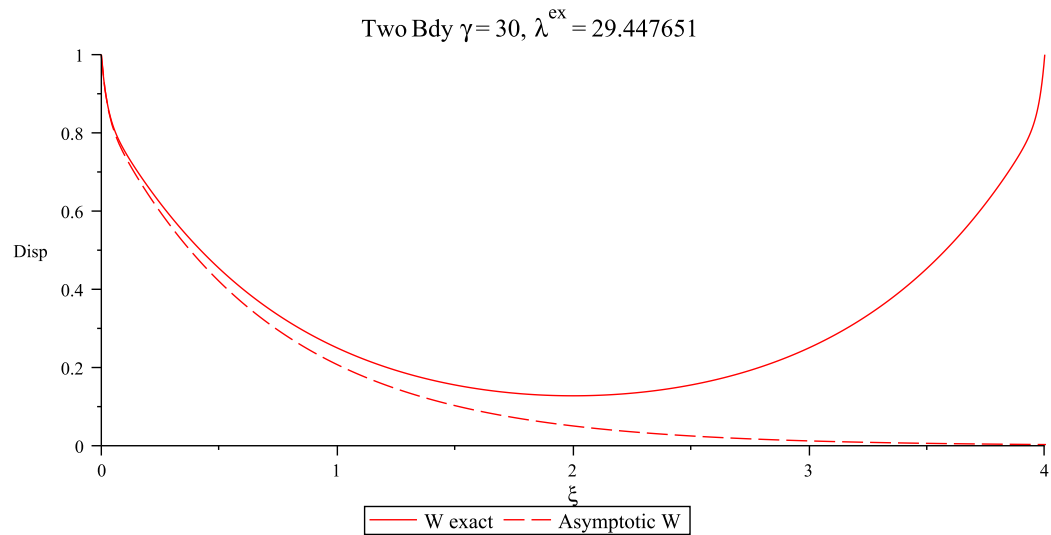


Figure 3.8: 2B

The effect of changing edge wavelength is minimal on the behaviour of vibration in 1B, as γ and λ increase, the vibration decays slightly slower. However in 2B the increase in edge wavelength increases the rate of decay.

3.3.2 Free-Fixed

For larger γ there is more accuracy between asymptotics and numerics so it is not necessary to visit graphs of $\gamma = 40$ again. Figure 3.9 for $\gamma = 25 \sim \eta^{-\frac{2}{3}}$ and $\psi, \xi = 1$ shows a smooth decay to the fixed edge of the numerics, however as expected the asymptotics are not so accurate.

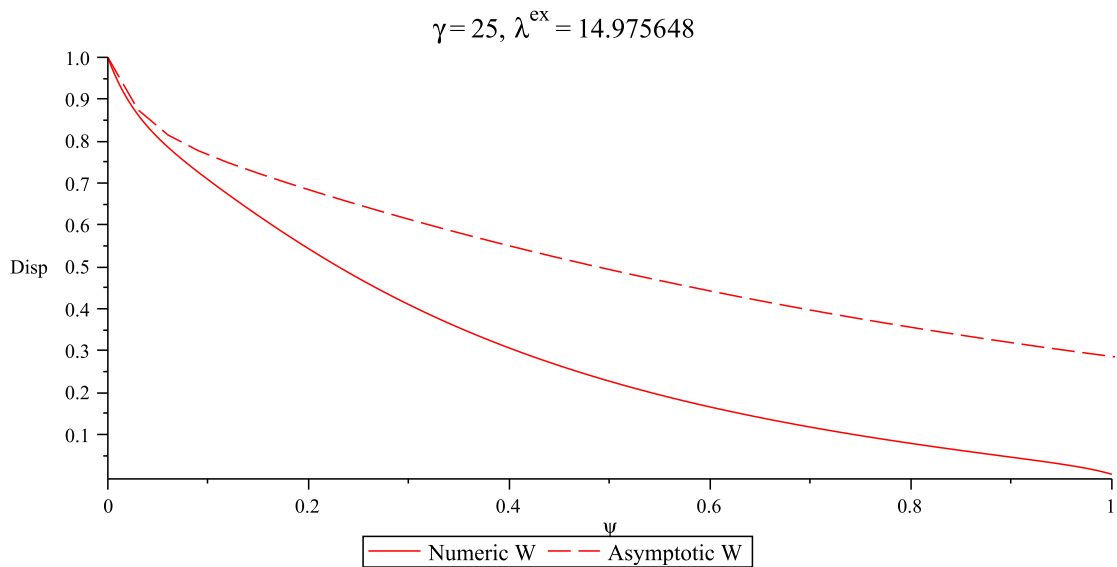


Figure 3.9: 1B

Similarly, Figure (3.10) for 2B shows the influence of the second fixed edge on the decay of the solution. Although decay is smooth, the fixed edge has some effect. Longer distances improve the accuracy of the asymptotics for Problem 2B, but not so for Problem 1A.

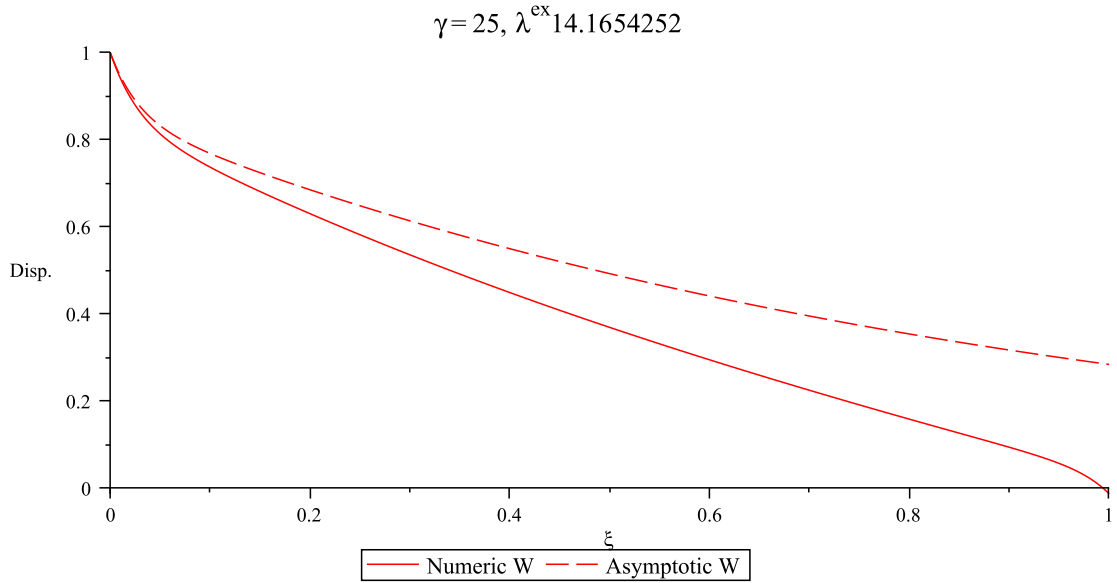


Figure 3.10: 1B

Figures (3.11) and (3.12) show a shorter and longer length of $\psi, \xi = 0.5$ and $\psi, \xi = 2$. It is clear that in all cases the decay is smooth and the effect of the fixed edge decreases as length increases. For problem 2B the asymptotics work well.

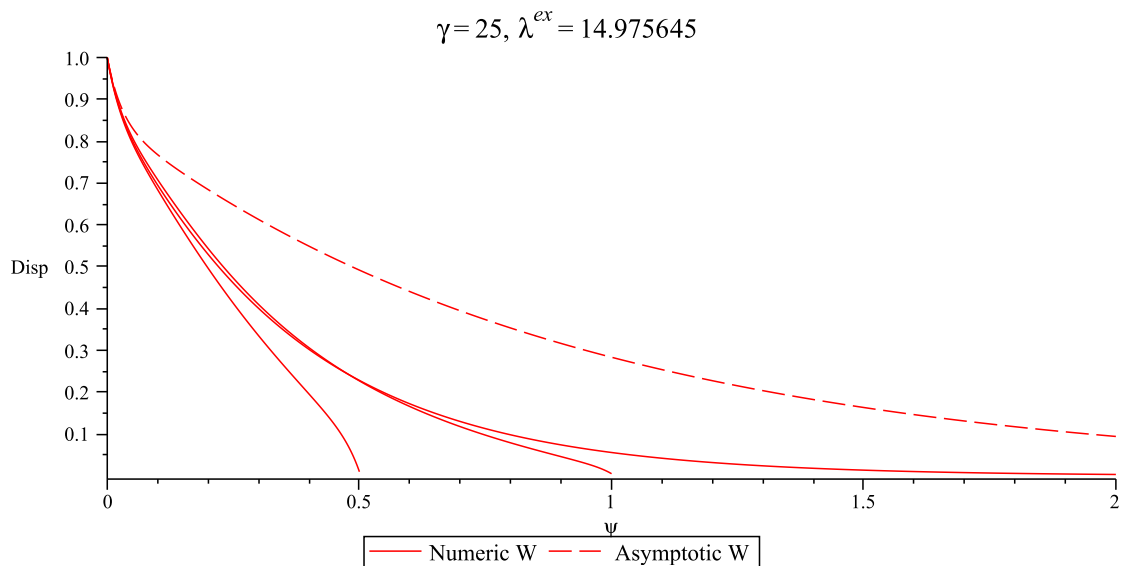


Figure 3.11: 1B

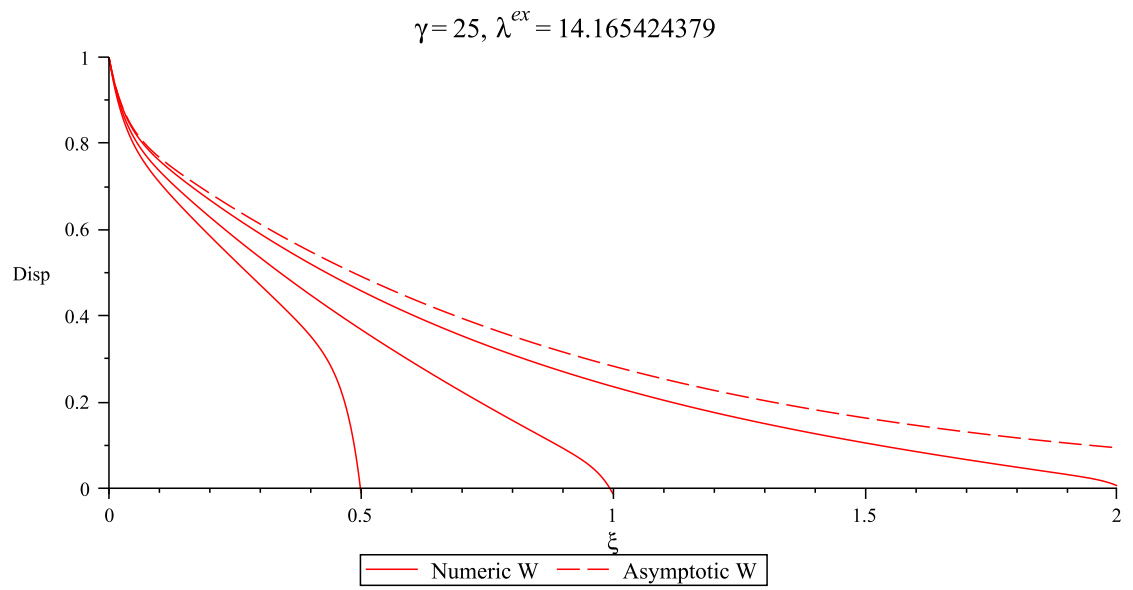


Figure 3.12: 2B

3.4 Numerical Results for Extensional Vibration

3.4.1 Free-Free

The results for extensional vibration observed in the previous chapter showed that the graphs are pretty similar. When a second free edge is introduced, although frequencies slightly differ, the leading order asymptotic forms remain accurate. For this section one graph per case will be shown as the graphs for Problems 1B and 2B are very visibly similar. Where in the legends of the graphs it is written ‘numeric,asymptotic U, V ’ it means that the corresponding line is U for Problem 1B and V for Problem 2B, and visa versa. They are not the same, but only visibly similar.

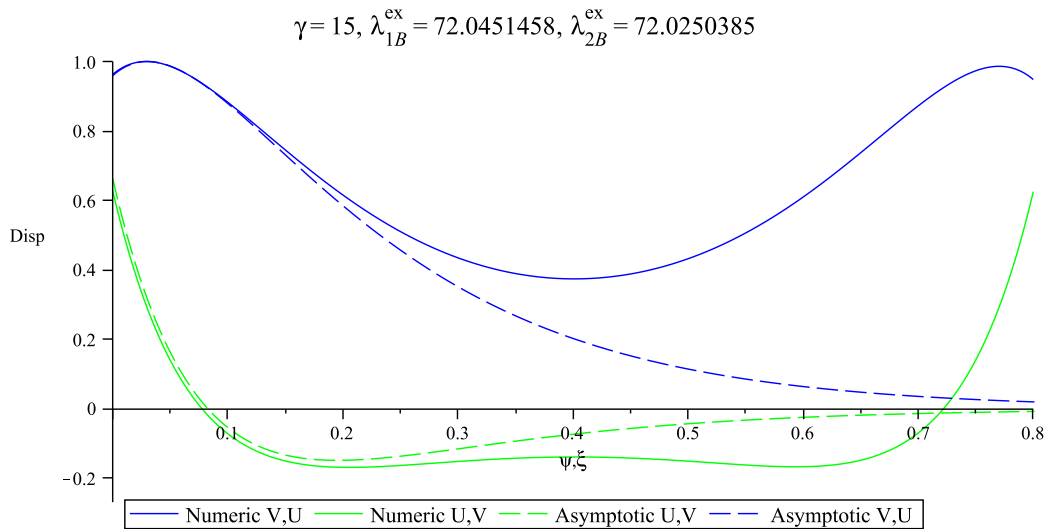


Figure 3.13: 1C

Figure (3.13) with $\eta = 0.001$, $\nu = 0.3$, $\gamma = 15 \sim \eta^{\frac{2}{3}}$ and $\psi, \xi = 0.8$, shows that the asymptotics are accurate within a short length, however within this distance the second boundary has a large effect. When the length of the panel is increased to $\psi, \xi = 3$ the asymptotics become more accurate as seen in Figure 3.14. In fact, the dashed asymptotic lines cannot even be seen.

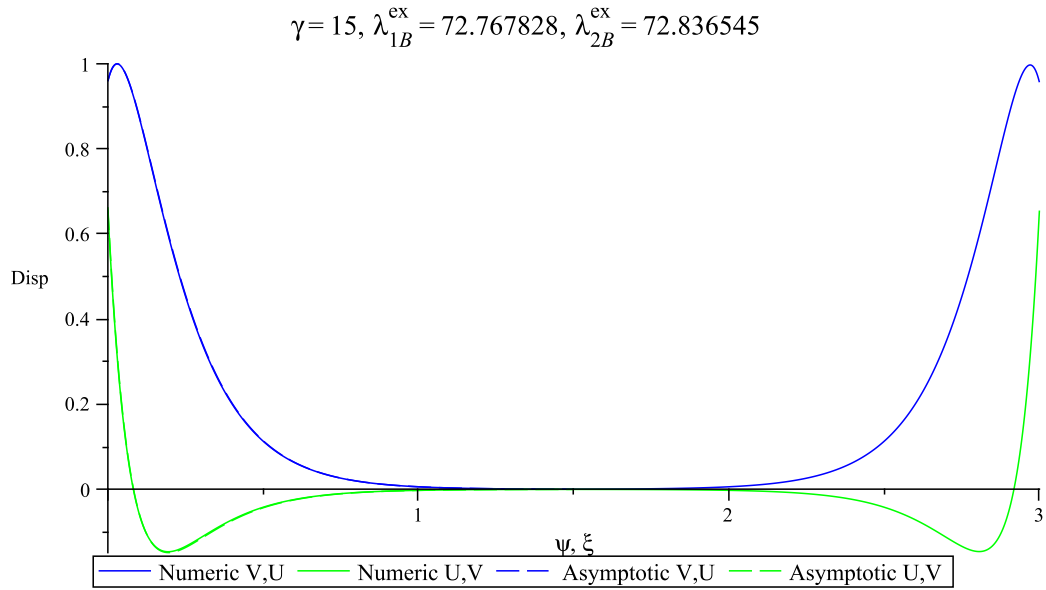


Figure 3.14: 1B and 2B

3.4.2 Free-Fixed

Fixed boundary conditions on the other edge do not significantly affect the difference between the leading order extensional vibration for 1B and 2B. Figure 3.15 is for $\gamma = 15$ and $\psi, \xi = 0.4$. Although this is a very short length, close to $\psi, \xi = 0$ the asymptotics are reliable.

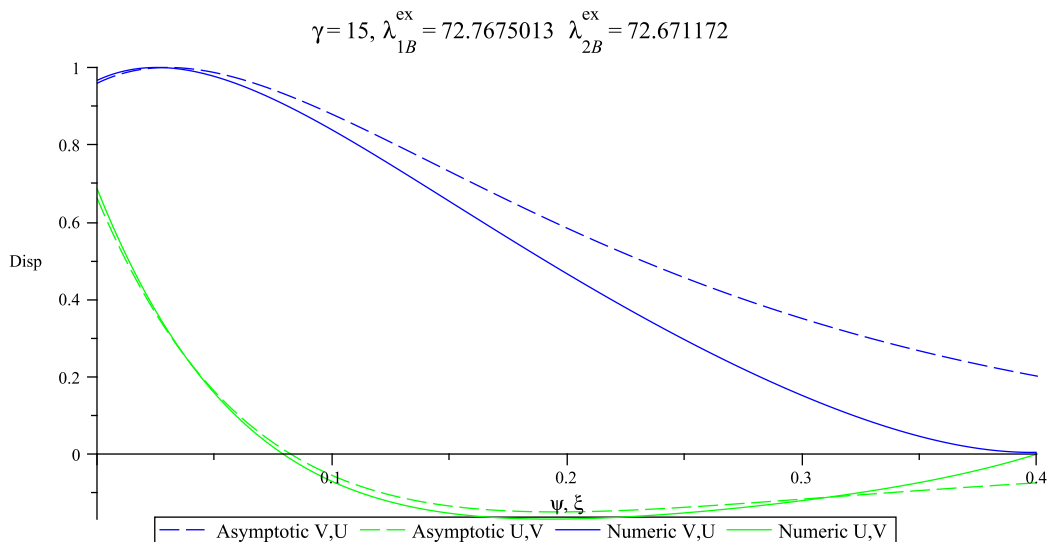


Figure 3.15: 1B and 2B

For a longer panel length of $\psi, \xi = 1.5$, Figure 3.16 shows that the asymptotics are very accurate.

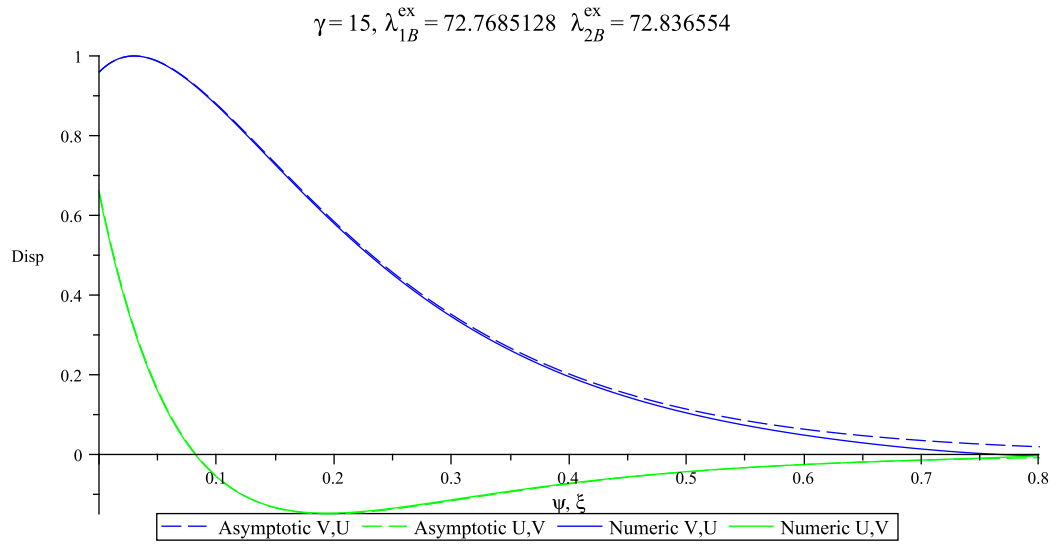


Figure 3.16: 1B and 2B

3.5 Numerical Results for Super-Low Frequency

3.5.1 Free-Free

In the previous chapter it was seen that the curvature of the panel greatly increases the decay of the wave in Problem 1A, whereas in Problem 2A without the effect of curvature the decay is much slower in comparison. Figure (3.17) shows the effect of the second free edge on the super-low frequency vibration at a length of $\psi, \xi = 1$, with $\eta = 0.001$, $\nu = 0.3$ and $\gamma = 10$.

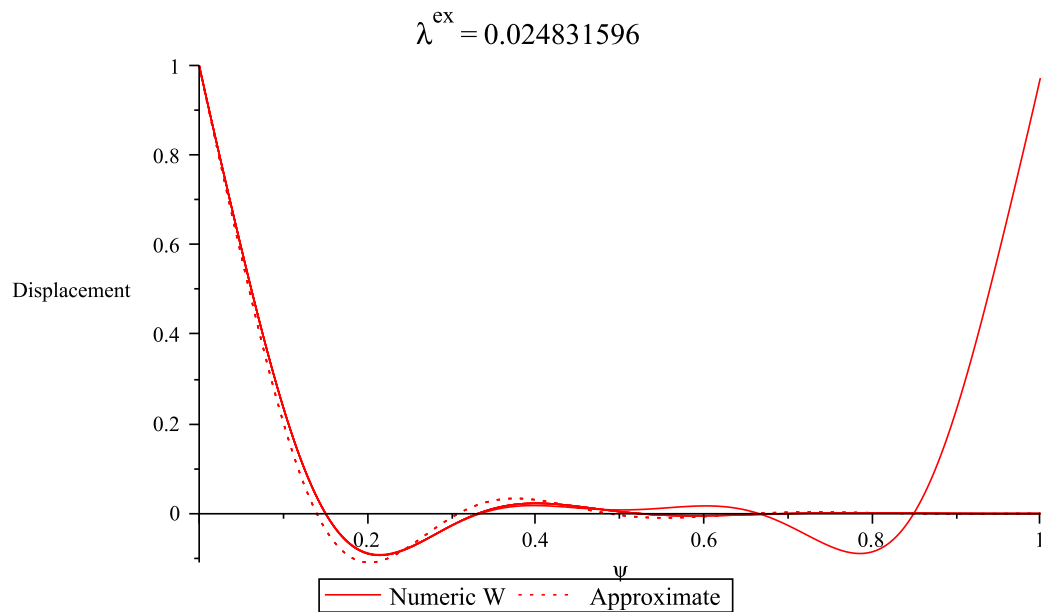


Figure 3.17: Asymptotic approximate and numeric form for the super-low frequency edge wave of Problem 1B with fixed parameters $\eta = 0.001$, $\nu = 0.3$, and $\gamma = 10$

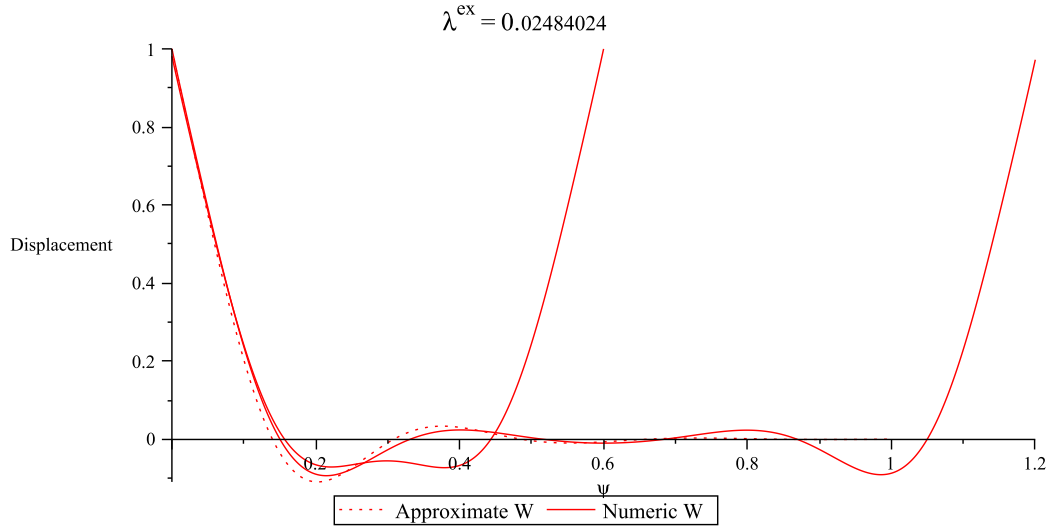


Figure 3.18: Asymptotic approximate and numeric form for the super-low frequency edge wave of Problem 1B with fixed parameters $\eta = 0.001$, $\nu = 0.3$, and $\gamma = 10$

Figure 3.18 for similar values to before, except with $\psi, \xi = 0.5$ and $\psi, \xi = 1.4$. As was found in subsection 2.5.3, changes in ν in Problem 1A had very little effect on the form of W . Again the same result is observed here.

For the same values of ν , η and γ , but a shell length of $\xi = 11$, Figures 3.19 for $\xi = 5$ and 3.20 for $\xi = 11$ show that the asymptotics are reasonably accurate over short shell lengths. Although both numeric and asymptotic curves seem to decay at a similar rate, the numerics indicate that there is some behaviour very close to the boundaries which affects the initial decay. This could be due to numerical error. As the shell length increases, however, the asymptotic and numeric lines become closer. Furthermore, results with change of ν do not affect the wave much.

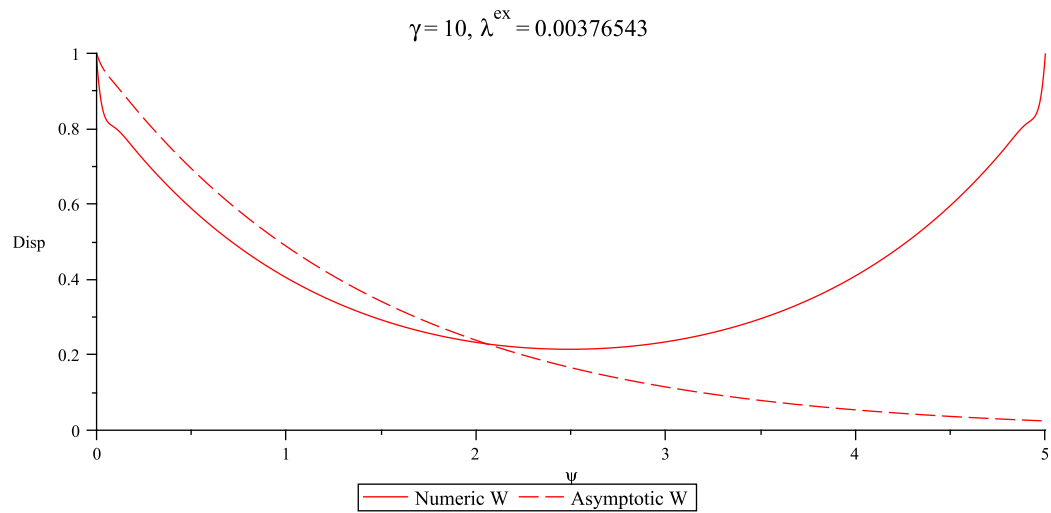


Figure 3.19: Asymptotic approximate and numeric form for the super-low frequency edge wave of Problem 2B with fixed parameters $\eta = 0.001$, $\nu = 0.3$, and $\gamma = 10$

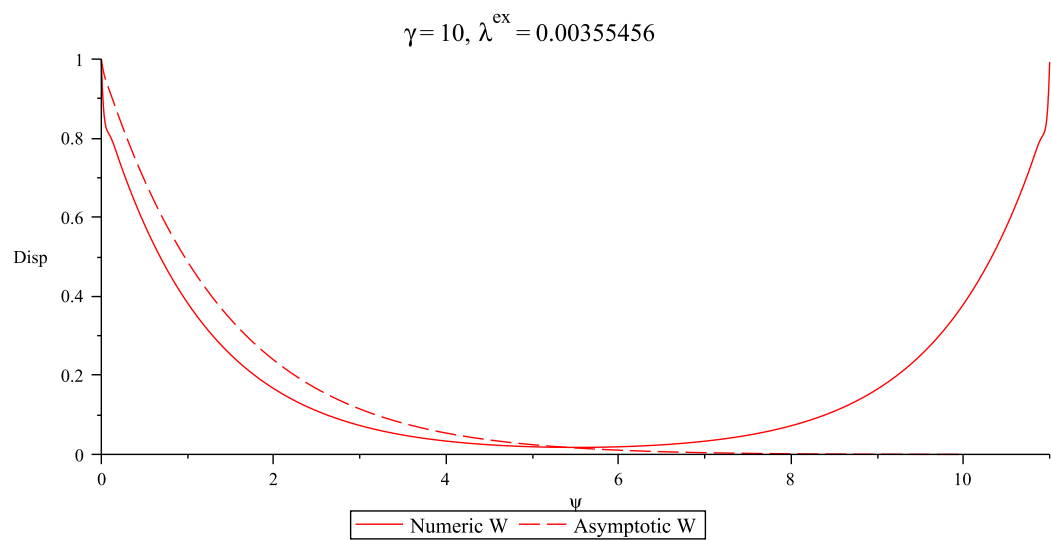


Figure 3.20: 2B

3.5.2 Free-Fixed

Figure 3.21 is for $\gamma = 10$ and $\psi = 0.7$. All results here are similar to this and subsection 2.5.3 due to the rapid decay of the wave in Problem 1A.

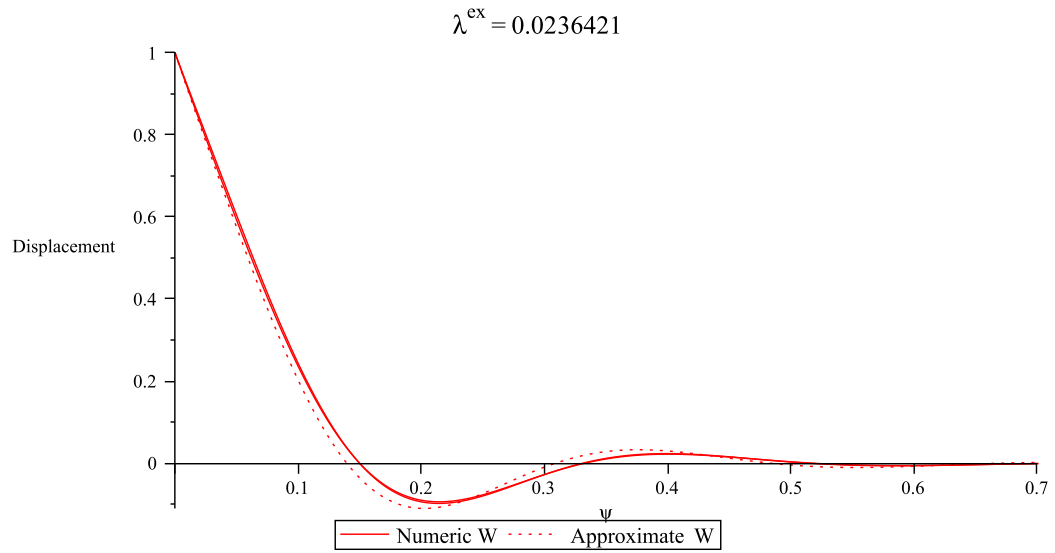


Figure 3.21: 1A

Chapter 4

Interfacial Vibration of Composite Cylindrical Shell

4.1 Statement of the Problem

In this chapter Problems 1A and 2A are extended by considering a simplified formulation of free interfacial vibration occurring at the joint, or perfect bond, of two non homogeneous cylindrical panels of the same curvature and thickness but different material properties, without taking into account the effects of a second edge on both smaller panels. These formulations will be called Problem 1C and 2C.

4.1.1 Problem 1C

Consider free harmonic vibrations of a circumferentially non homogeneous, infinite, isotropic, cylindrical panel which is composed of two panels of the same curvature and thickness which are perfectly bonded at their respective longitudinal edges, and are each homogeneous and isotropic. The surface is composed of two surfaces Γ_1 and Γ_2 which occupy the domains $0 \leq \psi < a$, $-\infty < \xi < \infty$ and $-b < \psi \leq 0$, $-\infty < \xi < \infty$ respectively. The values a and b are constant, and in this simplified set up similar to problem 1A, assume that $a \rightarrow \infty$ and $b \rightarrow -\infty$. The panels corresponding to Γ_1 and Γ_2 will be called panels 1 and 2 respectively. The non homogeneous panel that is formed is infinite in the circumferential direction, with one edge which is located at the interface $\psi = 0$.

The waves are localised at the perfect join, propagate along the longitudinal edge and decay in the circumferential direction away from the join in the positive and negative circumferential directions. In this simplified set up in which the effect of a second and third longitudinal edge, which make the panel finite, are not taken into account. However, as the waves are localised at the longitudinal join, this does become a good approximation as the circumferential length becomes large and the waves are localised at the join $\psi = 0$ and decay to infinity.

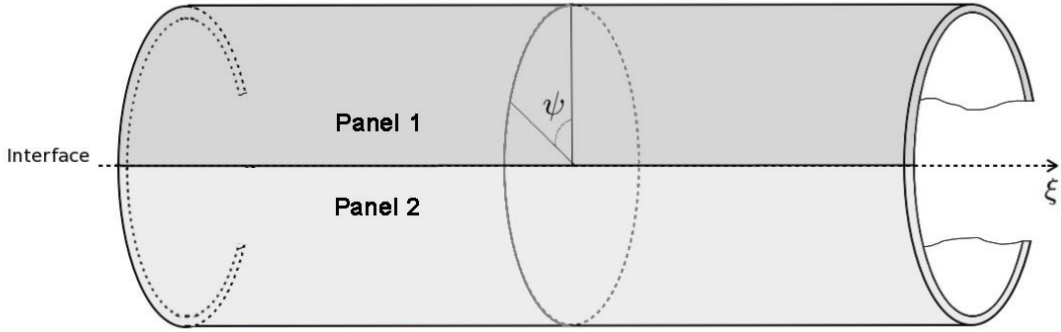


Figure 4.1

4.1.2 Problem 2C

This problem is studied in Kaplunov and Wilde (2002) and is replicated here for comparison. The authors considered free harmonic vibrations of a longitudinally non homogeneous, isotropic, infinite circular cylindrical shell composed of two semi-infinite homogeneous shells of the same curvature and thickness, which are perfectly joined together at their respective circumferential edges, and are each homogeneous, isotropic, and semi-infinite in the longitudinal direction. The mid-surface Γ occupies the domain $-\infty < \xi < \infty$ and $0 \leq \psi \leq 2\pi$. The panel corresponding to $\xi \geq 0$ will be called panel 1, and the panel corresponding to $\xi \leq 0$ will be called panel 2. The non homogeneous panel which is formed is infinite in its longitudinal direction with one edge which is located at the interface at $\xi = 0$. The waves are localised at the perfect join, propagate along the circumferential edge and decay in the longitudinal direction away from the join in both the positive and negative longitudinal directions, $\xi \rightarrow \pm\infty$.

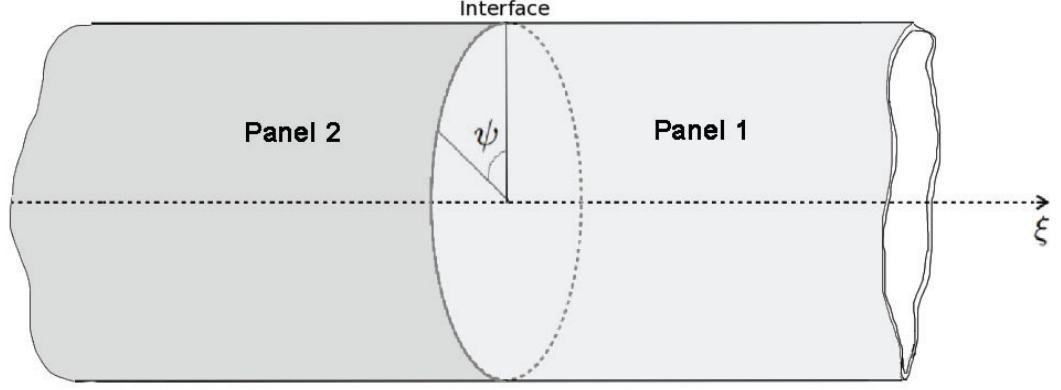


Figure 4.2

4.1.3 Equations of Motion

The governing equations from the Kirchhoff-Love theory of shells (2.4) can be rewritten as

$$\frac{\partial^2 U^{(k)}}{\partial^2 \xi} + \frac{1 - \nu^{(k)}}{2} \frac{\partial^2 U^{(k)}}{\partial \psi^2} + \frac{1 + \nu^{(k)}}{2} \frac{\partial^2 V^{(k)}}{\partial \psi \partial \xi} - \nu^{(k)} \frac{\partial W^{(k)}}{\partial \xi} + \lambda \bar{\rho}^{(k)} (1 - \nu^{(k)^2}) U^{(k)} = 0, \quad (4.1)$$

$$\begin{aligned} & \frac{\partial^2 V^{(k)}}{\partial \psi^2} + \frac{1 - \nu^{(k)}}{2} \frac{\partial^2 V^{(k)}}{\partial \xi^2} + \frac{1 + \nu^{(k)}}{2} \frac{\partial^2 U^{(k)}}{\partial \xi \partial \psi} - \frac{\partial W^{(k)}}{\partial \psi} \\ & + \frac{\eta^2}{3} \left[2(1 - \nu^{(k)}) \frac{\partial^2 V^{(k)}}{\partial \xi^2} + \frac{\partial^2 V^{(k)}}{\partial \psi^2} + \frac{\partial^3 W^{(k)}}{\partial \psi^3} + (2 - \nu) \frac{\partial^3 W^{(k)}}{\partial \xi^2 \partial \psi} \right] + \lambda \bar{\rho}^{(k)} (1 - \nu^{(k)^2}) V^{(k)} = 0, \end{aligned} \quad (4.2)$$

$$\begin{aligned} & \nu^{(k)} \frac{\partial U^{(k)}}{\partial \xi} + \frac{\partial V^{(k)}}{\partial \psi} - W^{(k)} - \frac{\eta^2}{3} \left[\frac{\partial^4 W^{(k)}}{\partial \xi^4} + 2 \frac{\partial^4 W^{(k)}}{\partial \xi^2 \partial \psi^2} \right. \\ & \left. + \frac{\partial^4 W^{(k)}}{\partial \psi^4} + \frac{\partial^3 V^{(k)}}{\partial \psi^3} + (2 - \nu^{(k)}) \frac{\partial^3 V^{(k)}}{\partial \xi^2 \partial \psi} \right] + \lambda \bar{\rho}^{(k)} (1 - \nu^{(k)^2}) W^{(k)} = 0, \end{aligned} \quad (4.3)$$

where superscript $k = 1, 2$ corresponds to panels 1 and 2 respectively, and non-dimensional frequency λ and the material parameter $\bar{\rho}$ are defined as

$$\lambda = \frac{\rho^{(1)} \omega^2 R^2}{E^{(1)}}, \quad \bar{\rho}^{(k)} = \bar{E}^{(k)} \frac{\rho^{(k)}}{\rho^{(1)}}, \quad (4.4)$$

where

$$\bar{E}^{(k)} = \frac{E^{(1)}}{E^{(k)}}. \quad (4.5)$$

All other parameters are as chapter 2 except that they are now with superscript k .

4.1.4 Perfect Contact Boundary Conditions

Problem 1C

The boundary conditions at $\psi = 0$, the join between panels 1 and 2 at their respective longitudinal edges are written as

$$U^{(1)} - U^{(2)} = 0, \quad V^{(1)} - V^{(2)} = 0, \quad W^{(1)} - W^{(2)} = 0, \quad \frac{\partial W^{(1)}}{\partial \psi} - \frac{\partial W^{(2)}}{\partial \psi} = 0, \quad (4.6)$$

$$bd1^{(1)} - bd1^{(2)} = 0, \quad bd2^{(1)} - bd2^{(2)} = 0, \quad bd3^{(1)} - bd3^{(2)} = 0, \quad bd4^{(1)} - bd4^{(2)} = 0, \quad (4.7)$$

where

$$\begin{aligned} bd1^{(k)} &= \frac{1}{(1 - \nu^{(k)2})\bar{E}^{(k)}} \left(\nu^{(k)} \frac{\partial U^{(k)}}{\partial \xi} + \frac{\partial V^{(k)}}{\partial \psi} - W^{(k)} \right), \\ bd2^{(k)} &= \frac{1}{2(1 + \nu^{(k)})\bar{E}^{(k)}} \left(\frac{\partial U^{(k)}}{\partial \psi} + \frac{\partial V^{(k)}}{\partial \xi} \right), \\ bd3^{(k)} &= \frac{\eta^2}{3(1 - \nu^{(k)2})\bar{E}^{(k)}} \left(\frac{\partial V^{(k)}}{\partial \psi} + \frac{\partial^2 W^{(k)}}{\partial \psi^2} + \nu^{(k)} \frac{\partial^2 W^{(k)}}{\partial \xi^2} \right), \\ bd4^{(k)} &= - \frac{\eta^2}{3(1 - \nu^{(k)2})\bar{E}^{(k)}} \left(\frac{\partial^2 V^{(k)}}{\partial \psi^2} + 2(1 - \nu^{(k)}) \frac{\partial^2 V^{(k)}}{\partial \xi^2} + \frac{\partial^3 W^{(k)}}{\partial \psi^3} + (2 - \nu^{(k)}) \frac{\partial^3 W^{(k)}}{\partial \psi \partial \xi^2} \right), \end{aligned}$$

and with $\bar{E}^{(k)} = \frac{E^{(1)}}{E^{(k)}}$.

Problem 2C

At the join between the respective circumferential edges of the two panels, $\xi = 0$, boundary conditions for perfect contact take the form

$$U^{(1)} - U^{(2)} = 0, \quad V^{(1)} - V^{(2)} = 0, \quad W^{(1)} - W^{(2)} = 0, \quad \frac{\partial W^{(1)}}{\partial \xi} - \frac{\partial W^{(2)}}{\partial \xi} = 0, \quad (4.8)$$

$$bd1^{(1)} - bd1^{(2)} = 0, \quad bd2^{(1)} - bd2^{(2)} = 0, \quad bd3^{(1)} - bd3^{(2)} = 0, \quad bd4^{(1)} - bd4^{(2)} = 0, \quad (4.9)$$

where the following notation is used

$$\begin{aligned}
 bd1^{(k)} &= \frac{1}{(1 - \nu^{(k)^2})\bar{E}^{(k)}} \left(\frac{\partial U^{(k)}}{\partial \xi} + \nu^{(k)} \frac{\partial V^{(k)}}{\partial \psi} - \nu^{(k)} W^{(k)} \right), \\
 bd2^{(k)} &= \frac{1}{2(1 + \nu^{(k)})\bar{E}^{(k)}} \left(\frac{\partial U^{(k)}}{\partial \psi} + \frac{\partial V^{(k)}}{\partial \xi} + \frac{2}{3}\eta^2 \left(\frac{\partial V^{(k)}}{\partial \xi} + \frac{\partial^2 W^{(k)}}{\partial \psi \partial \xi} \right) \right), \\
 bd3^{(k)} &= \frac{\eta^2}{3(1 - \nu^{(k)^2})\bar{E}^{(k)}} \left(\nu^{(k)} \frac{\partial V^{(k)}}{\partial \psi} + \frac{\partial^2 W^{(k)}}{\partial \xi^2} + \nu^{(k)} \frac{\partial^2 W^{(k)}}{\partial \psi^2} \right), \\
 bd4^{(k)} &= - \frac{\eta^2}{3(1 - \nu^{(k)^2})\bar{E}^{(k)}} \left((2 - \nu^{(k)}) \frac{\partial^2 V^{(k)}}{\partial \xi \partial \psi} + \frac{\partial^3 W^{(k)}}{\partial \xi^3} + (2 - \nu^{(k)}) \frac{\partial^3 W^{(k)}}{\partial \psi^2 \partial \xi} \right),
 \end{aligned}$$

4.2 Exact Solution

4.2.1 Problem 1C

A possible solution to the governing equation (4.3) can be written as

$$\begin{pmatrix} U^{(k)}(\psi, \xi) \\ V^{(k)}(\psi, \xi) \\ W^{(k)}(\psi, \xi) \end{pmatrix} = \begin{pmatrix} u^{(k)} \\ v^{(k)} \\ w^{(k)} \end{pmatrix} e^{i\gamma\xi + (-1)^k m^{(k)}\psi}, \quad (4.10)$$

where the longitudinal wavenumber γ is given, $u^{(k)}$, $v^{(k)}$, and $w^{(k)}$ are constants, and m should satisfy (2.10) taking into account decay at ∞ .

Substituting this into (4.3) yields the linear system

$$\begin{aligned}
 u^{(k)} \left[m^{(k)^2} \left(\frac{1 - \nu^{(k)}}{2} \right) + \lambda \bar{\rho}^{(k)} (1 - \nu^{(k)^2}) - \gamma^2 \right] \\
 + v^{(k)} \left[i m^{(k)} \gamma \left(\frac{1 + \nu^{(k)}}{2} \right) \right] + w^{(k)} [i \gamma \nu^{(k)}] = 0,
 \end{aligned} \quad (4.11a)$$

$$\begin{aligned}
 u^{(k)} \left[i m^{(k)} \gamma \left(\frac{1 + \nu^{(k)}}{2} \right) \right] + v^{(k)} \left[m^{(k)^2} \left(\frac{\eta^2}{3} + 1 \right) + \lambda \bar{\rho}^{(k)} (1 - \nu^{(k)^2}) \right. \\
 \left. - \gamma^2 \left(\frac{1 - \nu^{(k)}}{2} - \frac{2\eta^2}{3} (1 - \nu^{(k)}) \right) \right]
 \end{aligned} \quad (4.11b)$$

$$\begin{aligned}
 + w^{(k)} \left[m^{(k)^3} \left(-\frac{\eta^2}{3} \right) + m^{(k)} \left(1 + \gamma^2 \frac{\eta^2}{3} (2 - \nu^{(k)}) \right) \right] = 0, \\
 u^{(k)} [-i \gamma \nu^{(k)}] + v^{(k)} \left[m^{(k)^3} \left(\frac{\eta^2}{3} \right) - m^{(k)} \left(1 + \gamma^2 \frac{\eta^2}{3} (2 - \nu^{(k)}) \right) \right] + \\
 w^{(k)} \left[m^{(k)^4} \left(-\frac{\eta^2}{3} \right) + m^{(k)^2} \left(\gamma^2 \frac{2\eta^2}{3} \right) + \lambda \bar{\rho}^{(k)} (1 - \nu^{(k)^2}) - \frac{\gamma^4 \eta^2}{3} - 1 \right] = 0.
 \end{aligned} \quad (4.11c)$$

This system can be written in a matrix form as

$$M_{1C}^{(k)} X^{(k)} = 0, \quad (4.12)$$

where

$$M_{1C}^{(k)} = \begin{bmatrix} m^{(k)2} \tilde{a} + \tilde{b} & m^{(k)} \tilde{c} & -\tilde{d} \\ m^{(k)} \tilde{c} & m^{(k)2} \tilde{f} + \tilde{r} & -m^{(k)3} \tilde{h} + m^{(k)} \tilde{p} \\ \tilde{d} & -m^{(k)3} \tilde{h} + m^{(k)} \tilde{p} & -m^{(k)4} \tilde{h} + m^{(k)2} \tilde{q} + \tilde{s} \end{bmatrix}, \quad (4.13)$$

$$X^{(k)} = \begin{bmatrix} u^{(k)} \\ v^{(k)} \\ w^{(k)} \end{bmatrix}, \quad (4.14)$$

and

$$\begin{aligned} \tilde{a}^{(k)} &= \frac{1}{2} (1 - \nu^{(k)}), \quad \tilde{b}^{(k)} = \lambda \bar{\rho}^{(k)} (1 - \nu^{(k)2}) - \gamma^2, \quad \tilde{c}^{(k)} = \frac{1}{2} \gamma (1 + \nu^{(k)}) i, \\ \tilde{d}^{(k)} &= \gamma \nu^{(k)} i, \quad \tilde{f}^{(k)} = \frac{1}{3} \eta^2 + 1, \quad \tilde{h}^{(k)} = \frac{1}{3} \eta^2, \\ \tilde{p}^{(k)} &= 1 + \frac{1}{3} \gamma^2 \eta^2 (2 - \nu^{(k)}), \quad \tilde{q}^{(k)} = \frac{2}{3} \gamma^2 \eta^2, \\ \tilde{r}^{(k)} &= \lambda \bar{\rho}^{(k)} (1 - \nu^{(k)2}) - \frac{1}{2} \gamma^2 (1 - \nu^{(k)}) - \frac{1}{3} \eta^2 \gamma^2 (2 - 2\nu^{(k)}), \\ \tilde{s}^{(k)} &= \lambda \bar{\rho}^{(k)} (1 - \nu^{(k)2}) - 1 - \frac{1}{3} \gamma^4 \eta^2. \end{aligned}$$

The equations of motion (4.11) correspond to two eigenvalue problems for the roots m of panels 1 and 2. These must both be solved in order to formulate and solve the more difficult eigenvalue problem for λ using the boundary conditions. Equating the determinant of matrix $M_{1C}^{(k)}$ for $k = 1, 2$ in (4.12) to zero gives two algebraic equations in $m^{(k)}$ which corresponds to the characteristic equation

$$\det M_{1C}^{(k)} = 0, \quad (4.15)$$

where,

$$\begin{aligned}
 \det M_{1C}^{(k)} &= m^{(k)8} (\tilde{a}^{(k)} \tilde{h}^{(k)2} + \tilde{a}^{(k)} \tilde{f}^{(k)} \tilde{h}^{(k)}) \\
 &+ m^{(k)6} (\tilde{h}^{(k)} (\tilde{b}^{(k)} \tilde{h}^{(k)} - 2\tilde{a}^{(k)} \tilde{p}^{(k)} + \tilde{c}^{(k)2} - \tilde{b}^{(k)} \tilde{f}^{(k)} - \tilde{a}^{(k)} \tilde{r}^{(k)}) + \tilde{a}^{(k)} \tilde{f}^{(k)} \tilde{q}^{(k)}) \\
 &+ m^{(k)4} (2\tilde{c}^{(k)} \tilde{d}^{(k)} \tilde{h}^{(k)} - 2\tilde{b}^{(k)} \tilde{h}^{(k)} \tilde{p}^{(k)} + \tilde{a}^{(k)} \tilde{f}^{(k)} \tilde{s}^{(k)} + \tilde{a}^{(k)} \tilde{r}^{(k)} \tilde{q}^{(k)} + \tilde{b}^{(k)} \tilde{f}^{(k)} \tilde{q}^{(k)} \\
 &\quad - \tilde{b}^{(k)} \tilde{r}^{(k)} \tilde{h}^{(k)} + \tilde{a}^{(k)} \tilde{p}^{(k)2} - \tilde{c}^{(k)2} \tilde{q}^{(k)}) \\
 &+ m^{(k)2} (\tilde{b}^{(k)} \tilde{r}^{(k)} \tilde{q}^{(k)} + \tilde{b}^{(k)} \tilde{f}^{(k)} \tilde{s}^{(k)} + \tilde{a}^{(k)} \tilde{r}^{(k)} \tilde{s}^{(k)} - 2\tilde{c}^{(k)} \tilde{d}^{(k)} \tilde{p}^{(k)} \\
 &\quad + \tilde{b}^{(k)} \tilde{p}^{(k)2} + \tilde{d}^{(k)2} \tilde{f}^{(k)} - \tilde{c}^{(k)2} \tilde{s}^{(k)}) \\
 &\quad + \tilde{b}^{(k)} \tilde{r}^{(k)} \tilde{s}^{(k)} + \tilde{d}^{(k)2} \tilde{r}^{(k)}.
 \end{aligned} \tag{4.16}$$

This equation can be written as

$$a_8^{(k)} m^{(k)8} + a_6^{(k)} m^{(k)6} + a_4^{(k)} m^{(k)4} + a_2^{(k)} m^{(k)2} + a_0^{(k)} = 0, \tag{4.17}$$

where $a_8^{(k)}$ to $a_0^{(k)}$ are

$$a_8^{(k)} = \eta^2, \quad a_6 = \eta^2 [\lambda \bar{\rho}^{(k)} (1 + \nu^{(k)}) (3 - \nu^{(k)}) - 4\gamma^2 + 2],$$

$$\begin{aligned}
 a_4^{(k)} &= 2\lambda \bar{\rho}^{(k)2} \eta^2 (1 - \nu^{(k)2}) (1 + \nu^{(k)}) + \lambda \bar{\rho}^{(k)} (1 + \nu^{(k)}) [-3\gamma^2 \eta^2 (2 - \nu^{(k)}) \\
 &\quad + \eta^2 (3 + \nu^{(k)}) - 3(1 - \nu^{(k)})] - \frac{\eta^4 \gamma^4}{3} (1 - \nu^{(k)2}) + 6\gamma^4 \eta^2 - 8\gamma^2 \eta^2 + \eta^2,
 \end{aligned}$$

$$\begin{aligned}
 a_2^{(k)} &= -\lambda \bar{\rho}^{(k)2} (1 - \nu^{(k)2}) (1 + \nu^{(k)}) (\eta^2 (4\gamma^2 + 2) + 3(3 - \nu^{(k)})) \\
 &\quad - \lambda \bar{\rho}^{(k)} \frac{(1 + \nu^{(k)})}{3} (-2\eta^4 \gamma^4 (1 - \nu^{(k)2}) + \eta^2 (-9\gamma^4 (3 - \nu^{(k)}) + 6\gamma^2 (2 - \nu^{(k)}) - 6) \\
 &\quad - 18\gamma^2 (1 - \nu^{(k)}) - 9(1 - \nu^{(k)})) - \frac{4}{3} \gamma^6 \eta^4 - 2\gamma^4 \eta^2 (3\gamma^2 - (6 - \nu^{(k)2})) - 4\gamma^2 \eta^2,
 \end{aligned}$$

$$\begin{aligned}
 a_0^{(k)} &= -6\lambda \bar{\rho}^{(k)3} (1 - \nu^{(k)2})^2 (1 + \nu^{(k)}) + \lambda \bar{\rho}^{(k)2} (1 - \nu^{(k)2}) (1 + \nu^{(k)}) (2\gamma^4 \eta^2 + 4\gamma^2 \eta^2 (1 - \nu^{(k)}) \\
 &\quad - 3\gamma^2 (3 - \nu^{(k)}) + 6) + \lambda \bar{\rho}^{(k)} \left[\frac{1}{3} (1 + \nu^{(k)}) \gamma^6 \eta^2 (-4\eta^2 (1 - \nu^{(k)}) - 3(3 - \nu^{(k)})) \right. \\
 &\quad \left. - \gamma^4 (1 - \nu^{(k)2}) (4\eta^2 + 3) - \gamma^2 (1 - \nu^{(k)2}) (4\eta^2 + 3(3 + 2\nu^{(k)})) \right].
 \end{aligned}$$

Similarly to chapter 2, solving (4.17) yields four roots for $k = 1, 2$ which can then be used to find $u^{(k)}$, $v^{(k)}$ and $w^{(k)}$. The solution to (4.11) is then

$$\begin{pmatrix} U^{(k)}(\psi, \xi) \\ V^{(k)}(\psi, \xi) \\ W^{(k)}(\psi, \xi) \end{pmatrix} = \sum_i^4 C_i^{(k)} \begin{pmatrix} u_i^{(k)} \\ v_i^{(k)} \\ w_i^{(k)} \end{pmatrix} e^{i\gamma\xi + (-1)^k m_i^{(k)} \psi}. \tag{4.18}$$

The constants $C_i^{(k)}$ are found using the boundary conditions. Substituting (4.18) into the perfect contact boundary conditions (4.7) yields the equation

$$b_{ij}^{(1C)} C_j^{(k)} = 0, \quad \text{for } i, j = 1..8, \tag{4.19}$$

where

$$b_{1j}^{(1C)} = bd1_j^{(1)} - bd1_j^{(2)}, \quad b_{2j}^{(1C)} = bd2_j^{(1)} - bd2_j^{(2)}, \quad (4.20a)$$

$$b_{3j}^{(1C)} = bd3_j^{(1)} - bd3_j^{(2)}, \quad b_{4j}^{(1C)} = bd4_j^{(1)} - bd4_j^{(2)}, \quad (4.20b)$$

$$b_{5j}^{(1C)} = bd5_j^{(1)} - bd5_j^{(2)}, \quad b_{6j}^{(1C)} = bd6_j^{(1)} - bd6_j^{(2)}, \quad (4.20c)$$

$$b_{7j}^{(1C)} = bd7_j^{(1)} - bd7_j^{(2)}, \quad b_{8j}^{(1C)} = bd8_j^{(1)} - bd8_j^{(2)}, \quad (4.20d)$$

with the notation

$$bd1_{1,j}^{(k)} = u_j^{(k)}, \quad bd2_{1,j}^{(k)} = v_j^{(k)}, \quad (4.21a)$$

$$bd3_{1,j}^{(k)} = w_j^{(k)}, \quad bd4_{1,j}^{(k)} = w_j^{(k)}(-1)^k m_j^{(k)}, \quad (4.21b)$$

$$bd5_{1,j}^{(k)} = \frac{1}{(1 - \nu^{(k)^2})\overline{E}^{(k)}} \left[u_j^{(k)}(\nu^{(k)}\gamma i) + v_j^{(k)}(-1)^k m_j^{(k)} + w_j^{(k)} \right], \quad (4.21c)$$

$$bd6_{2,j}^{(k)} = \frac{1}{2(1 + \nu^{(k)})\overline{E}^{(k)}} \left[u_j^{(k)}(-1)^k m_j^{(k)} + v_j^{(k)}\gamma i \right], \quad (4.21d)$$

$$bd7_{3,j}^{(k)} = \frac{\eta^2}{3(1 - \nu^{(k)^2})\overline{E}^{(k)}} \left[v_j^{(k)}(-1)^k m_j^{(k)} - w_j^{(k)}(m_j^{(k)^2} - \nu^{(k)}\gamma^2) \right], \quad (4.21e)$$

$$bd8_{4,j}^{(k)} = -\frac{\eta^2}{3(1 - \nu^{(k)^2})\overline{E}^{(k)}} \left[v_j^{(k)}[m_j^{(k)^2} - 2(1 - \nu^{(k)})\gamma^2] \right. \\ \left. - w_j^{(k)}[-(2 - \nu^{(k)})(-1)^k m_j^{(k)}\gamma^2 + (-1)^k m_j^{(k)^3}] \right], \quad (4.21f)$$

where $j = 1..4$ for $k = 1$ and $j = 5..8$ for $k = 2$. From (4.3) the following equation can be written

$$\det|b_{ij}^{(1C)}| = 0. \quad (4.22)$$

This is the essential eigenvalue problem for the edge wave frequency of interfacial waves, and should be solved numerically using the roots from (4.17) and the constants $u_j^{(k)}$, $v_j^{(k)}$ and $w_j^{(k)}$. The numerical scheme to solve (4.22) iterates through a region of λ where a root is predicted to lie using the asymptotics. A sign change then occurs where the root lies, and so through further careful iteration λ can be isolated to a good accuracy.

4.2.2 Problem 2C

For the problem of vibration propagating on the circumferential edge and decaying longitudinally, a solution to the equations of motion (2.4) can be written

as

$$\begin{pmatrix} U^{(k)}(\psi, \xi) \\ V^{(k)}(\psi, \xi) \\ W^{(k)}(\psi, \xi) \end{pmatrix} = \begin{pmatrix} u^{(k)} \\ v^{(k)} \\ w^{(k)} \end{pmatrix} \begin{pmatrix} \sin n\psi \\ \cos n\psi \\ \sin n\psi \end{pmatrix} e^{(-1)^k r^{(k)} \xi}. \quad (4.23)$$

where the circumferential wavenumber n is given, $u^{(k)}$, $v^{(k)}$ and $w^{(k)}$ are constants, and the roots r are chosen using condition (2.23) and satisfying decay at ∞ .

Substituting this into the governing equations (4.3) gives

$$\begin{aligned} u^{(k)} \left[r^{(k)2} - \frac{1 - \nu^{(k)}}{2} n^2 + \lambda \bar{\rho}^{(k)} (1 - \nu^{(k)2}) \right] \\ + v^{(k)} \left[-\frac{1 + \nu^{(k)}}{2} r^{(k)} n \right] + w^{(k)} [-\nu^{(k)} r^{(k)}] = 0, \end{aligned} \quad (4.24)$$

$$\begin{aligned} u^{(k)} \left[\frac{1 + \nu^{(k)}}{2} r^{(k)} n \right] + v^{(k)} \left[\frac{1 - \nu^{(k)}}{2} r^{(k)2} - n^2 + \frac{\eta^2}{3} (2(1 - \nu^{(k)}) r^{(k)2} \right. \\ \left. - n^2) + (1 - \nu^{(k)2}) \lambda \bar{\rho}^{(k)} \right] + w^{(k)} \left[\frac{\eta^2}{3} n ((2 - \nu^{(k)}) r^{(k)2} - n^2) - n \right] = 0, \end{aligned} \quad (4.25)$$

$$u^{(k)} [-\nu^{(k)} r^{(k)}] + v^{(k)} \left[n - \frac{\eta^2}{3} n ((2 - \nu^{(k)}) r^{(k)2} - n^2) \right] \quad (4.26)$$

$$+ w^{(k)} \left[1 + \frac{\eta^2}{3} (r^{(k)4} - 2n^2 r^{(k)2} + n^4) - (1 - \nu^{(k)2}) \lambda \bar{\rho}^{(k)} \right] = 0. \quad (4.27)$$

This can be written in matrix form as

$$M_{2C}^{(k)} X^{(k)} = 0, \quad (4.28)$$

where

$$M_{2C}^{(k)} = \begin{bmatrix} r^{(k)2} + \hat{b} & -r^{(k)} \hat{c} & -r^{(k)} \hat{d} \\ r^{(k)} \hat{c} & r^{(k)2} \hat{f} + \hat{r} & r^{(k)2} \hat{h} - \hat{p} \\ -r^{(k)} \hat{d} & -r^{(k)2} \hat{h} + \hat{p} & r^{(k)4} \hat{t} - r^{(k)2} \hat{q} + \hat{s} \end{bmatrix}, \quad (4.29)$$

and

$$\begin{aligned} \hat{b} &= \lambda \bar{\rho}^{(k)} (1 - \nu^{(k)2}) - \frac{1 - \nu^{(k)}}{2} n^2, \quad \hat{c} = \frac{1}{2} n (1 + \nu^{(k)}), \\ \hat{d} &= \nu^{(k)} r^{(k)}, \quad \hat{f} = \frac{1 - \nu^{(k)}}{2} + \frac{2}{3} (1 - \nu^{(k)}) \eta^2, \quad \hat{h} = \frac{1}{3} (2 - \nu^{(k)}) \eta^2 n, \\ \hat{p} &= n \left(\frac{1}{2} \eta^2 n^2 + 1 \right), \quad \hat{q} = \frac{2}{3} n^2 \eta^2, \\ \hat{r} &= \lambda \bar{\rho}^{(k)} (1 - \nu^{(k)2}) - n^2 \left(1 + \frac{1}{2} \eta^2 \right), \\ \hat{s} &= 1 - \lambda \bar{\rho}^{(k)} (1 - \nu^{(k)2}) + \frac{1}{3} \eta^2 n^4, \quad \hat{t} = \frac{1}{3} \eta^2. \end{aligned}$$

The system of equations (4.27) corresponds to two eigenvalue problems for r for $k = 1, 2$. Numerically solving these two problems allows solving for the more complicated larger eigenvalue problem for λ formed using the boundary conditions. Equating the determinant of matrix M_{2C} in (2.28) to zero yields the characteristic equation

$$\det M_{2A}^{(k)} = 0, \quad (4.30)$$

where

$$\begin{aligned} \det|M_{2A}^{(k)}| &= r^{(k)8} (\hat{f}\hat{t}) + r^{(k)6} (\hat{c}^2\hat{t} + \hat{b}\hat{f}\hat{t} - \hat{f}\hat{q} + \hat{r}\hat{t} + \hat{h}^2) \\ &+ r^{(k)4} (\hat{b}\hat{h}^2 + \hat{b}\hat{r}\hat{t} + 2\hat{c}\hat{d}\hat{h} + \hat{f}\hat{s} - 2\hat{h}\hat{p} - \hat{b}\hat{f}\hat{q} - \hat{d}^2\hat{f} - \hat{r}\hat{q} - \hat{c}^2\hat{q}) \\ &+ r^{(k)2} (\hat{p}^2 + \hat{b}\hat{f}\hat{s} + \hat{c}^2\hat{s} + \hat{r}\hat{s} - 2\hat{b}\hat{h}\hat{p} - \hat{d}^2\hat{r} - 2\hat{c}\hat{d}\hat{p} - \hat{b}\hat{r}\hat{q}) + \hat{p}^2\hat{b} + \hat{b}\hat{r}\hat{s}, \end{aligned} \quad (4.31)$$

which in a simpler notation is written as

$$b_8 r^{(k)8} + b_6 r^{(k)6} + b_4 r^{(k)4} + b_2 r^{(k)2} + b_0 = 0, \quad (4.32)$$

where b_8 to b_0 are given in the paper Kaplunov and Wilde (2002).

The characteristic equation (4.32) is numerically solved for all roots r with $k = 1, 2$, which are used to find the constants $u_i^{(k)}$, $v_i^{(k)}$, and $w_i^{(k)}$, enabling a solution to (4.27) to be written in the form

$$\begin{pmatrix} U^{(k)}(\psi, \xi) \\ V^{(k)}(\psi, \xi) \\ W^{(k)}(\psi, \xi) \end{pmatrix} = \sum_i^4 B_i^{(k)} \begin{pmatrix} u_i^{(k)} \\ v_i^{(k)} \\ w_i^{(k)} \end{pmatrix} \begin{pmatrix} \sin n\psi \\ \cos n\psi \\ \sin n\psi \end{pmatrix} e^{(-1)^k r_i^{(k)} \xi}, \quad (4.33)$$

where $B_i^{(k)}$ are constants to be found by using the boundary conditions.

The main eigenvalue problem is now formulated by substituting (4.33) into the perfect contact boundary conditions (4.9) giving

$$b_{ij}^{(2C)} B_j^{(k)} = 0, \quad \text{for } i, j = 1..8, \quad (4.34)$$

where

$$b_{1j}^{(2C)} = bd1_j^{(1)} - bd1_j^{(2)}, \quad b_{2j}^{(2C)} = bd2_j^{(1)} - bd2_j^{(2)}, \quad (4.35a)$$

$$b_{3j}^{(2C)} = bd3_j^{(1)} - bd3_j^{(2)}, \quad b_{4j}^{(2C)} = bd4_j^{(1)} - bd4_j^{(2)}, \quad (4.35b)$$

$$b_{5j}^{(2C)} = bd5_j^{(1)} - bd5_j^{(2)}, \quad b_{6j}^{(2C)} = bd6_j^{(1)} - bd6_j^{(2)}, \quad (4.35c)$$

$$b_{7j}^{(2C)} = bd7_j^{(1)} - bd7_j^{(2)}, \quad b_{8j}^{(2C)} = bd8_j^{(1)} - bd8_j^{(2)}, \quad (4.35d)$$

with

$$bd1_{1,j}^{(k)} = u_j^{(k)}, \quad bd2_{1,j}^{(k)} = v_j^{(k)}, \quad (4.36a)$$

$$bd3_{1,j}^{(k)} = w_j^{(k)}, \quad bd4_{1,j}^{(k)} = w_j^{(k)}(-1)^k r_j^{(k)}, \quad (4.36b)$$

$$bd5_{1,j}^{(k)} = \frac{1}{(1 - \nu^{(k)^2})\bar{E}^{(k)}} \left[u_j^{(k)}(-1)^k r_j^{(k)} + v_j^{(k)}\nu^{(k)}n + w_j^{(k)}\nu^{(k)} \right], \quad (4.36c)$$

$$bd6_{2,j}^{(k)} = \frac{1}{2(1 + \nu^{(k)})\bar{E}^{(k)}} \left[u_j^{(k)}n + v_j^{(k)}(-1)^k r_j^{(k)} + \frac{2}{3}\eta^2(-1)^k r_j^{(k)}(v_j^{(k)} + w_j^{(k)}n) \right], \quad (4.36d)$$

$$bd7_{3,j}^{(k)} = \frac{\eta^2}{3(1 - \nu^{(k)^2})\bar{E}^{(k)}} \left[-v_j^{(k)}\nu^{(k)}n + w_j^{(k)}(r_j^{(k)^2} - \nu^{(k)}n^2) \right], \quad (4.36e)$$

$$bd8_{4,j}^{(k)} = -\frac{\eta^2}{3(1 - \nu^{(k)^2})\bar{E}^{(k)}} \left[-v_j^{(k)}n(-1)^k r_j^{(k)}(2 - \nu^{(k)}) + w_j^{(k)}(-1)^k r_j^{(k)}(r_j^{(k)^2} - (2 - \nu^{(k)})n) \right], \quad (4.36f)$$

where $j = 1..4$ for $k = 1$ and $j = 5..8$ for $k = 2$. Equation (4.34) is the main important eigenvalue problem. It represents a system of size 8x8 from which the equation

$$\det|b_{ij}^{(2C)}| = 0, \quad (4.37)$$

can be solved numerically to find the non-dimensional frequency λ . The asymptotic analysis for Problem 2C can be found in Kaplunov and Wilde (2002).

4.3 Flexural Vibrations

The asymptotics and relations between terms are taken from subsection 2.3.1. From section 2.4 the leading order asymptotic equation is known and can be rewritten with as

$$m^{(k)4} - 2m^{(k)2}\gamma^2 + \gamma^4 = \frac{3\lambda\bar{\rho}^{(k)}(1 - \nu^{(k)2})}{\eta^2}. \quad (4.38)$$

This equation is analogous to the governing equation of the Stoneley-type flexural wave on a plate (1.31). As a result the solution to this equation is

$$W^{(k)} = \sum_{j=1}^2 w_j^{(k)} e^{i\gamma\xi + (-1)^k m_j^{(k)}}, \quad (4.39)$$

Also from section 2.4 the leading order boundary conditions are known, and applying the asymptotic terms to conditions (4.6) allows writing the interfacial boundary conditions as where $bd_{ij}^{(1C)}$ are

$$bd_{1j}^{(1C)} = w_j^{(1)} - w_j^{(2)}, \quad bd_{2j}^{(1C)} = -w_j^{(1)}m_j^{(1)} - w_j^{(2)}m_j^{(2)}, \quad (4.40a)$$

$$bd_{3j}^{(1C)} = -\frac{\eta^2}{3(1 - \nu^{(1)2})\bar{E}^{(1)}} \left[w_j^{(1)}(m_j^{(1)2} - \nu^{(1)}\gamma^2) \right] \\ + \frac{\eta^2}{3(1 - \nu^{(2)2})\bar{E}^{(2)}} \left[w_j^{(2)}(m_j^{(2)2} - \nu^{(2)}\gamma^2) \right], \quad (4.40b)$$

$$bd_{4j}^{(1C)} = \frac{\eta^2}{3(1 - \nu^{(1)2})\bar{E}^{(1)}} \left[w_j^{(1)} \left((2 - \nu^{(1)})m_j^{(1)}\gamma^2 - m_j^{(1)3} \right) \right] \\ + \frac{\eta^2}{3(1 - \nu^{(2)2})\bar{E}^{(2)}} \left[w_j^{(2)} \left(-(2 - \nu^{(2)})m_j^{(2)}\gamma^2 + m_j^{(2)3} \right) \right], \quad (4.40c)$$

which are analogous to the perfect contact boundary conditions for the Stoneley-type flexural waves on a plate (1.26) and (1.34). and the frequency can be found from (1.39) as shown in subsection 1.2.3.

4.3.1 Numerical Results

Some relevant data have been presented in table 4.1 for γ and n from 20 to 40.

Table 4.1: Natural Frequencies with $\nu^{(1)} = 0.3$, $\nu^{(2)} = 0.4$, and $\eta = 0.001$

γ, n	1C λ^{ex}	2C λ^{ex}	asymptotic λ^{as}
20	7.19071633	6.2775268	6.328183596
25	16.3388262	15.3715586	15.44966698
30	32.9367056	31.92394078	32.03642946
40	102.513922	101.046959	101.2509375

Similarly to subsection 2.4.1, the results indicate that for larger wavenumbers the asymptotics are more accurate in Problem 1C, but at smaller wavenumbers the asymptotics become less reliable. For all of the graphs here $\nu^{(1)} = 0.3$ and $\nu^{(2)} = 0.4$. Figure 4.3 for $\gamma = 40$ shows a clear difference between asymptotic and numeric forms, which increases as γ decreases, seen in Figure 4.4. For $\gamma = 25$ in Figure 4.5 the difference is extremely visible, especially in the decay as $\psi \rightarrow -\infty$. In comparison to Problem 2C in Figure 4.6 the asymptotics remain more accurate for smaller γ .

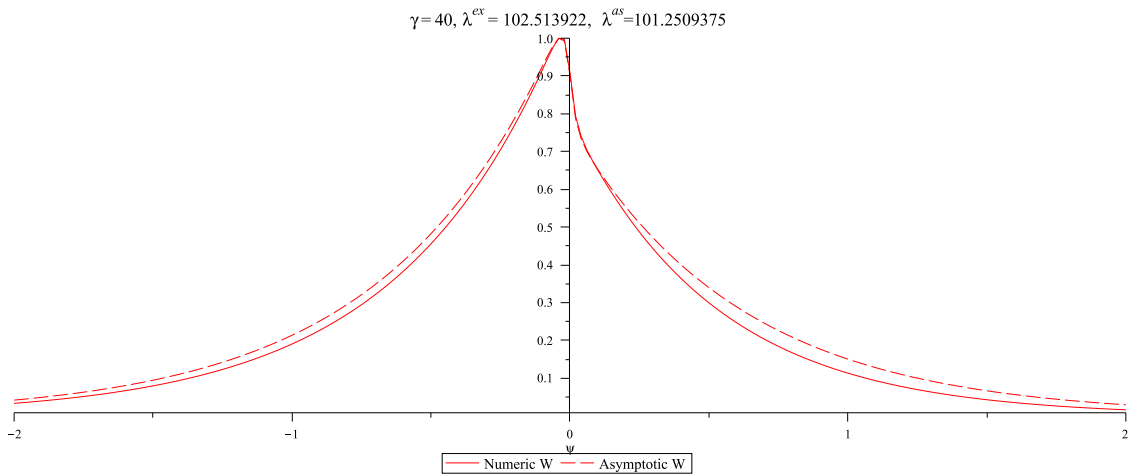


Figure 4.3: Asymptotic and numeric forms for the interfacial flexural edge wave of Problem 1C with fixed parameters $\eta = 0.01$, $\nu^{(1)} = 0.3$, $\nu^{(2)} = 0.4$, and $\gamma = 40$

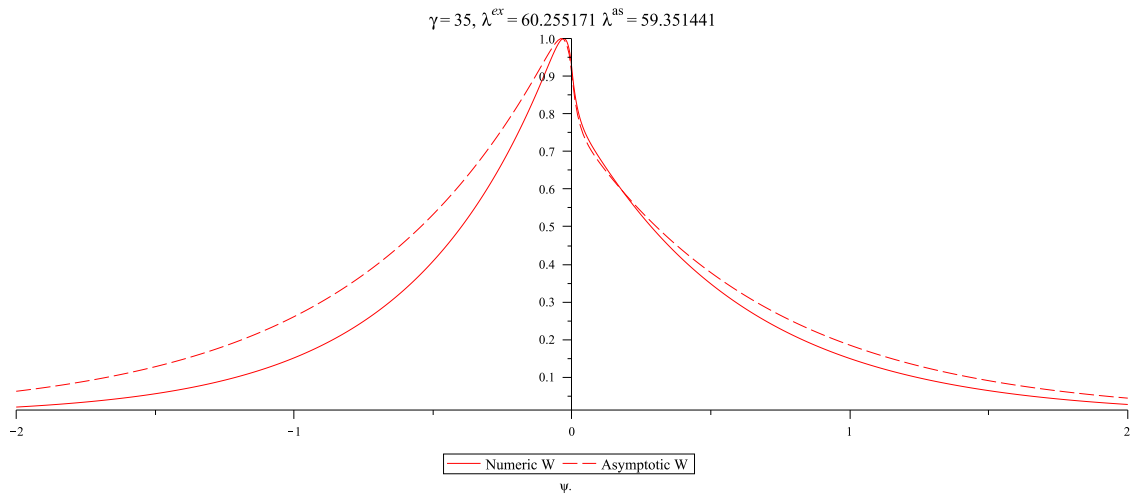


Figure 4.4: Asymptotic and numeric forms for the interfacial flexural edge wave of Problem 1C with fixed parameters $\eta = 0.01$, $\nu^{(1)} = 0.3$, $\nu^{(2)} = 0.4$, and $\gamma = 35$

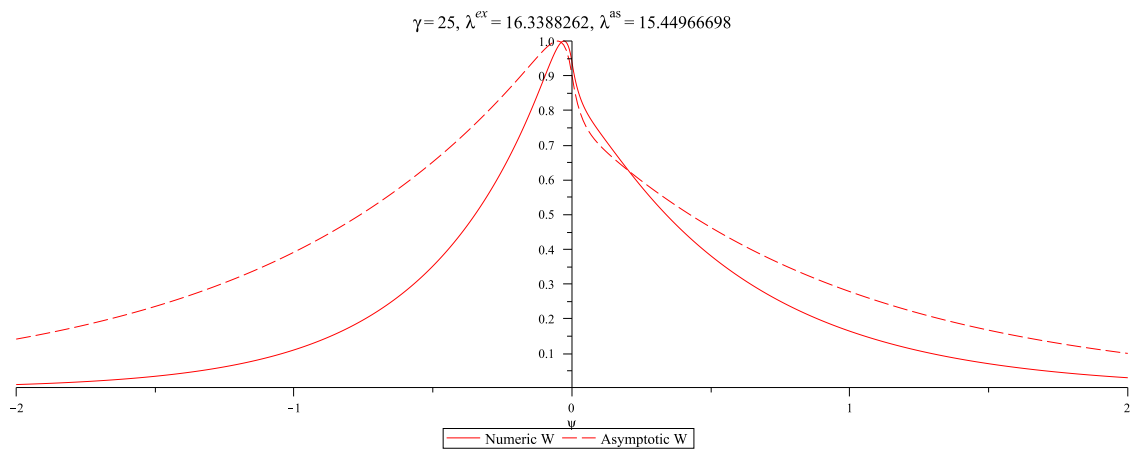


Figure 4.5: Asymptotic and numeric forms for the interfacial flexural edge wave of Problem 1C with fixed parameters $\eta = 0.01$, $\nu^{(1)} = 0.3$, $\nu^{(2)} = 0.4$, and $\gamma = 25$

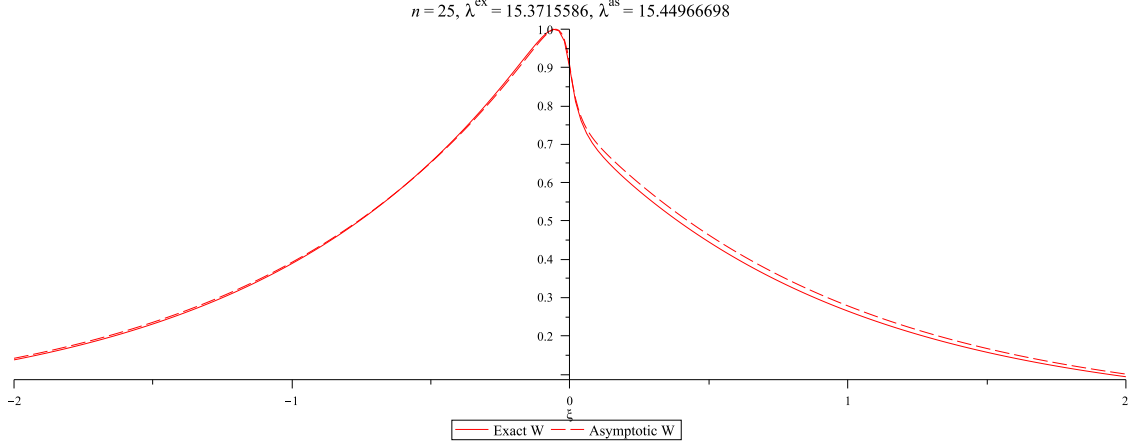


Figure 4.6: Asymptotic and numeric forms for the interfacial flexural edge wave of Problem 2C with fixed parameters $\eta = 0.01$, $\nu^{(1)} = 0.3$, $\nu^{(2)} = 0.4$, and $n = 25$.

4.4 Extensional Vibrations

The asymptotics and relations are taken from subsection 2.3.1, and from section 2.5. (4.4), the leading order asymptotic equations can be rewritten as

$$\begin{aligned} u^{(k)} \left[m^{(k)2} - \gamma^2 \left(\frac{1 - \nu^{(k)}}{2} \right) + (1 - \nu^{(k)2}) \lambda \bar{\rho}^{(k)} \right] + v^{(k)} \left[-i\gamma m^{(k)} \left(\frac{1 + \nu^{(k)}}{2} \right) \right] &= 0, \\ u^{(k)} \left[-i\gamma m^{(k)} \frac{1 + \nu^{(k)}}{2} \right] + v^{(k)} \left[m^{(k)2} \frac{1 - \nu^{(k)}}{2} - \gamma^2 (1 - \nu^{(k)2}) \lambda \bar{\rho}^{(k)} \right] &= 0. \end{aligned} \quad (4.41)$$

These equations are analogous to the governing equations of the Stoneley-type extensional waves on a plate (1.43) derived in subsection 1.2.4. A solution to this equation can be written as

$$\begin{pmatrix} U^{(k)}(\psi, \xi) \\ V^{(k)}(\psi, \xi) \end{pmatrix} = \sum_{j=1}^2 \begin{pmatrix} u_0^{(k)} \\ iu_0^{(k)} \left(\frac{(-1)^k m_j^{(k)}}{\gamma} \right)^{3-2j} \end{pmatrix} C_j^{(k)} e^{i\gamma\xi + (-1)^k m_j^{(k)} \psi}. \quad (4.42)$$

Using the results from section 2.5 and applying the asymptotic terms to (4.6), $bd_{ij}^{(1C)}$ in the boundary conditions (4.3) become

$$bd1_{i,j}^{(k)} = u_j^{(1)} - u_j^{(2)}, \quad bd2_{i,j}^{(k)} = v_j^{(1)} - v_j^{(2)}, \quad (4.43a)$$

$$bd3_{i,j}^{(k)} = \frac{1}{(1 - \nu^{(1)^2})\bar{E}^{(1)}} \left[u_j^{(1)} i\nu^{(1)}\gamma - v_j^{(1)} m_j^{(1)} \right] - \frac{1}{(1 - \nu^{(2)^2})\bar{E}^{(2)}} \left[u_j^{(2)} i\nu^{(2)}\gamma + v_j^{(2)} m_j^{(2)} \right], \quad (4.43b)$$

$$bd4_{i,j}^{(k)} = \frac{1}{2(1 + \nu^{(1)})\bar{E}^{(1)}} \left[-u_j^{(1)} m_j^{(1)} + v_j^{(1)} i\gamma \right] - \frac{1}{2(1 + \nu^{(2)})\bar{E}^{(2)}} \left[u_j^{(2)} m_j^{(2)} + v_j^{(2)} i\gamma \right]. \quad (4.43c)$$

This is the same as the perfect contact boundary conditions for the Stoneley-type extensional waves on a plate (1.41) and (1.47).

4.4.1 Numerical Results

Table 4.2 below presents some relevant interfacial frequencies for different wavenumbers, with $\nu = 0.3$ and $\eta = 0.01$.

Table 4.2: Natural Frequencies with $\nu^{(1)} = 0.3$, $\nu^{(2)} = 0.4$, and $\eta = 0.01$

γ, n	1C λ^{ex}	2C λ^{ex}	asymptotic λ^{as}
5	8.039828	8.6551465	8.394243987
10	33.2883071	33.8576356	33.57697594
15	75.271057	75.653902	75.54819588

As mentioned earlier in chapters 2 and 3 the results are very similar for both problems, and again here too. Only several graphs have been presented to illustrate this.

Figure 4.7 for Problem 1C for $\nu^{(1)} = 0.3$, $\nu^{(2)} = 0.4$, $\eta = 0.01$ and $\gamma = 15$, the asymptotics have been coloured black to show their good agreement with the numerics. There is smooth decay away from the interface in both directions with very similar behaviour to that mentioned before. The larger ν causes more rapid decay with no change of sign, whereas the smaller ν causes a sign change in U .

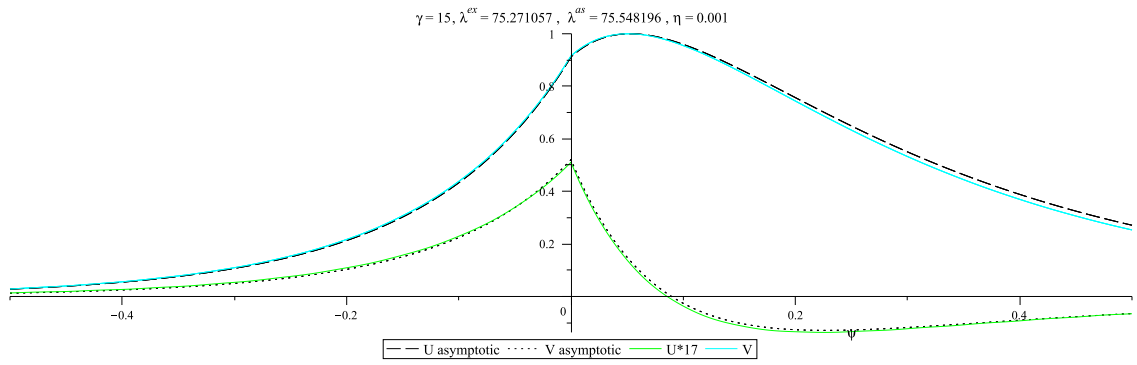


Figure 4.7: Asymptotic and numeric forms for the interfacial extensional edge wave of Problem 1C with fixed parameters $\eta = 0.001$, $\nu^{(1)} = 0.3$, $\nu^{(2)} = 0.4$, and $\gamma = 15$

Figures 4.8 and 4.9 for Problem 2C with $n = 5$ and $n = 10$ illustrate that when the wavenumber is smaller, the rate of decay reduces. However the asymptotics remain accurate and cannot be seen on the graphs.

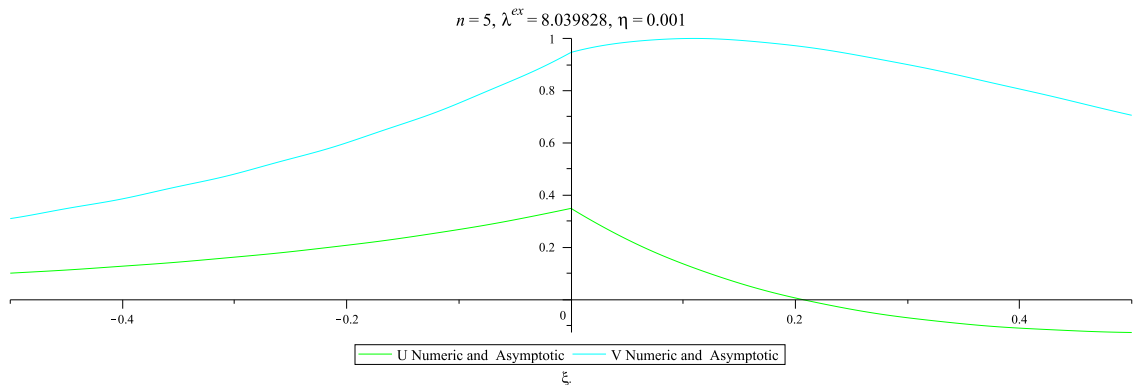


Figure 4.8: Asymptotic and numeric forms for the interfacial flexural edge wave of Problem 2C with fixed parameters $\eta = 0.001$, $\nu^{(1)} = 0.3$, $\nu^{(2)} = 0.4$, and $n = 5$

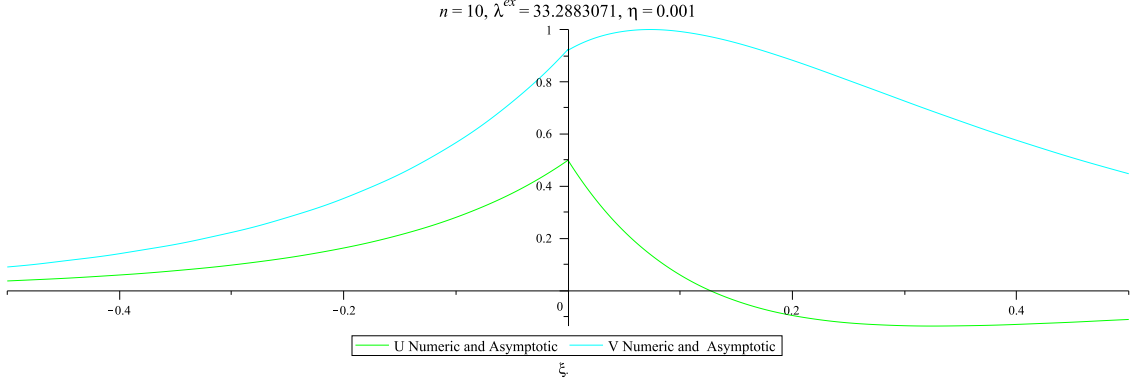


Figure 4.9: Asymptotic and numeric forms for the interfacial flexural edge wave of Problem 1C with fixed parameters $\eta = 0.001$, $\nu^{(1)} = 0.3$, $\nu^{(2)} = 0.4$, and $n = 10$

4.5 Super-Low Frequency Vibrations

Using the asymptotics and notations from subsection 2.3.1 and 2.5.2 the leading order system of equations (2.77) can be rewritten with all quantities having superscript (k) , and using the notation (4.4). The characteristic equation (2.78) then becomes

$$-m_*^{(k)8} \frac{1}{3} + m_*^{(k)4} \lambda \bar{\rho}^{(k)} (1 - \nu^{(k)2}) - \gamma^4 (1 - \nu^{(k)2}) = 0. \quad (4.44)$$

A solution to this problem is written as

$$\begin{pmatrix} U^{(k)}(\psi, \xi) \\ V^{(k)}(\psi, \xi) \\ W^{(k)}(\psi, \xi) \end{pmatrix} = \sum_{i=1}^4 C_i^{(k)} \begin{pmatrix} u_i^{(k)} \\ v_i^{(k)} \\ w_i^{(k)} \end{pmatrix} e^{i\gamma\xi - m_i^{(k)}\psi}, \quad (4.45)$$

Following this, $u_i^{(k)}$ and $v_i^{(k)}$ are expressed through $v_i^{(k)}$ as

$$w_i^{(k)} m_i^{(k)} = -v_i^{(k)} \left[m_i^{(k)2} + \gamma^2 \nu^{(k)} \epsilon + \frac{1}{m_i^{(k)2}} \gamma^4 (1 + \nu^{(k)})^2 \epsilon^2 \right]. \quad (4.46)$$

and

$$w_i^{(k)} m_i^{(k)} = -v_i^{(k)} \left[m_i^{(k)2} + \gamma^2 \nu^{(k)} \epsilon + \frac{1}{m_i^{(k)2}} \gamma^4 (1 + \nu^{(k)})^2 \epsilon^2 \right]. \quad (4.47)$$

Similarly to what was done in subsection 2.5.2 for Problem 1A, the boundary conditions (4.3) can be rewritten with subscript (k) notation and expressed through $v_i^{(k)}$ using (4.46) and (4.47).

4.5.1 Numerical Results

The results in this subsection are very similar to those in subsection 2.5.2. Figure 4.10 for Problem 1C with $\nu = 0.3$, $\eta = 0.001$ and $\gamma = 10$ shows the good agreement between the numerics and the asymptotics with leading order terms and some smaller terms.

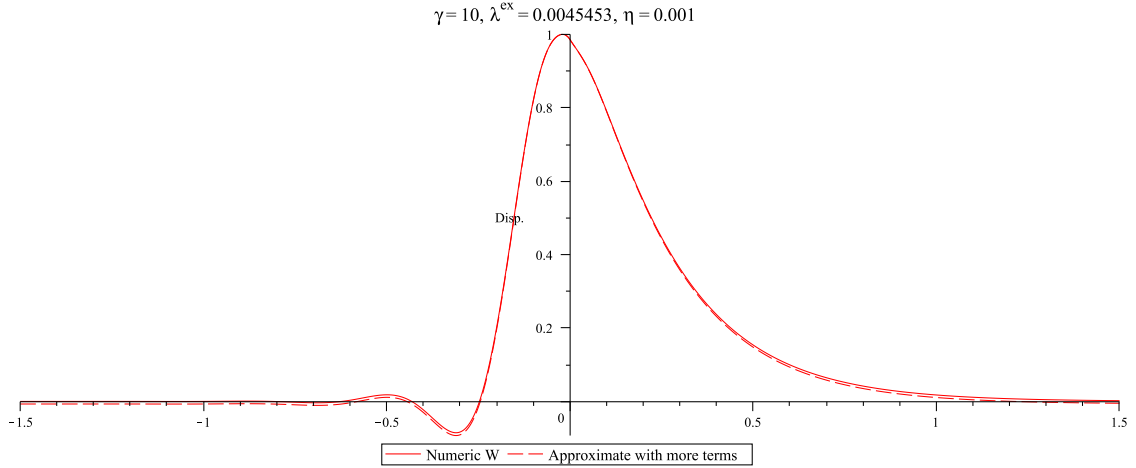


Figure 4.10: Asymptotic and numeric forms for the interfacial super-low edge wave of Problem 1C with fixed parameters $\eta = 0.001$, $\nu^{(1)} = 0.3$, $\nu^{(2)} = 0.4$, and $\gamma = 10$

Figure 4.11 with the same values for Problem 2C is shown for comparison.

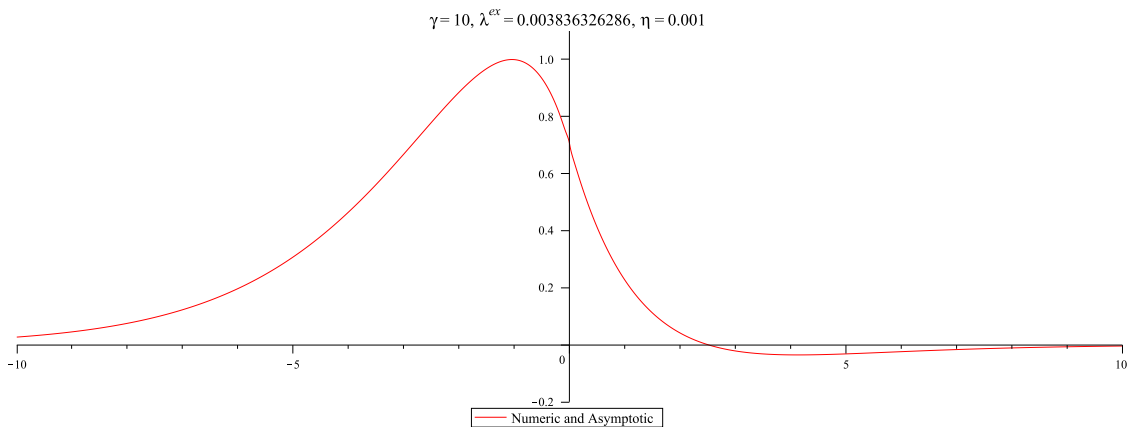


Figure 4.11: Asymptotic and numeric forms for the interfacial flexural edge wave of Problem 2C with fixed parameters $\eta = 0.001$, $\nu^{(1)} = 0.3$, $\nu^{(2)} = 0.4$, and $\gamma = 10$

4.6 Concluding Remarks

We observed three different types of edge and interfacial vibrations, they are the Rayleigh-type and Stoneley-type flexural and extensional vibrations, and super-low frequency. For the first two there are counterparts in plate edge waves. The third one is specific only for shells, being affected by curvature. Throughout the thesis we compared the results with the former investigation for a cylindrical shell in the papers by Kaplunov et al. (1999) and Kaplunov and Wilde (2002). All of the asymptotics were tested by comparison with the exact solution which basically consists of two eigenvalue problems. The first eigenvalue problem is used to find eigen forms for the equations of motion, and the second one takes into account the boundary conditions leading to the sought for dispersion relation.

It appears that the asymptotic results for the Rayleigh and Stoneley-type extensional vibrations are very accurate for both problems investigated. However, for the Rayleigh and Stoneley-type flexural vibrations that propagate on the cylindrical panel with straight longitudinal edge and decay over the curvature of the cylindrical panel, the asymptotics are not a good approximate for some cases. This is due to the effect of curvature which is not taken into account in the asymptotics. Unfortunately for the so called super-low frequency vibration there is a greater deviation, in this case it was not possible to formulate an explicit frequency equation using the leading order terms. Instead, we suggest a numerical scheme to treat the leading order equations of motion and boundary conditions. Another new insight we made in this thesis is the effect of the second edge on the localised vibration. We compare these results with the semi infinite setup. The results obtained have the potential to be extended to more sophisticated situations including non-circular cylindrical shells as well as anisotropic structures, and also for more realistic setups of interfaces including a shell with a patch of different material.

Bibliography

- D. N. Alleyne and P. Crawley. The interaction of lamb waves with defects. *EEE Transactions on Ultrasonics, Ferroelectrics, and Frequency Control*, 39, 1992.
- D. N. Alleyne and P. Crawley. The use of lamb waves for the long range inspection of large structures. *EEE Transactions on Ultrasonics, Ferroelectrics, and Frequency Control*, 34, 1996.
- I. V. Andrianov. Boundary resonance in a cylindrical shell with free ends in the ring direction. 1991.
- I. V. Andrianov and J. Awrejcewicz. Edge localized effects in buckling and vibration of a shell with free in circumferential direction ends. *Acta Mechanica*, 2004.
- D. M. Barnett, J. Lothe, S. D. Gavazza, and M. J. P. Musgrave. Considerations of the existence of interfacial (stoneley) waves in bonded anisotropic elastic half-spaces. *Proceedings of the Royal Society of London*, 402:153–166, Nov 1985.
- E. R. Baylis. Flexural elastic waves in an isotropic internal stratum. 1986.
- V. L. Berdichevskii. High-frequency long-wave vibration of plates. *Akademiia Nauk SSSR*, 1977.
- P. Chadwick and P. Borejko. Existence and uniqueness of stoneley waves. *Geophysical Journal International*, 1994.
- P. Chadwick and D. A. Jarvis. Interfacial waves in a pre-strained neo-hookean body i. biaxial states of strain. *Q. Ji mech. appl. Math*, 1979a.

- P. Chadwick and G. D. Smith. Foundations of the theory of surface waves in anisotropic elastic materials. *Adv. Appl. Mech*, pages 303–376, 1977.
- M. A. Dowaiikh and R. W. Ogden. Interfacial waves and deformations in pre-stressed elastic media. *Proceedings: Mathematical and Physical Sciences*, 433: 313–328, May 1991.
- V.G. Yakovleva D.P. Kouzov, T.S. Kravtsova. On the scattering of the vibrational waves on a knot contact of plates. *Soviet Acoustical Physics*, 1989.
- K. O. Friedrichs. Kirchhoff's boundary conditions and the edge effects for elastic plates. *Proc. Symp. Appl. Math*, 1950.
- K. O. Friedrichs. Asymptotic phenomena in mathematical physics. *Bulletin of the American Mathematical Society*, 1955a.
- K.O. Friedrichs. Asymptotic phenomena in mathematical physics. *Bulletin of the American Mathematical Society*, 1955b.
- V. G. Gogoladse. Rayleigh waves on the interface between a compressible fluid medium and a solid elastic half-space. *Trudy Seismologicheskogo Instituta Akademii Nauk SSSR*, 1948.
- A. L. Goldenveizer. *Theory of Elastic Thin Shells*. 1961.
- A. L. Goldenveizer and A. V. Kolos. On the derivation of two-dimensional equations in the theory of thin elastic plates. *Proc. Symp. Appl. Math*, 29, 1965.
- A. L. Goldenveizer, V. B. Lidskii, and P. E. Tovstik. *Free Vibrations of Thin Elastic Bodies*. 1979.
- A. L. Goldenveizer, J. D. Kaplunov, and E.V. Nolde. On timoshenko-reissner type theories of plates and shells. *International Journal of Solids and Structures*, 30, 1993.
- L.G. Gulgazaryan G.R. Gulgazaryan and R.D. Saakyan. The vibrations of a thin elastic orthotropic cylindrical shell with free and hinged edges. *Journal of Applied Mathematics and Mechanics*, 2008.

- L.G. Gulgazaryan G.R. Gulgazaryan and D. L. Srapionyan. Vibrations of a thin-walled structure consisting of orthotropic non-closed elastic cylindrical shells with free and hinge-mounting conditions at boundary generators. 69, 2007.
- L.G. Gulgazaryan G.R. Gulgazaryan and D. L. Srapionyan. Localized vibrations of a thin-walled structure consisted of orthotropic elastic non-closed cylindrical shells with free and rigid-clamped edge generators. *Journal of Applied Mathematics and Mechanics*, 2012.
- A. E. Green. Boundary layer equations in the linear theory of thin elastic shells. *Proc. R. Soc*, 1963.
- M. A. Hayes and R. S. Rivlin. Surface waves in deformed elastic materials. 1961.
- D. Vassiliev I. Roitberg and T. Weidl. Edge resonance in an elastic semi-strip. 1998.
- A. Y. Ishlinskii. On a limiting process in the theory of the stability of elastic rectangular plates. 1954.
- J. D. Kaplunov. Integration of the dynamic boundary-layer equations. *Izv. Akad. Nauk SSSR*, 1990.
- J. D. Kaplunov and M. V. Wilde. Edge and interfacial vibrations in elastic shells of revolution. *Z. angew. Math. Phys*, 2000.
- J. D. Kaplunov and M. V. Wilde. Free interfacial vibrations in cylindrical shells. 2002.
- J. D. Kaplunov, L. Yu. Kossovich, and E.V. Nolde. *Dynamics of Thin Walled Elastic Bodies*. 1998.
- J. D Kaplunov, L. Y Kossovich, and M. V Wilde. Free localized vibrations of a semi-infinite cylindrical shell. 1999.
- J.D. Kaplunov, D.A. Prikazchikov, and G.A. Rogerson. Edge vibration of a pre-stressed semi-infinite strip with traction-free edge and mixed face boundary conditions. *Zeitschrift fur Angewandte Mathematik und Physik (ZAMP)*, 2004.

- C. Kauffmann. A new bending wave solution for the classical plate equation. 1998a.
- C. Kauffmann. Response to flexural edge waves and comments on ‘a new bending wave solution for the classical plate equation’. 1998b.
- G. Kirchhoff. Uber das gleichewicht und die bwegung einer elastischen scheibe. *Journal fur die reine und angewandte Mathematik*, 1850.
- A. V. Kolos. Methods of refining the classical theory of bending and extension of plates. *Prik. Mat. Mekhan*, 1965.
- Yu. K. Konenkov. On a rayleigh-type bending wave. 1960.
- A. A. Krushynska. Flexural edge waves in semi-infinite elastic plates. *Journal of Sound and Vibration*, 330, 2011.
- K. E Kurrer. *The History of the Theory of Structures: From Arch Analysis to Computational Mechanics*. 2008.
- H. Lamb. On waves in an elastic plate. *Proc. Roy. Soc. London, Ser.*, 1917.
- J. B. Lawrie and J. Kaplunov. Edge waves and resonance on elastic structures: An overview. *Journal of Mathematics and Mechanics of Solids*, 2011.
- K. Chau Le. *Vibrations of Shells and Rods*. Springer, 1999.
- A. E. H. Love. *A Treatise on the Mathematical Theory of Elasticity, 2nd Edition*. 1906.
- A. E. H. Love. *On the Small Free Vibrations and Deformations of Elastic Shells*. CRC Press, 1988.
- M. Marsenne. *Trait de l’harmonie Universelle*. 1637.
- D. M. McCann and M. C. Forde. Edge waves and resonance on elastic structures: An overview. *NDT and E International 34*, 2001.
- R. Mindlin. Influence of rotary inertia and shear on flexural vibrations of isotropic elastic plates. *Journal of Applied Mechanics*, 1951.

- R. Mindlin and M. Onoe. Mathematical theory of vibrations of elastic plates. *Proc. 11th Ann. Symp. Freq. Cont*, pages 17–40, 1957.
- A. N. Norris, V. V. Krylov, and I. D. Abrahams. Flexural edge waves and comments on a new bending wave solution for the classical plate equation. 1998.
- V. Pagneux. Complex resonance and localized vibrations at the edge of a semi-infinite elastic cylinder. 2011.
- A. V. Pichugin and G. A. Rogerson. Edge vibration of a pre-stressed semi-infinite strip with traction-free edge and mixed face boundary conditions. *Zeitschrift für Angewandte Mathematik und Physik (ZAMP)*, 2011.
- M. Ratassepp, A. Klauson, F. Chati, F Leon, and G Maze. Edge resonance in semi-infinite thick pipe: Numerical predictions and measurements. *J Acoust Soc Am*, 2008.
- Lord Rayleigh. On the electromagnetic theory of light. *Philos. Mag*, 1881.
- Lord Rayleigh. On waves propagated along the plane surface of an elastic solid. *Proc. London Math. Soc*, 1885.
- E. Reissner. The effect of transverse shear deformation on the bending of elastic plates. *ASME Journal of Applied Mechanics*, 12, 1945.
- G.A. Rogerson. Some asymptotic expansions of the dispersion relation for an incompressible elastic plate. *International Journal of Solids and Structures*, 34:2785–2802, Aug 1997.
- M. V. Belubekyan S. A. Ambartsumyan. On bending waves localized along the edge of a plate. *Institute of Mechanics, Armenian Academy of Sciences, Erevan*, 30:61, February 1994.
- J. G. Scholte. On the stoneley-wave equation. *Proc. K. Ned. Akad. We*, 45:20–25, 1942.
- J. G. Scholte. The range of existence of rayleigh and stoneley waves. *Geophysical Journal International*, 5:120–126, 1947.

- K. Sezawa and K. Kanai. The range of possible existence of stoneley waves, and some related problems. 1939.
- E. A. G. Shaw. On the resonant vibrations of thick barium titanate disks. *J. Acoust. Soc*, 1956.
- A. S. Silbergleit and I. B. Suslova. Contact bending waves in thin plates. 1983.
- B. K. Sinha. Some remarks on propagation characteristics of ridge guides for acoustic waves at low frequencies. 1974.
- A. Sommerfeld. Jahresbericht der d. m. v. pages 309–353, 1912.
- R. Stoneley. Elastic waves at the surface of separation of two solids. *Proceedings of the Royal Society of London*, 1924.
- A. N. Stroh. Steady state problems in anisotropic elasticity. 1962.
- R. N. Thurston and J. McKenna. Flexural acoustic waves along the edge of a plate. 1974.
- P. J. Torvik. Reflection of wave trains in semi-infinite plate. *Acoust. Soc. Am*, 1967.
- A.V. Pichugin V. Zernov and J. Kaplunov. Eigenvalue of a semi-infinite elastic strip. *Proc. R. Soc*, April 2006.
- D. D. Zakharov. Analysis of the scoustical edge flexural mode in a plate using refined asymptotics. *Journal of the Acoustical Society of America*, 2004.
- V. Zernov and J. Kaplunov. Three-dimensional edge waves in plates. *Proceedings of the Royal Society of London*, page 301, 2008.